Dispersal and remineralisation of biodeposits: Ecosystem impacts of mussel aquaculture

A thesis
submitted in partial fulfilment
of the requirements for the degree of

Doctor of Philosophy
at
The University of Waikato

by

Hilke Giles

THE UNIVERSITY OF
WAIKATO
Te Whare Wānanga o Waikato

The University of Waikato
2006

For Tony and Tana

Abstract

Suspension-feeding bivalves produce biodeposits (faeces and pseudofaeces) that have much higher sinking velocities than their constituent particles. Consequently they cause sedimentation of material that might otherwise not be deposited. The benthic remineralisation of biodeposits increases sediment oxygen demand and nutrient regeneration, thus enhancing the benthic-pelagic coupling of nearshore ecosystems. In New Zealand the mussel *Perna canaliculus* has a high natural abundance and is also intensively cultured. This thesis examines the dispersal and remineralisation characteristics of mussel *P. canaliculus* biodeposits and the impacts of sedimentation from a mussel farm in the Firth of Thames on sediment biogeochemistry by combining laboratory, field and modelling studies.

Dispersal characteristics were examined in the laboratory by measuring sinking velocities and erosion thresholds of biodeposits produced by mussels of a wide size range fed three experimental diets. The results show that biodeposit dispersal is a function of mussel diet and size and thus could differ significantly between locations and seasons. Estimates of dispersal distances based on these results demonstrated that the initial dispersal of biodeposits produced by cultured mussels is not far. Depending on the hydrodynamic conditions, secondary dispersal via resuspension potentially plays a more important role in the dispersal of biodeposits from mussel farms than initial dispersal and almost certainly serves as the major means of transport of biodeposits from natural mussel beds.

Biodeposit mineralisation was studied by incubating coastal sediments with added biodeposits and measuring oxygen and nutrient fluxes as well as sediment characteristics over an 11 d period. Sediment oxygen consumption and ammonium release increased immediately after biodeposit addition and remained elevated compared to control cores without additions for the incubation period. A biodeposit decay rate (0.16 d^{-1}) was calculated by fitting a first-order G model to the observed increase in oxygen consumption. This rate is 1 – 2 orders of magnitude higher than published decay rates of coastal sediments without organic enrichment or plant material. Nutrient fluxes during the incubation period illustrated that biodeposit remineralisation alters the stoichiometry of the nutrients

released from the sediments which may potentially be more significant than the changes of the individual fluxes.

To determine the impact of a mussel farm in the Firth of Thames I measured sediment oxygen and nutrient fluxes by deploying benthic chambers, sediment characteristics by collecting sediment cores and sedimentation rates by deploying sediment traps in four seasons. Oxygen consumption and sediment nutrient release rates were generally higher under the farm compared to a reference site, demonstrating the typical response to increased organic input. Unusually low nitrogen release rates measured in summer may indicate enhanced denitrification under the farm. A simple budget demonstrated the importance of benthic nutrient regeneration in maintaining primary production in this region and that mussel culture can lead to a redistribution of nutrients. This study showed that site-specific hydrodynamic and biogeochemical conditions have to be taken into account when planning new mussel farms to prevent excessive modifications of nutrient dynamics.

Results of the laboratory and field studies conducted in this thesis were used to parameterise, calibrate and validate models of mussel biodeposit dispersal and remineralisation. A particle tracking model showed that the maximum initial dispersal of faecal pellets from the mussel farm is approximately 300 m and that pellets can be transported several times this distance via resuspension. The remineralisation model was able to simulate the increased nitrogen fluxes from the sediments well and highlighted the need for thorough calibration and parameterisation of the model.

This thesis contributed to the current understanding of the ecosystem impacts of mussel culture and provided numerical models and model parameters that will assist in the assessment of mussel culture sustainability and the contribution of mussels to the nutrient cycling in nearshore ecosystems.

Table of Contents

List of Figures

List of Tables

Acknowledgements

First, I would like to thank my chief supervisor Conrad Pilditch for his never-ending enthusiasm, motivation and believe in me. I am grateful for your ideas, guidance, grammar lessons and for introducing me to many great people. I could not have wished for a better supervisor.

I also greatly appreciate the support from my supervisors Niall Broekhuizen and Karin Bryan. Thanks Karin for your diagrams of tidal dynamics and DHI tutorials and Niall, thank you for the discussions on the mysterious paths of particles and currents.

My field work would not have been possible without Dudley Bell. Thank you for your tremendous energy, ideas and support and for the laughs after long days of hard work. I value your knowledge and experience and thoroughly enjoyed working with you.

Special thanks to Kent Ericksen who helped with my field work because he enjoys challenges and is a true friend. I sincerely appreciate your support and enjoyed diving and sharing my chocolates with you.

Many thanks to Dean and Mark Aislabe for providing access to their mussel farm.

Many people provided support for this study which I greatly appreciate. Scott Nodder gave advice and loaned sediment traps. John Oldman and Scott Stevens helped with the modelling and Dr. Alec Zwart with statistical analyses. Carolyn Lundquist, Kay Vopel and John Zeldis kindly reviewed manuscripts and gave valuable suggestions. Bill, Wendy, Elizabeth, Sally and the rest of the Ecoquest team were very hospitable and provided accommodation and lab space. Chris and Brian from the Science and Engineering workshop were always helpful and brought my plans into reality. Alex Ring, Ellie, Dave West, Dean, Erin, Nina and Amanda: Thanks for your practical and mental support and coffee breaks. I am very lucky to have great parents who have always been there for me. You feel much closer than 18000 km away.

Special thanks to Ting-Ling, Sun, Jane, Sonia and the rest of the Campus crèche nursery team for looking so well after Tana.

Tana, thank you for your big smiles and for sleeping through the night during the last phase of this thesis. Tony, you cheered me up when I needed it and put it all into perspective. We achieved this together.

Throughout this work, I was supported by a University of Waikato Doctoral Scholarship.

Preface

The main body of this thesis comprises four chapters (Chapters 2-5). Chapters 2 – 4 have been published or are accepted for publication in peer reviewed international scientific journals. I assumed the responsibility of the field work programme, laboratory and data analysis, and for writing this thesis. Except where referenced, the material in this thesis was produced from my own ideas and work undertaken under the supervision of Conrad Pilditch, Niall Broekhuizen and Karin Bryan.

Chapter 2 has been published by *Marine Ecology Progress Series*, Vol. 282: *pp.* 205-219, under the title "Effects of diet on sinking rates and erosion thresholds of mussel (*Perna canaliculus*) biodeposits" by H. Giles and C. A. Pilditch.

At the time of submission Chapter 3 is in press at *Marine Biology* under the title "Effects of mussel (*Perna canaliculus*) biodeposit decomposition on benthic respiration and nutrient fluxes" by H. Giles and C. A. Pilditch.

At the time of submission Chapter 4 is in press at *Aquaculture* under the title "Sedimentation from mussel (*Perna canaliculus*) culture in the Firth of Thames, New Zealand: Impacts on sediment oxygen and nutrient fluxes" by H. Giles, C. A. Pilditch and D.G. Bell.

Chapter 1

General introduction

1.1 Introduction

Suspension feeding bivalves, such as mussels, are often the dominant component of the macrofauna community in many coastal ecosystems and play a key role in the coupling of pelagic and benthic ecosystems (e.g. Kautsky and Evans 1987, Loo and Rosenberg 1989, Dame 1993, Newell 2004). They gather particles from the water column, which are either bound in mucus and rejected as pseudofaeces or ingested and subsequently egested as faeces. The amount and composition of suspended seston fluctuate widely within nearshore environments (e.g. Widdows et al. 1979, Fegley et al. 1992) and therefore the composition of egested faeces and pseudofaeces (biodeposits) may vary considerably spatially and temporally. Bivalves can selectively retain and reject captured particles and are capable of enhancing the organic content of ingested matter compared to that of the available seston (Hawkins et al. 1999). Biodeposits are much larger than their constituent particles and hence have much greater sinking rates (Haven and Morales-Alamo 1968, Wotton and Malmqvist 2001), thus a by-product of suspension feeding is increased sedimentation of organic matter that might otherwise not be deposited (Kautsky and Evans 1987, Dame 1993) diverting energy from pelagic to benthic food webs (Cloern 1982).

The benthic remineralisation of organic material increases sediment oxygen consumption due to a combination of chemical oxygen demand and microbial activity and results in the release of nutrients into the overlying water. In shallow coastal ecosystems benthic nutrient regeneration is a very important process that may account for over 80 % of the nutrients required for primary production (e.g. Rowe et al. 1975, Nixon 1981, Jensen et al. 1990). Biodeposition by bivalves stimulates the benthic metabolism and enhances the regeneration of nutrients (e.g. Smaal and Prins 1993, Gibbs et al. 2005). Furthermore, biodeposits are a food

resource and can also be utilised by animals for constructing tubes and similar structures (Wotton and Malmqvist 2001). Consequently, biodeposition can affect sediment texture, chemistry and benthic community composition (e.g. Dame 1993, Hertweck and Liebezeit 1996, Norkko et al. 2001).

In addition to their often high natural abundance, mussels are also cultivated in the upper water column where they are attached to ropes hanging off floating longlines and feed on the water flowing through these structures. In New Zealand the cultivation of the Greenshell™ mussel *Perna canaliculus* has increased dramatically over the last 25 years and more major expansions are planned (Jeffs et al. 1999, Christensen et al. 2003). Most mussel farms are located in the Marlborough Sounds, South Island, but currently there are also more than 2000 ha of existing and approved farm area in the Firth of Thames, North Island, with applications pending for approximately another 6000 ha (Broekhuizen et al. 2004). The environmental impacts of biodeposition from mussel culture range from little (e.g. Crawford et al. 2003) to severe (e.g. Nizzoli et al. 2005). Three previous studies have examined the impacts of mussel culture in the Marlborough Sounds (Kaspar et al. 1985, Christensen et al. 2003) and found significant effects on sediment characteristics and nutrient dynamics. Shellfish culture is generally considered to have less severe effects than finfish culture because farmed shellfish feed solely on ambient phytoplankton and organic particles and no external feed is added (e.g. Naylor et al. 2000, Newell 2004). However, in regions with little water movement where biodeposits are deposited in the vicinity of the farm impacts from shellfish culture can be equivalent or even higher (Nizzoli et al. 2005) and several studies have shown that the degree of environmental impact is directly related to the systems ability to disperse the organic material originating from the farm (Chamberlain et al. 2001, Newell 2004).

Simulation modelling provides an effective means to evaluate the potential interactions of bivalve aquaculture and the supporting coastal marine ecosystem. Several models have been developed to describe aspects of bivalve culture such as bivalve growth and carrying capacity (e.g. Dowd 1997, Campbell and Newell 1998, Gangnery et al. 2001). However, even though biodeposition is one of the most important potential effects of suspended bivalve culture (Grant et al. 2005)

the dynamics of bivalve biodeposition, including sinking velocity and resuspension, are poorly understood (Cranford et al. 2003) and only few models separate biodeposits from other sedimenting material and benthic detritus (Chapelle et al. 2000, Grant et al. 2005, Hartstein and Stevens 2005). The value of numerical models is dependent on the representation of simulated processes and their parameterisation. Only Hartstein and Stevens (2005) used measured mussel biodeposit sinking velocities whereas the model by Grant et al. (2005) avoided most mechanics of deposition and Chapelle et al. (2000) do not specify how sedimentation is calculated in their lagoon ecosystem model. Of the previous models simulating the impacts of biodeposition on benthic-pelagic nutrient fluxes (Bacher et al. 1995, Chapelle et al. 2000, Dowd 2005) only Chapelle et al. (2000) separated biodeposits from other benthic detritus, yet they used identical decay rates for both compartments. Mussel biodeposits show high bacterial activity and decompose rapidly (Kaspar et al. 1985, Grenz et al. 1990, Fabiano et al. 1994), suggesting that not using specific decay rates will lead to an underestimation of benthic oxygen and nutrient fluxes following biodeposit sedimentation. Consequently there is a need for more well-parameterised models simulating the deposition and subsequent remineralisation of biodeposits from suspended bivalve culture (Henderson et al. 2001). Because the level of environmental impact of mussel culture is strongly linked to the local hydrodynamics (Chamberlain et al. 2001, Hartstein and Stevens 2005) models need to consider the spatial dispersal as well as the sedimentary remineralisation processes of biodeposits.

While sinking through the water column biodeposits can be dispersed horizontally and their dispersal distance depends primarily on current speed and biodeposit sinking velocity. Biodeposit sinking rates depend on their size, shape and specific gravity (Wotton and Malmqvist 2001) and therefore differ not only with species or animal size but also with diet. The natural diet of bivalves may include a variety of organic and inorganic components and the composition of the food may vary widely in space and time (e.g. Fegley et al. 1992, Bayne 1993). Several studies have examined sinking velocities of faecal pellets produced by copepods, blackfly larvae and other aquatic organisms (e.g. review by Wotton and Malmqvist 2001) to estimate the flux of organic material in the deep ocean or in riverine ecosystems. Only two previous studies have examined biodeposit sinking

velocities of mussels (Miller et al. 2002, Hartstein and Stevens 2005) that predominantly live in coastal regions. Miller et al. (2002) measured higher sinking velocities for biodeposits produced on a mixed phytoplankton and silt diet compared to a phytoplankton diet, however, neither study has assessed sinking velocity as a function of mussel size. If bed shear velocities exceed the critical biodeposit shear velocity (erosion threshold) biodeposits can be resuspended after initial contact with the sediment surface, leading to their redistribution over a large area. Biodeposits are more easily resuspended than the surrounding sediments (Nowell et al. 1981, Minoura and Osaka 1992, Roditi et al. 1997, Widdows et al. 1998) but no previous studies have examined the erosion thresholds of mussel biodeposits.

Biodeposits contain predominantly broken down material and are already colonised by large populations of microorganisms when they are expelled (Harris 1993, Fabiano et al. 1994). This promotes their decomposition leading to significantly higher nutrient release rates at their deposition sites compared to sediments devoid of biodeposits (Asmus and Asmus 1992, Dame 1993, Prins and Smaal 1994, Newell et al. 2002). Despite their important function as substrate in the remineralisation of organic matter and hence the benthic-pelagic coupling of nutrient cycling in coastal ecosystems, no bivalve biodeposit decay rates have been published. Consequently, measurements of mussel biodeposit decay rates are essential in order to understand and quantify their contribution to the benthic regeneration of nutrients and enable accurate parameterisations of numerical models.

This thesis examines the dispersal and remineralisation characteristics of mussel *Perna canaliculus* biodeposits and the impacts of sedimentation from a mussel farm on surrounding sediments and nutrient dynamics. Because of the high natural abundance and intensive cultivation of *P. canaliculus* in New Zealand's nearshore ecosystems, it is important to quantify the spatial extent of their biodeposit dispersal and consequent ecosystem modifications. The goal of this thesis is to further our understanding of these processes and provide numerical models and model parameters that will assist in the assessment of mussel culture sustainability and the contribution of mussels to the nutrient cycling in nearshore ecosystems.

1.2 Organisation of thesis

This main body of this thesis comprises four chapters (2 – 5) each assessing a different aspect of the dispersal and remineralisation of mussel (*Perna canaliculus*) biodeposits. Chapter 2 examines the dispersal of mussel biodeposits and Chapter 3 their sedimentary remineralisation. Chapter 4 presents the environmental impacts of a mussel farm in the Firth of Thames and Chapter 5 is a modelling study of biodeposit dispersal and remineralisation.

The specific objectives of each chapter were:

- (Chapter 2) to examine the factors regulating the dispersal of biodeposits by using laboratory experiments to measure sinking velocities and erosion thresholds of biodeposits produced under varying diets and to verify the laboratory results with *in situ* measurements of biodeposit sinking velocities.
- (Chapter 3) to examine the changes in biogeochemical processes over time as mussel biodeposits age and calculate a biodeposit decay rate by incubating sediment cores with added biodeposits and tracking changes in sediment oxygen consumption and nutrient release rates over time.
- (Chapter 4) to investigate the effects of sedimentation from a mussel farm on sediment characteristics and benthic nutrient regeneration by deploying sediment traps and benthic chambers and analysing sediment samples at sites with different impact levels over four seasons.
- (Chapter 5) to develop models of biodeposit dispersal and benthic remineralisation of sedimenting material from a mussel farm by applying existing models using parameters determined in Chapters 2 and 3 and verifying them using the results from Chapter 4.

Chapter 2

Effects of diet on sinking rates and erosion thresholds of mussel (*Perna canaliculus*) biodeposits

2.1 Introduction

Suspension-feeding bivalves, such as mussels, live as benthos within nearshore environments and play an important role in the coupling of pelagic and benthic ecosystems (e.g. Kautsky and Evans 1987, Loo and Rosenberg 1989, Dame 1993). They gather particles from the water column, that are either rejected as pseudofaeces or ingested and subsequently egested as faeces (Griffiths and Griffiths 1987). Because the egested faeces and pseudofaeces (biodeposits) are compacted aggregates of particles in the water column their sinking rates can be much greater than the rates of their constitute particles (Haven and Morales-Alamo 1968, McCall 1979). Upon reaching the sediment surface, bottom currents can initiate the erosion of the biodeposits leading to redistribution. Thus a by-product of suspension-feeding is increased sedimentation and redistribution of particles that might otherwise not be deposited, leading to changes in the textural and chemical characteristics of the existing sediments as well as variations in the benthic community structure (Haven and Morales-Alamo 1968, Dahlbaeck and Gunnarsson 1981, Kaspar et al. 1985, Mirto et al. 2000, Norkko et al. 2001). Even though biodeposits are often very abundant, represent a repackaging of available organic matter and are readily transported, many contemporary studies continue to focus on the top-down effect of suspension-feeders on phytoplankton dynamics and much less attention has been paid to the role of biodeposits (Wotton and Malmqvist 2001).

The extent to which biodeposits modify the existing sediments and affect benthic communities depends on their quality and quantity, the physical and chemical characteristics of the existing sediments, composition of the benthos and hydrodynamic conditions. Biodeposits of suspension-feeding bivalves can be rich

in carbon and nitrogen (Kautsky and Evans 1987) and C:N ratios between 4.8 and 8.5 (Stuart et al. 1982, Kautsky and Evans 1987, Loo and Rosenberg 1989, Ahn 1993, Miller et al. 2002) suggest a high nutritional value (Parsons et al. 1984), indicating that biodeposits may represent a significant proportion of the energy potentially available to the benthos (Johannes and Satomi 1966, Tenore et al. 1982). The nutritional value of biodeposits is dependent on diet (Butler and Dam 1994, Miller et al. 2002). The natural diet of bivalves may include a variety of organic and inorganic components and the composition of the food may vary widely in space and time (e.g. Fegley et al. 1992, Bayne 1993). Tidal currents and storm conditions can periodically resuspend the sediments in mussel habitats, increasing the silt proportion of the diet (Falconer and Owens 1990, Sobral and Widdows 2000) and algae blooms can lead to an organic enrichment of the ingested material.

In most coastal marine systems the flux of organic matter to the sediment significantly increases benthic productivity (Nixon 1981, Grall and Chauvaud 2002) and affects primary production by supplying regenerated nutrients to the overlying water (Hargrave 1973). Faeces and pseudofaeces are characterised by a large bioavailability to microbial assemblages as well as rapid degradation rates (Grenz et al. 1990, Fabiano et al. 1994, La Rosa et al. 2002) and the mineralisation of biodeposits in the sediment causes higher nutrient release rates compared to sediments devoid of biodeposits (Asmus and Asmus 1992, Dame 1993, Smaal and Prins 1993, Newell et al. 2002). Where mussel beds are located in a well-mixed or the trophogenic zone of a stratified ecosystem, nutrients regenerated by the mussels and biodeposits are immediately available to primary producers (Nixon 1981, Kautsky and Evans 1987). Besides their significant role in coupling the pelagic and benthic compartments of coastal ecosystems and their function as food resource, biodeposits can also be utilised by animals for constructing tubes and similar structures (Wotton and Malmqvist 2001).

Depending on the prevailing currents, biodeposits can be dispersed horizontally while sinking through the water column. In regions of high current velocities biodeposits will be spread over a large area reducing the flux to the benthos whereas in low energy environments biodeposits may accumulate at a greater rate.

Thus the extent of their impact on sediment properties and the benthos is likely to vary greatly between these systems. Biodeposits can also be redistributed over a large area because they are more easily eroded than the surrounding sediments (Nowell et al. 1981, Minoura and Osaka 1992, Roditi et al. 1997, Widdows et al. 1998, Austen et al. 1999). Few studies have examined the quantitative effects of faecal pellets produced by benthic organisms on particle fluxes (Graf and Rosenberg 1997) and measured bed shear velocities required to erode biodeposits (Minoura and Osaka 1992, Widdows et al. 1998, Austen et al. 1999, Andersen 2001). To predict the dispersal of biodeposits and hence their flux to the benthos I quantified the sinking velocities and erosion thresholds of biodeposits produced by the common mussel *Perna canaliculus*.

The green-lipped mussel *Perna canaliculus* is endemic to New Zealand and found in a variety of habitats, attached to rock faces, wharf piles, among algal holdfasts in the intertidal zone and in deeper water over mud or sand (Morton and Miller 1973). Mussels typically grow 100 to 170 mm long and are widely distributed throughout the country. *P. canaliculus* is also intensively cultured and the extremely rapid growth of the aquaculture production of this species has lead to constraints on further expansion (Jeffs et al. 1999). Because of the high natural abundance and intensive cultivation of *P. canaliculus* in New Zealand's nearshore ecosystems, it is important to understand the spatial extent of their biodeposit dispersal. A recent review of the use of ecosystem models for managing environmental impacts of mussel culture concluded that the key areas of modelling uncertainty include the parameterisation of biodeposit settling velocities, quality and erosion characteristics (Henderson et al. 2001).

As a first step toward analysing the spatial dispersal of biodeposits and potential effects of mussel farms on the benthos I measured sinking velocities and erosion thresholds of faeces and pseudofaeces produced by *Perna canaliculus*. Mussels of a wide size range were fed three experimental diets under controlled laboratory conditions to examine the influence of animal size and diet on biodeposit dispersal characteristics. In addition, *in situ* biodeposit sinking velocities were measured on two separate occasions.

2.2 Materials and methods

2.2.1 Biodeposit production

Rope-cultured *Perna canaliculus* were collected by SCUBA from a commercial mussel farm in the Firth of Thames, New Zealand (175°17' E, 36°59' S), a historic site of large mussel beds (Greenway 1969). Mussels were scraped clear of epibionts, transported to the laboratory and allowed to acclimatise to laboratory conditions for 8 d before exposure to the experimental diet in an aerated recirculating sea water system at 17 ± 2 °C on a 12 : 12 h light / dark cycle. During this time no food was added to the system and mussels completely emptied their guts. Mussels were divided into five size classes (1: <40 mm, 2: 41 – 60 mm, 3: 61 – 80 mm, 4: 81 – 100 mm and 5: >100 mm shell length). Three mussels of the smallest two size classes and two of each remaining size class were randomly selected from the acclimatised animals for exposure to the experimental diet and biodeposit production.

To examine the effects of diet on biodeposit dispersal characteristics, mussels were fed three experimental diets composed of natural sea water (N diet) and filtered (5 μm) sea water mixed with either cultured algae (A diet) or silt (S diet; Table 2.1). The amounts of algae and silt added were chosen to represent situations such as dense algae blooms that occur in shallow or unmixed eutrophic waters and high concentrations of silt caused by resuspension of sediments or riverine input in coastal ecosystems (Hawkins et al. 1999). The natural seawater was collected from Raglan, New Zealand (174°57' E, 37°48' S), and used within two days of collection. The A diet was composed of 4.2 ml of the cultured flagellate *Isochrysis galbana* per litre of filtered (5 μm) sea water. For the S diet sediment was collected from intertidal mud banks near the mussel farm, sieved (<63 μm; median grain size = 17.2 μm) and 1.1 ml of the slurry added per litre of filtered sea water.

Biodeposits were produced by exposing mussels contained in eight flow-through feeding chambers (length = 15.5 cm, width = 13 cm, vol. = 1.4 l) to the experimental diets. For the larger size classes (3 – 5; n = 2 mussels per size class) a single mussel was placed in a feeding chamber but for the smaller size classes (1

Table 2.1. Summary of experimental (N: natural, A: algae, S: silt) and *in situ* diet (Field) characteristics. Data are the treatment means of water samples collected during biodeposit production (n = 2 – 4) and *in situ* (Field 1: n = 10, Field 2: n = 4). Standard deviations are given when more than two replicates were determined. Suspended particulate material (SPM), particulate organic matter (POM), organic content (OC), chlorophyll *a* (chl *a*), phaeopigment (phaeo), particulate carbon and nitrogen (PC, PN) and C:N ratio. ND = no data

	N diet	A diet	S diet	Field 1	Field 2
SPM ($mg\ l^{-1}$)	20.9 ± 8.1	53.6 ± 4.9	101.5 ± 15.4	7.3 ± 2.3	5.6 ± 0.7
POM ($mg\ l^{-1}$)	2.5 ± 0.8	37.1 ± 5.1	12.3 ± 2.7	2.1 ± 0.5	1.6 ± 0.3
OC (%)	12.3 ± 4.1	70.2 ± 6.4	12.2 ± 2.4	30.1 ± 6.6	29.0 ± 4.0
Chl *a* ($\mu g\ l^{-1}$)	2.56 ± 0.41	578 ± 39	2.52 ± 0.63	2.07 ± 0.60	4.26 ± 0.99
Phaeo ($\mu g\ l^{-1}$)	1.50 ± 0.28	26.1 ± 1.3	6.04 ± 0.94	0.91 ± 0.21	1.74 ± 0.43
PC ($\mu g\ l^{-1}$)	827	14652	2814	ND	ND
PN ($\mu g\ l^{-1}$)	98	2200	381	ND	ND
C:N (by weight)	8.5	6.7	7.4	ND	ND

& 2) there were three mussels per chamber and size class. A header tank supplied the chambers with diet at a flow rate of 200 ml min^{-1} which was fast enough to prevent depletion within the chamber (Bayne 1993, Hawkins et al. 1996, Hawkins et al. 1998). Water leaving the chambers was collected and pumped back into the header tank for the A and S diets. Water samples were taken from the header tank at the start of each experiment and from the collection tank approximately every hour thereafter for the analysis of suspended particulate material (S diet, Hach DR/890 colorimeter) and *in vivo* fluorescence (A diet, Turner Designs 10-AU Fluorometer). If necessary more algae or silt-slurry was added to ensure consistent experimental conditions. For the N diet experiments only fresh seawater was used which was discarded once it had passed through the chambers. All biodeposit production experiments were conducted at 16 ± 1 °C at a salinity of 31.5 ± 0.5

ppt. Four water samples for diet analysis were taken from the header tank during the biodeposit production period.

Mussels were allowed to acclimatise in the feeding chambers for one hour before start of the experiment (Hawkins et al. 1999). All biodeposits produced during the acclimatisation period were removed with pipettes without disturbing the animals. Pseudofaeces were fragile but stayed intact in the feeding chambers and when handled with care. Occasionally pseudofaeces were damaged during handling but these were discarded from further analysis. During the feeding experiment biodeposits were removed from the chambers approximately every hour until the end of the experiment (after 3.25 – 7 h). For the sinking velocity measurements biodeposits from each mussel were individually placed into vials filled with filtered seawater and photographed immediately under a Leica MZ12 microscope. From the digital images biodeposit length, cross-sectional width and cross-sectional area were measured using image analysis software (Image-Pro Plus V. 4.5.1.22). For the erosion threshold measurements only biodeposits produced by mussels of size classes 1, 3 and 5 were used which captured the size range of biodeposits produced by all size classes. Biodeposits were kept dark and on ice in filtered seawater until the start of the erosion measurements (within 4 h). Additional biodeposits were collected during the feeding experiments for analysis of their composition.

2.2.2 Biodeposit sinking velocities and erosion thresholds

Biodeposit sinking velocities were determined by timing the rate of descent of individual faecal pellets and pseudofaeces in a temperature controlled settling tank (height = 2 m, ID = 19 cm) filled with filtered (1.2 μm) sea water (T = 18.4 – 18.7 °C, S = 31.2 – 31.5 ppt). The temperature was controlled by pumping tap water through an outer column surrounding the tank for 24 h prior to and during the measurements. Preliminary experiments have shown that this reduces the spatial temperature variation in the tank (top, mid and lower section) to 0.08 °C and the variation over a ten-hour period (maximum duration of measurements) to 0.25 °C. Biodeposits were transferred into the settling tank using a pipette and released approximately one centimetre below the water surface. They were allowed to sink untimed for 30 cm to eliminate momentum due to release, then the time taken to

fall three consecutive 30 cm intervals was recorded. For all analyses an average of these three readings was used. Sinking velocity measurements of biodeposits coming within 3 cm of the sidewall were discarded.

Biodeposit erosion thresholds (here defined as the bed shear stress required to initiate transport) were determined in a recirculating flume (7.23 m long, 50 cm wide) described by Miller et al. (2002) that was filled to 15 cm with filtered (5 μm) sea water (T = 19 ± 1 °C, S = 31.5 ppt). Located in the working section of the flume 5.5 m downstream of the entrance are two core inserts, whose centres are located 20 cm from the side walls. Sediment cores (ID = 5.2 cm) were placed into the inserts ensuring that the sediment surface was flush with the flume floor. Sediment for the cores was collected from a mid-intertidal sandflat, prepared by wet-sieving through a 500 μm mesh (median grain size = 33.7 μm) to remove macrofauna, and frozen until use.

Erosion thresholds were measured separately for biodeposits produced by mussels of size classes 1, 3 and 5 for each diet. Fifty freshly collected faecal pellets were placed onto one sediment core by letting them sink through a tube of the same diameter as the sediment core and approximately 50 pseudofaeces were placed onto the second core. By arranging the biodeposits this way I tried to simulate the natural distribution of biodeposits on the sediment surface. The flume motor speed was increased by 2 Hz every 10 minutes and the number of faecal pellets eroded off the sediment cores recorded. Pseudofaeces partly broke up when exposed to the flow resulting in an almost even coverage of the sediment core area. Therefore, the percentage of the core area exposed was estimated after each incremental increase in flow speed. These measurements were conducted once for each of the three mussel size classes.

To convert flume motor output to estimates of bed shear velocity (u_*, cm s^{-1}) velocity profiles were measured at the centre of the cores using a Sontek 10-MHz Acoustic Doppler Velocimeter (ADV) for the range of motor settings used during the erosion measurements. Flow profiles started 0.8 cm above the bed to ensure that the bed is not included within the sampling volume (Finelli et al. 1999) and measurements were made at nine additional heights (z = 1, 1.5, 2, 2.5, 3, 4, 5, 6

and 7 cm). For each motor setting (4, 8, 12, 16 and 20 Hz) flow velocities were measured for 60 s at each height. Flow profiles were generated for both cores and shear velocities derived from the regression of velocity and log transformed height above the sediment (r^2 = 0.95 – 0.97). No significant differences were found between the slopes or intercepts for the two cores (t-test, $p > 0.05$) so one common regression equation was calculated (u_* (cm s^{-1}) = 0.0234 + 0.0343 × Hz, $r^2 = 0.98$, $p < 0.0005$).

2.2.3 Biodeposit and diet analysis

Biodeposit and diet samples were processed the same day they were collected. Unless specified duplicate samples were analysed and prior to sub-sampling biodeposits were homogenised by vigorous shaking in filtered (1.2 µm) sea water. For the determination of organic content (OC, %) approximately 30 biodeposits were filtered onto ashed and pre-weighed 25 mm Whatman GF/C filters, rinsed with 20 ml distilled water to remove salts, dried at 60 °C for 24 h and ashed at 450 °C for 4 h. Suspended particulate material (SPM, mg l^{-1}) concentration, particulate organic matter (POM, mg l^{-1}) concentration and OC of the diet samples were measured by filtering 500 ml onto ashed and pre-weighed 47 mm Whatman GF/C filters which were treated as described above for biodeposits. Chlorophyll *a* (chl *a*) and phaeopigment (phaeo) content of biodeposits (µg mg dw^{-1}) and diet (µg l^{-1}) samples were determined by filtering 30 biodeposits or 100 ml water, respectively, onto 25 mm Whatman GF/C filters that were frozen for <6 weeks until analysis using the 90 % acetone extraction method on a Turner Designs 10-AU Fluorometer (Arar and Collins 1997). For analysis of particulate carbon (PC, µg mg dw^{-1}) and particulate nitrogen (PN, µg mg dw^{-1}) content, faecal pellets and pseudofaeces were rinsed with distilled water and dried at 60 °C for 24 h. Water samples were filtered onto 25 mm Whatman GF/C filters and analysed the same way for PC (µg l^{-1}) and PN (µg l^{-1}) concentration. PC and PN analyses were done using a Europa Scientific 20/20 isotope analyser.

2.2.4 Field measurements of biodeposit sinking velocities

Biodeposit sinking velocities were measured on two separate occasions in summer at the Firth of Thames mussel farm. A video camera and a cylindrical sediment trap (aspect ratio = 8.3, height = 58 cm) were attached to a frame, so that the

camera recorded the lower section of the trap in which a grid was placed. Biodeposits captured in the trap sank past the grid and sinking velocities were derived from the time it took an individual biodeposit to travel the recorded distance. The frame holding the camera and sediment trap was set-up approximately 2 m off the bottom. On the first occasion baffles were used to diminish turbulence and to create a calm layer in the trap allowing sinking velocity measurements (Bloesch and Burns 1980). When analysing the video footage of these measurements I noticed that pseudofaeces were absent. To ensure that pseudofaeces entered the trap I repeated the experiment attaching a funnel covered by a mesh to the sediment trap and placed mussels onto the mesh so that biodeposits produced by the mussels descended directly into the trap.

All collected biodeposits were visually examined to ensure that they were *Perna canaliculus* biodeposits. On both occasions only mussel biodeposits were collected. Pseudofaeces area was determined by image analysis of the videographed pseudofaeces. Faecal pellet width could not be reliably determined from the video because of the pellets' orientation while settling. Instead, faecal pellets were collected from the sediment trap material and their width analysed as described above for biodeposits produced in the laboratory. This precluded assigning a width to each measured sinking velocity and the average width of all captured faecal pellets was calculated instead. Water samples were taken and analysed as described above to compare the *in situ* diet composition (SPM, POM, OC, chl *a* and phaeo) to the laboratory diets (Table 2.1).

2.2.5 Statistical analysis

I fitted general linear models (GLMs) to determine the relationships between biodeposit size (faecal pellet width and pseudofaeces area) and mussel size class and experimental diet using GenStat (V. 6.1.0.200, copyright 2002 Lawes Agricultural Trust). I performed Tukey post-hoc tests using MINITAB™ (Release 13.32) to investigate the difference between individual treatments for significant GLM results (α = 0.05). GLMs were also fitted to biodeposit sinking velocity with factors biodeposit size, mussel size class and experimental diet. I conducted additional multiple comparison tests (t-test, GenStat) to examine differences between slopes and intercepts. Sinking velocity and biodeposit morphometric data

(faecal pellet width and pseudofaeces area) were $\log_{10}$ transformed to satisfy the assumptions of homogeneity of variance and normality. I used GLMs because they allow categorical variables as predictors (such as mussel size class and experimental diet) and do not assume slopes of fitted lines to be equal. To quantify the relationship between sinking velocity and biodeposit size linear regression analyses were conducted for faecal pellets and pseudofaeces using MINITAB™. Although I could assign each biodeposit to the individual mussel that produced them preliminary analysis indicated that the variation in the size of biodeposits produced by a single individual was greater than the variation between individual mussels of the same size class. I therefore treated each biodeposit as a replicate for statistical analyses.

2.3 Results

2.3.1 Diets

The characteristics of the three experimental diets were very different (Table 2.1). The N diet had a SPM concentration of 20.9 mg l^{-1}, OC of 12.3 % and a chl *a* concentration of 2.56 µg l^{-1}. The A diet was characterised by a very high chl *a* concentration (578 µg l^{-1}) and OC of 70.2 %. On the other hand the S diet had a 5 × higher SPM concentration compared to the N diet but a similar OC and chl *a* concentration possibly a result of microphytobenthos and/or sediment bacteria. PC and PN concentrations were highest for the A diet, followed by the S and N diets. The C:N ratio of the A diet was 6.7 and increased for the S (7.4) and N diet (8.5). The *in situ* diets were most similar to the N diet but on both occasions had lower SPM concentrations and higher OC (Table 2.1).

2.3.2 Biodeposit shape and composition

Mussels produced pseudofaeces within a few minutes of being placed into the feeding chambers and faeces after approximately 30 minutes. Faecal pellet production rates differed among the three diets so to ensure sufficient pellets for analysis feeding time varied between 3.25 h for the N diet to 7 h for the A diet. However, despite the extended duration of the A diet treatment mussels produced only 79 pellets, compared to 174 on the N and 192 on the S diet.

Faecal pellets had a cylindrical shape but rather than being a closed cylinder, the edges curled up and rolled over inwards creating a longitudinal groove (Fig. 2.1a). Pellets produced on the N and S diets were light brown and had an even, slightly rough texture compared to those produced on the A diet which were dark green with a soft, silky texture. Because of this distinctive shape it was not possible to measure the volume of faecal pellets produced by *Perna canaliculus* and pellet length, width and cross-sectional area were chosen as size parameters. Pseudofaeces were readily distinguished from faeces. They were amorphous in shape (Fig. 2.1b), consisting of a fluffy texture and colour identical to that of the faecal pellets. It was not possible to define volume, length or width of the pseudofaeces and therefore cross-sectional area was used to describe their size.

The composition of biodeposits reflected the diets mussels were fed (Tables 2.1 and 2.2). Biodeposits produced on the A diet had an ~8 × higher OC compared to those produced on the N and S diets and values of faecal pellets and pseudofaeces were very similar. The chl *a* content was higher for pseudofaeces than faeces for

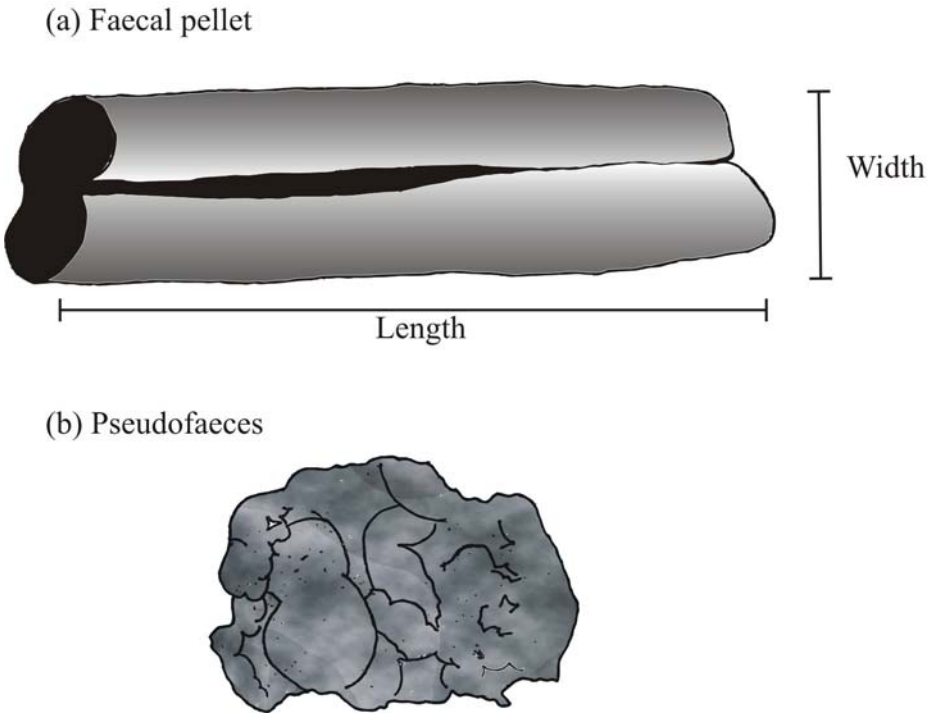

Figure 2.1. Drawing of *Perna canaliculus* (a) faecal pellet and (b) pseudofaeces. Faecal pellets ranged in length from 1.0 - 65.2 mm and in width from 0.22 - 1.86 mm whereas pseudofaeces were between 0.6 - 10.0 mm^2 in area.

Table 2.2. Summary of biodeposit characteristics (mean ± SD, n = 4 and for remainder n = 2) produced on the three experimental diets (N: natural, A: algae, S: silt).

	Faeces	Pseudofaeces
Organic content (%)		
N diet	11.9 ± 0.9	9.6 ± 0.3
A diet	93.8	93.4
S diet	11.8 ± 0.7	12.1 ± 2.2
Chlorophyll *a* content (µg mg dw^{-1})		
N diet	0.10 ± 0.03	0.12 ± 0.01
A diet	3.68	4.42
S diet	0.033 ± 0.004	0.035 ± 0.007
Phaeopigment content (µg mg dw^{-1})		
N diet	0.167 ± 0.04	0.047 ± 0.003
A diet	12	29
S diet	0.087 ± 0.02	0.042 ± 0.005
Carbon content (µg mg dw^{-1})		
N diet	30.1	34.7
A diet	287	392
S diet	29.7	24.8
Nitrogen content (µg mg dw^{-1})		
N diet	3.54	4.02
A diet	40.1	59.9
S diet	3.98	3.24
C:N (by weight)		
N diet	8.5	8.6
A diet	7.2	6.6
S diet	7.5	7.7

all diets and ~37 × higher on the A diet compared to the N and ~120 × higher compared to the S diet. Phaeo concentrations were lower for pseudofaeces than faeces for the N and S diets but increased for the A diet. They were also much higher for biodeposits produced on the A diet (~72 to >600 ×) compared to the other two diets. The C:N ratio was higher for biodeposits produced on the N diet compared to those on the S diet and A diet (Table 2.2).

2.3.3 Biodeposit size

A correlation analysis of faecal pellet sinking velocity with pellet morphometrics (length, width and area) revealed that the best correlations (Pearson's correlation coefficient, r) occurred with width for all diets (N diet: $r = 0.85$, A diet: $r = 0.73$, S diet: $r = 0.74$, $p < 0.0005$). Correlations of pellet sinking velocity with length and area were also highly significant ($p < 0.0005$) but the correlation coefficients were reduced by 0.10 – 0.34 compared to width. Faecal pellet width was therefore chosen as the size description variable for the statistical analyses. The correlations between pseudofaeces sinking velocity and cross-sectional area were also highly significant (N diet: $r = 0.46$, A diet: $r = 0.75$, S diet: $r = 0.73$, $p < 0.0005$).

Larger mussels produced larger biodeposits (Table 2.3). The average width of faecal pellets produced on the N diet ranged from 0.54 mm (mussel size class 1) to 1.49 mm (mussel size class 5). Pellets produced on the S diet were slightly narrower for all size classes, ranging from 0.50 mm to 1.19 mm, and those produced on the A diet had widths between 0.42 mm and 1.29 mm. Mean pseudofaeces area of mussels fed the N diet was 1.76 mm^2 for size class 1 and increased to 4.25 mm^2 for size class 5. Those produced on the A diet had a greater disparity between small and large mussels with mean pseudofaeces area ranging from 1.31 mm^2 to 7.13 mm^2. Average area of pseudofaeces produced on the S diet was 1.74 mm^2 for size class 1 and 5.50 mm^2 for size class 5. Pseudofaeces produced by mussels of size class 3 on the S diet were unusually large (5.57 mm^2) compared to size classes 4 and 5.

To analyse the effects of mussel size and diet on biodeposit size I fitted GLMs to $\log_{10}$ transformed faecal pellet width and pseudofaeces area with mussel size class and diet as factors. The model of faecal pellet width indicated significant effects of mussel size class and diet ($p < 0.001$) as well as a significant interaction term of the two factors ($p < 0.001$). It explained 80.8 % of the variation (r^2) in faecal pellet width ($p < 0.001$) and had a standard error (SE) of 0.0814 ($n = 445$). The GLM of pseudofaeces area ($p < 0.001$, $r^2 = 60.7$ %, SE = 0.176, $n = 74$) also showed significant effects of mussel size class ($p < 0.001$) and diet ($p = 0.005$) on biodeposit size but the interaction term did not contribute significantly to the explanation of the data ($p = 0.210$). Therefore a simpler model could be fitted,

Table 2.3. Mean faecal pellet width (± SD) and mean (± SD) pseudofaeces area produced by mussels of different size classes (range of shell lengths given below size class) on the experimental diets (N: natural, A: algae, S: silt). Numbers of biodeposits measured are given in brackets.

	N diet	A diet	S diet
Faecal pellet width (mm)			
Size class 1 27.3 – 36.1 mm	0.54 ± 0.06 (34)	0.42 ± 0.12 (30)	0.50 ± 0.07 (39)
Size class 2 45.3 – 58.7 mm	0.85 ± 0.07 (31)	0.87 ± 0.29 (17)	0.76 ± 0.13 (39)
Size class 3 63.2 – 78.7 mm	1.07 ± 0.12 (38)	0.98 ± 0.14 (10)	0.99 ± 0.14 (38)
Size class 4 63.2 – 78.7 mm	1.37 ± 0.16 (38)	1.27 ± 0.30 (17)	1.18 ± 0.20 (39)
Size class 5 101.0 – 114.1 mm	1.49 ± 0.19 (33)	1.29 ± 0.34 (5)	1.19 ± 0.23 (37)
Pseudofaeces area (mm^2)			
Size class 1 27.3 – 36.1 mm	1.76 ± 1.00 (5)	1.31 ± 0.76 (5)	1.74 ± 0.43 (5)
Size class 2 45.3 – 58.7 mm	1.82 ± 0.88 (4)	2.65 ± 0.78 (5)	2.45 ± 0.47 (5)
Size class 3 63.2 – 78.7 mm	2.67 ± 1.00 (5)	4.28 ± 1.94 (5)	5.57 ± 1.65 (5)
Size class 4 63.2 – 78.7 mm	3.42 ± 1.13 (5)	6.65 ± 2.99 (5)	4.90 ± 1.41 (5)
Size class 5 101.0 – 114.1 mm	4.25 ± 1.49 (5)	7.13 ± 3.11 (5)	5.50 ± 1.31 (5)

omitting the interaction term of mussel size class and diet. The simplified model explained 58.7 % of the variation in pseudofaeces area ($p < 0.001$, SE = 0.181) with significant effects of mussel size class ($p < 0.001$) and diet ($p = 0.006$).

To examine differences in faecal pellet width and pseudofaeces area among mussel size classes, I conducted multiple comparison tests for each diet (Tukey test, $\alpha = 0.05$). Faecal pellets produced by mussels of size class 1 were significantly smaller than those produced by larger mussels for all experimental diets (Table 2.4). The difference between mean pellet width was significant for all

Table 2.4. Multiple comparisons of mean biodeposit sizes between mussel size classes for experimental diets (N: natural, A: algae, S: silt). Separate lines represent significant differences (Tukey test, $p < 0.05$) and where lines are joined no significant differences were observed.

	Mussel size class				
	1	2	3	4	5
Faecal pellet width					
N diet	—	—	—	—	—
A diet	—	———			
			———		
S diet	—	—	—	———	
Pseudofaeces area					
N diet	———				
		———			
A diet	———				
		———			
			———		
S diet	———		———		

mussel size classes fed the N diet and for those fed the S diet only the difference between size classes 4 and 5 were non-significant. Faecal pellets produced on the A diet were not significantly different between size classes 2 and 3 as well as 3, 4 and 5. Comparing the mean pseudofaeces areas revealed that the distinction among size classes was not as great as for faecal pellets (Table 2.4). The only significant size difference of pseudofaeces produced on the N diet was between mussel size classes 1 and 5 and on the A diet significant differences were found between size classes 1 and 3 or higher as well as 2 and 5. Pseudofaeces area for mussels produced on the S diet were not significantly different between size classes 1 and 2 as well as 3, 4 and 5.

2.3.4 Biodeposit sinking velocities

Biodeposit sinking rates varied with diet and were generally lower for pseudofaeces compared to faeces (Figs. 2.2 and 2.3). Sinking velocities of faecal pellets produced on the N diet ranged from 0.9 to 4.3 cm s^{-1} whereas the corresponding rates for pseudofaeces were only about half as large (0.5 to 2.2 cm

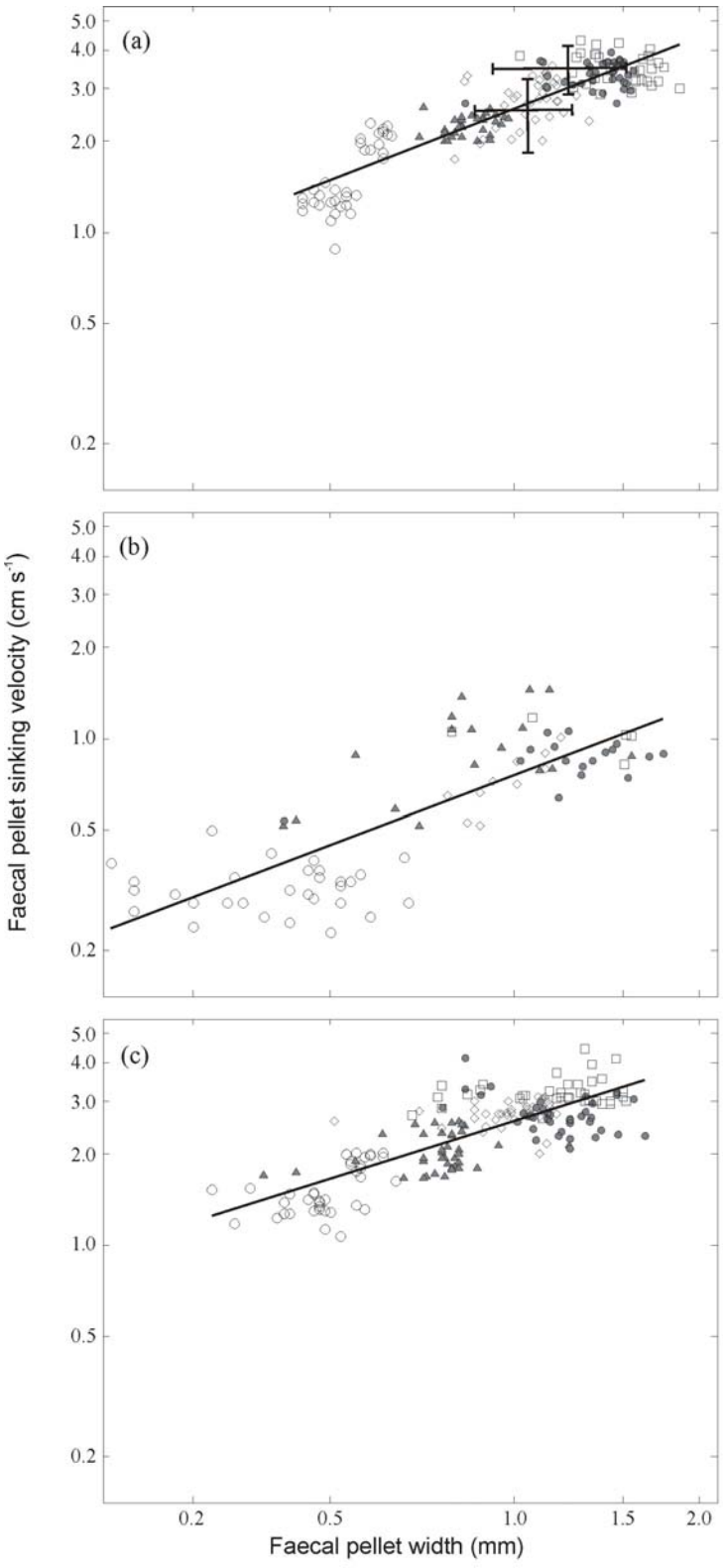

Figure 2.2. Relationship between faecal pellet sinking velocity and width for the experimental diets: (a) Natural diet, (b) Algae diet and (c) Silt diet. Mussel size classes are indicated by symbols: (O) <40 mm, (▲) 41 - 60 mm, (◇) 61 - 80 mm, (●) 81 - 100 mm and (□) >100 mm shell length. The crosses in Fig. (a) represent the mean ± SD of width and sinking velocity of the two *in situ* measurements (Field 1 and Field 2). The solid lines represent linear regression lines fitted to the data. Regression statistics are given in Table 2.5.

s^{-1}). Faecal pellets that were produced on the S diet had similar sinking velocities (1.1 to 4.5 cm s^{-1}) to those on the N diet and pseudofaeces sank equally fast (1.1 to 4.0 cm s^{-1}). Both faeces and pseudofaeces produced on the A diet had much lower sinking velocities than those produced on the other two diets (faeces: 0.2 to 1.5 cm s^{-1}, pseudofaeces: 0.1 to 0.8 cm s^{-1}).

To examine how biodeposit sinking velocity was affected by diet, biodeposit size and mussel size class I fitted GLMs to $\log_{10}$ transformed faecal pellet and pseudofaeces sinking velocity. In the GLM of faecal pellet sinking velocity all three independent variables were significant ($p < 0.001$) but the order in which biodeposit size and mussel size class were fitted in the model determined which of these variables described the greater amount of variation in sinking velocity. I decided that faecal pellet width was the most important variable for the model since it is commonly used to characterise biodeposit size, whereas mussel size class is a rather arbitrary definition. Furthermore, adding mussel size class to the model only explained an additional 3.1 % of the variation in the data. These arguments and the close relationships of mussel size class and biodeposit size described above suggested that it was acceptable to omit mussel size class in favour of faecal pellet width in the model of faecal pellet sinking velocity.

Table 2.5. Linear regression analysis of biodeposit sinking velocity (cm s^{-1}) vs. biodeposit size for experimental (N: natural, A: algae, S: silt) and *in situ* diets. Faecal pellet sinking velocity = a + b × width (mm) and pseudofaeces sinking velocity = a + b × area (mm^2). All data was $\log_{10}$ transformed before analysis.

	a	b	r^2	p	n
Faecal pellets (sinking velocity vs. width)					
N diet	0.410	0.789	0.79	< 0.0005	174
A diet	-0.120	0.769	0.65	< 0.0005	79
S diet	0.412	0.632	0.64	< 0.0005	192
Pseudofaeces (sinking velocity vs. area)					
N diet	-0.099	0.504	0.43	< 0.0005	24
A diet	-0.650	0.501	0.66	< 0.0005	25
S diet	0.163	0.370	0.43	< 0.0005	25
In situ	0.157	0.291	0.49	0.011	12

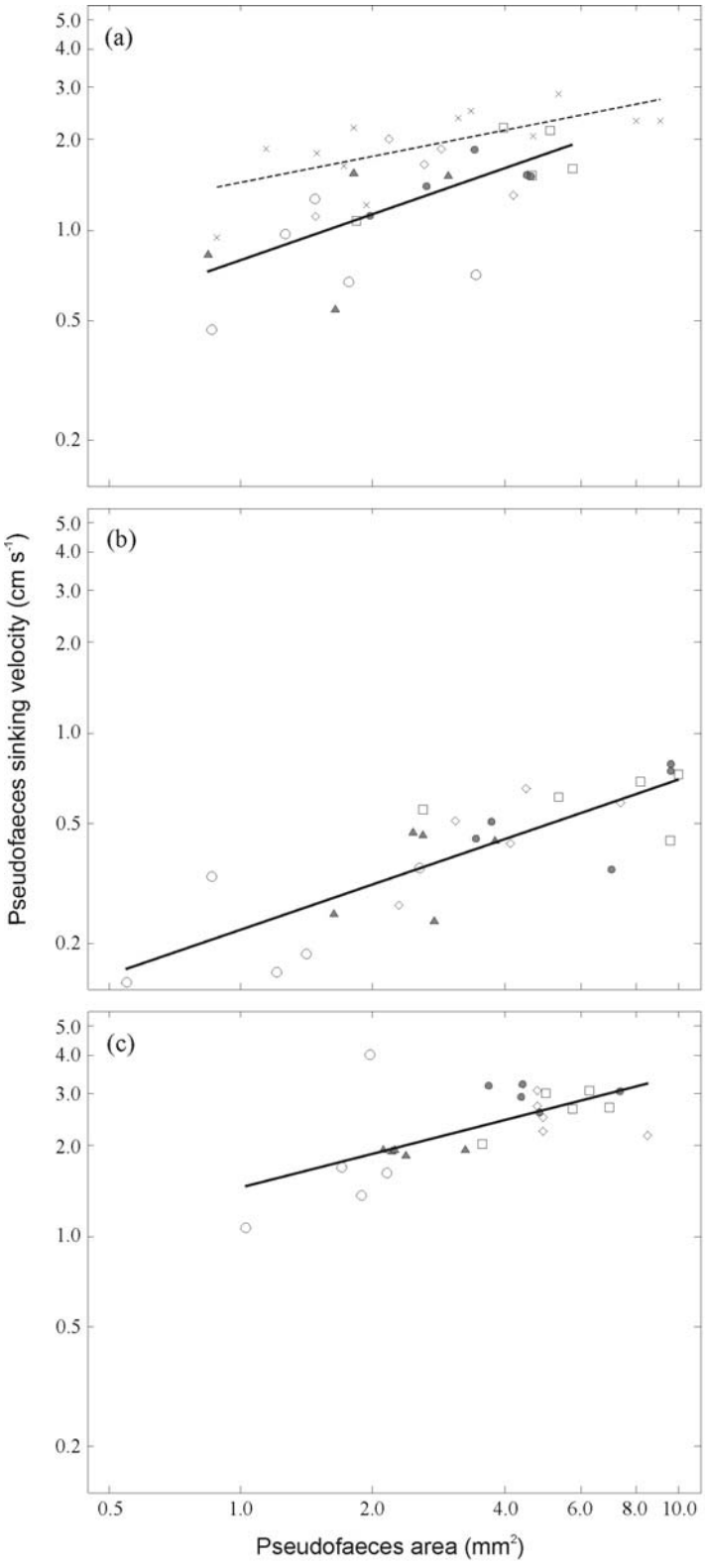

Figure 2.3. Relationship between pseudofaeces sinking velocity and area for the experimental diets: (a) Natural diet, (b) Algae diet and (c) Silt diet. Mussel size classes are indicated by symbols: (O) <40 mm, (▲) 41 - 60 mm, (◇) 61 - 80 mm, (●) 81 - 100 mm and (□) >100 mm shell length. *In situ* pseudofaeces measurements are indicated by (×) in (a). The solid lines represent linear regression lines fitted to the data. Regression statistics are given in Table 2.5.

The GLM explained 91 % of the variation in faecal pellet sinking velocity ($p < 0.001$, SE = 0.0873, n = 445). Faecal pellet width and diet had significant effects on sinking velocity ($p < 0.001$) and the interaction between these two variables was also significant ($p = 0.010$). Further multiple comparison tests (t-test, GenStat) showed significant differences between the slopes for the N and S diet ($p = 0.005$) as well as the A and S diet ($p = 0.017$) but no significant difference between the N and A diets ($p = 0.711$). The intercepts of the regression lines for the N and A diets were significantly different ($p < 0.001$).

The GLM for pseudofaeces sinking velocity explained 88 % of the variation in the data ($p < 0.001$, SE = 0.124, n = 74) and revealed significant contributions of pseudofaeces area and diet ($p < 0.001$) but not mussel size class ($p = 0.191$). The interaction term of pseudofaeces area and diet was not significant ($p = 0.580$), indicating equal slopes of sinking velocity versus pseudofaeces area for all three experimental diets. The GLM showed significant differences between the intercepts of all three regression lines ($p < 0.001$) indicating significantly higher sinking velocities for pseudofaeces produced on the S diet and the lowest rates for those produced on the A diet.

To quantify the relationships between sinking velocity and biodeposit size (faecal pellet width and pseudofaeces area), a simple linear regression analysis was conducted (Table 2.5). All regressions were significant ($p < 0.0005$), and regressions generally had stronger fits (i.e. higher coefficients of determination, r^2) for faecal pellets ($r^2 = 0.64 – 0.79$) than pseudofaeces ($r^2 = 0.43 – 0.66$). The amount of variation in biodeposit sinking velocity explained by biodeposit size was highest for faecal pellets produced on the N diet and pseudofaeces produced on the A diet.

The faecal pellet size and sinking velocities measured *in situ* on both occasions were well within the range of those produced in the laboratory under the natural diet (Fig. 2.2). During the time of our deployments the mussels at the commercial farm were approximately 55 to 100 mm long and hence did not represent the very small (<40 mm) and very large (>100 mm) mussels used in the laboratory measurements. This is illustrated by the lack of very small (<0.50 mm width) and

very large (>1.79 mm width) faecal pellets collected in the sediment trap. The size range of pseudofaeces captured represented the complete range of pseudofaeces analysed in the laboratory (Fig. 2.3) and their sinking velocities (0.95 to 2.84 cm s^{-1}) were most similar to those measured in the laboratory on the N diet. Sinking velocities also increased significantly with pseudofaeces size ($p = 0.011$, $r^2 = 0.49$; Table 2.5).

2.3.5 Biodeposit erosion

The erosion thresholds of faecal pellets produced by mussels of different size classes fed different diets were analysed by comparing the bed shear velocities (u_*) required to erode 10, 50 and 90 % of the pellets. These u_* were determined from logistic curves that describe the relationship between number of faecal pellets eroded and the bed shear stress ($r^2 = 0.98 – 1.00$). Three of the 9 data sets could not be modelled by a logistic curve because most of the biodeposits eroded simultaneously. In these cases a straight line was fitted to describe the erosion phase. Because pseudofaeces partly broke up during the measurements we compared the u_* required to expose 10, 50 and 90 % of the area initially covered by pseudofaeces. Because the erosion measurements were only performed once no statistical analysis was possible.

Faecal pellets and pseudofaeces produced on the A diet had lower erosion thresholds than those produced on the other two diets (Fig. 2.4). Ten percent of the faecal pellets produced on the A diet were eroded at a u_* of 0.17 cm s^{-1} and at 0.28 cm s^{-1} 90 % of these pellets were removed from the sediment. In comparison, the bed shear velocity required to erode faecal pellets produced on the N and S diets was about twice as high for 10 % (N diet: 0.36 cm s^{-1}, S diet: 0.32 cm s^{-1}) and 90 % erosion (N diet: 0.67 cm s^{-1}, S diet: 0.59 cm s^{-1}). Pseudofaeces generally eroded over a wider range of u_* and the differences between the three diets were less distinctive compared to faecal pellets. Ten percent of pseudofaeces produced on the A diet eroded at a u_* of 0.16 cm s^{-1} and those produced on the N and S diets at 0.30 cm s^{-1}. A u_* of 0.44 cm s^{-1} eroded 90 % of all pseudofaeces produced on the A diet whereas 0.57 cm s^{-1} was required to remove 90 % of all pseudofaeces produced on the other two diets. No consistent pattern was found in the bed shear

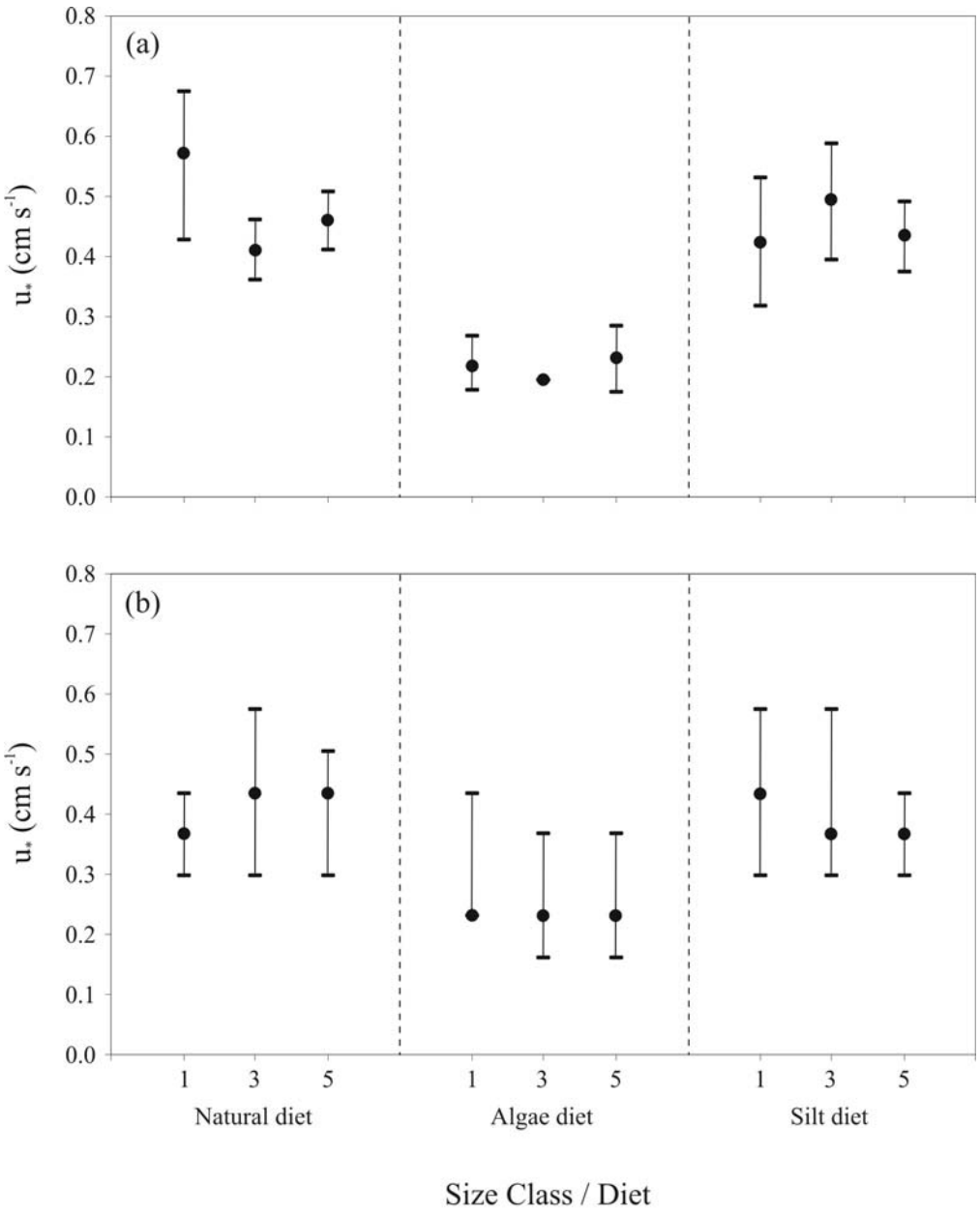

Figure 2.4. Bed shear velocities (u_*) required to erode 50 % (•) of (a) individual faecal pellets and (b) pseudofaeces area coverage produced by mussels of size class 1 (<40 mm), 3 (61 - 80 mm) and 5 (>100 mm) fed on the three experimental diets (N: natural, A: algae, S: silt). The position of the upper and lower bars (**‒**) represent the bed shear velocity required to erode 90 and 10 % of the biodeposits, respectively. In some instances the bars are covered by the 50 % marker.

velocities required to erode biodeposits produced by mussels of the three different size classes.

2.4 Discussion

2.4.1 Biodeposit sinking velocities and diet

Sinking velocities were significantly lower for faecal pellets produced on the A diet compared to pellets produced on the N or S diets due to the high proportion of low-density phytoplankton in the A diet. This was indicated by the dark green colour of these biodeposits as well as their high OC and chl *a* content. Because of the similar high inorganic content of the N and S diets faecal pellets produced on these diets had similar compositions, resulting in similar sinking velocities. Pseudofaeces generally settled slower than faecal pellets and rates varied significantly between all three diets. Sinking velocities were more variable for pseudofaeces than for faeces, which was most likely due to their more variable shape. Because the A diet was of very high quality mussels did not have to sort the filtered material before ingestion (Hawkins et al. 1999). Therefore, pseudofaeces contained a high proportion of phytoplankton, indicated by a high OC and chl *a* content, resulting in low sinking velocities. The S and N diets both contained heavy silt particles, but their concentration was about 5× higher in the S diet causing denser and heavier pseudofaeces with higher sinking rates. Pseudofaeces produced on the N diet had a lower OC compared to faeces due to the preingestive selection of filtered material (Ahn 1993, Rueda and Smaal 2002). In contrast, the OC of pseudofaeces produced on the S diet was slightly elevated, most possibly a result of the high amount of mucus required to package the silt particles (Owen 1966, Prins and Smaal 1989, Davies and Hawkins 1998).

Generally there was little difference in composition between faeces and pseudofaeces for the three diets and this probably reflects a high proportion of intestinal faeces relative to glandular faeces. At low seston concentrations all particles selected for ingestion are transported to the digestive gland and the unassimilated matter is rejected as glandular faeces (Widdows et al. 1979). When seston concentrations exceed the maximum digestible concentration the excess material bypasses the digestive gland, is transported through the gut undigested

and rejected as intestinal faeces. This sorting mechanism precedes the production of pseudofaeces and considering the large amounts of pseudofaeces produced it is very likely that faecal pellets collected in this study contained a high proportion of intestinal faeces.

The sinking velocities of *Perna canaliculus* biodeposits measured in this study (0.1 – 4.5 cm s^{-1}) fall within the range observed for other aquatic invertebrates. Biodeposit sinking velocities range from approximately 0.02 cm s^{-1} for copepod to 5.94 cm s^{-1} for polychaete faecal pellets (Wotton and Malmqvist 2001). This variation originates mainly from the differences in organism size and physiology between species, which obviously effects biodeposit size, as well as feeding habits. Aquatic animals living in the water column grazing primarily on algae (such as copepods) and benthic suspension-feeders are likely to produce less dense biodeposits compared to deposit feeders (such as polychaetes). Similar to this study lower sinking rates have been measured for biodeposits produced on diets with higher algae concentrations for the horse mussel *Atrina zelandica* (Miller et al. 2002) and the copepod *Acartia tonsa* (Butler and Dam 1994). Higher faecal pellet sinking velocities have been obtained for deposit feeders who are exposed to diets with high proportions of inorganic material (Taghon et al. 1984, Ladle et al. 1987).

No previous studies have examined settling characteristics of pseudofaeces, yet this may represent a significant fraction of the filtered material for suspension-feeding bivalves in coastal environments. *Perna canaliculus* produce pseudofaeces at SPM concentrations as low as 3 mg l^{-1} and at 40 mg l^{-1} the proportion of filtered material rejected as pseudofaeces is as high as 90 % (Hawkins et al. 1999). The results from this study showed that pseudofaeces have generally lower sinking velocities than faecal pellets. Pseudofaeces are therefore likely to disperse farther from their origin compared to faecal pellets and their impact on the sediment becomes diffused by being spread over a larger area. In addition, I observed that pseudofaeces were easily destroyed and in energetic coastal environments turbulence would promote the breakdown of pseudofaeces reducing their settling velocity and increasing mineralisation in the water column so that they may never reach the benthos. This could have been the reason why

during the first field measurements pseudofaeces were absent in the sediment traps which were placed approximately four metres below cultured mussels suspended in the water column. Once some of the material trapped by *P. canaliculus* is rejected as pseudofaeces, the ingestion and faeces production rates remain relatively constant with further increments in SPM concentration (Hawkins et al. 1999). Therefore, above a certain threshold increased SPM concentrations do not inevitably lead to increased sedimentation load. This functional response to high seston concentrations has been demonstrated for a several species, e.g. the blue mussel *Mytilus edulis* and the Eastern oyster *Crassostrea virginica* (Griffiths and Griffiths 1987). However, some bivalves, such as the hard clam *Mercenaria mercenaria*, show a different response (Tenore and Dunstan 1973) which has to be taken into account when making biodeposit dispersal estimates.

The results of this study demonstrate that changes in diet composition lead to variations in biodeposit sinking velocity and therefore influence the potential dispersal of biodeposits. The suspended particle concentration in coastal environments is influenced by a wide range of factors, such as storms, currents or seasonal conditions, creating tidal, seasonal and inter-annual fluctuations in the diet available to suspension-feeding bivalves (Berg and Newell 1987). The impact of mussel biodeposition on the benthos is dependent on the flux to the sediment (amount of biodeposits per unit area and unit time), which, in turn, is a function of production rate and dispersal characteristics as well as biodeposit quality. The biodeposit C:N ratios obtained in this study indicate their high nutritional value compared to sediments which generally have a C:N ratio of 10 or more (Parsons et al. 1977) and fall into the range of previously measured C:N ratios of suspension-feeding bivalves (e.g. Ahn 1993, Miller et al. 2002). Biodeposits produced on the A diet had the lowest C:N ratios, reflecting the high quality of the A diet. Aquaculture leases are preferentially located in highly productive areas to sustain growth and prevent phytoplankton depletion. Therefore, the diet of cultured mussels is likely to contain a higher proportion of chl *a* compared to mussels living in natural beds, which could result in higher quality biodeposits.

2.4.2 Predicting biodeposit sinking velocity

Larger mussels produced larger biodeposits and sinking velocity increased significantly with biodeposit size for faeces and pseudofaeces produced on all three diets. Faecal pellet width is solely determined by mussel morphology and hence mussel size. Mussels produce a string of faecal material which breaks into sections creating individual pellets (pers. obs.) whose length (and hence also area) depends on mussel orientation and ambient flow and is therefore very variable. The significant effect of mussel size class in the GLMs of biodeposit size and the strong relationship of biodeposit size and sinking velocity indicate that mussel size governs biodeposit dispersal. Bivalve populations are often dominated by few distinctive cohorts (Loo and Rosenberg 1989, Strasser et al. 1999, Cole et al. 2000, Witbaard and Bergman 2003) and if biodeposit dispersal is a function of animal size then biodeposit dispersal could vary considerably with population size structure.

Various efforts have been made to calculate sinking rates from faecal pellet size, density and seawater characteristics using the equations of Komar et al. (1981), Stoke's law and Newton's second law (Komar et al. 1981, Taghon et al. 1984, Ladle et al. 1987, Deibel 1990, Butler and Dam 1994, Yoon et al. 2001). All equations used to calculate sinking velocities are valid only for certain geometrical shapes (spherical, cylindrical, ellipsoidal, conical or rectangular) and chosen for the best approximation to the shape of the examined faecal pellets. Most comparisons of measured and calculated sinking rates showed inconsistencies, predominantly caused by inaccurate density estimates and/or the deviation of actual pellet shape to the shape assumed for the equation (Taghon et al. 1984, Deibel 1990, Yoon et al. 2001) and good agreements were only found by Komar et al. (1981) for copepod pellets. Since neither faecal pellets nor pseudofaeces produced by *Perna canaliculus* fit any of the shapes listed above, and no mathematical description exists of *P. canaliculus* biodeposit shape, I was not able to calculate sinking velocities. This demonstrates the importance of empirical relationships of biodeposit size and sinking velocity to estimate dispersal characteristics. However, according to Stoke's law and the equation of Komar, which is a semi-empirically derived version of Stokes' law, changes in faecal pellet width cause greater changes in the sinking velocity than changes in

faecal pellet length which is consistent with the strong correlation of faecal pellet width and sinking velocity I found.

2.4.3 Biodeposit erosion

This study provides a first order approximation of the bed shear velocities required to initiate the erosion of mussel biodeposits as a function of size and composition. Biodeposits produced on the A diet had lower erosion thresholds than those produced on the other two diets, most likely due to their lower density and potentially because of their smoother surface which reduces the friction between biodeposit and sediment. The similar composition of biodeposits produced on the N and S diets resulted in equal erosion thresholds. The range of bed shear stresses over which pseudofaeces eroded was much higher compared to faeces. The erodibility of particles can be affected by their exposure to the flow which is dependent on particle size, shape and orientation (Jumars and Nowell 1984). Pseudofaeces had a more variable shape compared to faecal pellets. Furthermore, pseudofaeces partly broke down during movement and at high flow speeds created an almost even layer on the sediment surface, hence reducing their exposure to the flow. No specific pattern was noticeable in the order in which the biodeposits produced by mussels of the three size classes eroded off the sediment cores. This was probably due to the trade-off between the higher bed shear velocity required to erode larger and hence heavier particles and the lower bed shear velocity sufficient to initiate the erosion of particles with greater exposure to the flow.

The biodeposit erosion thresholds I measured are similar to the few obtained in previous studies, all of which involved organisms feeding on natural diets. Faecal pellets produced by the deposit feeder *Hydrobia ulvae* were transported at a u_* of 0.10 to 0.44 cm s^{-1} (Austen et al. 1999, Andersen 2001) comparable to those required to erode faecal pellets produced on the algal diet (0.17-0.28 cm s^{-1}). Polychaete faecal pellets started to erode at a free stream velocity of 3 cm s^{-1} measured 5 cm above the sediment (z_5) and were completely transported at approximately 11 cm s^{-1} (Minoura and Osaka 1992). The width of these cylindrical pellets was approximately 0.35 mm, similar to faecal pellets produced by mussels of the smallest size class I examined. The flow at z_5 required to erode

90 % of faecal pellets of the smallest size class ranged from 7 (A diet) – 18 (N diet) cm s^{-1}. Widdows et al. (1998) showed that at current velocities of 20 cm s^{-1} ten centimetres above the bed (z_{10}) mussel (*Mytilus edulis*) pseudofaeces and faeces were resuspended. Because of the water depth in the flume and ADV configuration I could not directly measure flow velocities at this height, however, by extrapolation of the flow profile data an estimate could be obtained (flow velocity at z_{10} (cm s^{-1}) = 30.8 × u_* - 1.1, r^2 = 0.99). In this study the flow at z_{10} required to erode 90 % of all biodeposits produced on the N diet ranged between 12.3 – 19.6 cm s^{-1} which is very similar to the flow speed measured by Widdows et al. (1998).

The erosion thresholds obtained in this study should only be used as an approximation since they were measured under idealistic laboratory conditions with a smooth sediment surface devoid of macrofauna or other obstacles. In natural sediments faecal material reduces sediment stability (e.g. Andersen et al. 2002) but because in this study biodeposits were placed on top of the experimental sediments prior to the measurements this effect was not observed. Suspension-feeding bivalves alter their physical habitat, bed roughness and water flow over the seabed (Frechette et al. 1989, Green et al. 1998) through bioturbation, surface tracking and the production of faecal pellet mounds as well as by their own presence (Willows et al. 1998, Widdows et al. 2000, Andersen 2001, Andersen et al. 2002). Because of these factors comparisons of erosion thresholds measured in different environments should be done with care. To attain more realistic erosion thresholds in the laboratory intact sediment cores should be used to simulate the effect of bioturbating macrofauna and the presence of other animals and structures. Experimental set-ups should also consider realistic bottom topographies which significantly alter the flow dynamics above the sediment bed.

In this study I examined freshly egested biodeposits which have not been exposed to any further modification. However, biodeposits provide an important food supply for the benthos and may be eaten and hence repackaged by many marine animals (Johannes and Satomi 1966, Frankenberg and Smith 1967, Tenore and Dunstan 1973, Wotton et al. 1998) including the species that produced them (Newell 1965). Furthermore, biodeposits are mineralised rapidly with peak

activity in the first three days of degradation followed by a decline to initial levels after 8 – 30 d (Turner and Ferrante 1979, Stuart et al. 1982, Grenz et al. 1990, Fabiano et al. 1994). The significance of biodeposit modification is dependent on the composition of the benthos. Repackaging and ageing alters biodeposit density, composition and sinking rates (Gonzales and Biddanda 1990, Fabiano et al. 1994, Yoon et al. 1996) and would likely affect erosion thresholds. The implications of biodeposit modification by the benthos should therefore be examined to obtain a more comprehensive understanding of biodeposit redistribution.

2.4.4 Estimated dispersal distances of mussel biodeposits

Perna canaliculus naturally forms dense beds of up to 100 m^{-2} (Jeffs et al. 1999) which are predominantly found subtidally or in the low intertidal. In suspended cultures, mussels are attached to dropper lines hanging off floating longlines. To examine the spatial extent of biodeposit dispersal from mussel farms I calculated the approximate initial dispersal distance from the commercial farm described above as a function of biodeposit sinking velocity, water depth and current velocity. Based on the mean depth of the water underneath the dropper lines (6 m), the mean current velocity measured one metre above the sediment (12.8 cm s^{-1}) and the average sinking velocities of biodeposits produced on the N diet, the initial contact with the sediment would be 31 m (faecal pellets) and 62 m (pseudofaeces) away from the release point. Applying the lower sinking rates of biodeposits produced on the algae dominated diet resulted in initial dispersal distances of 124 m (faecal pellets) and 181 m (pseudofaeces). To estimate the significance of secondary dispersal via erosion at the farm I transformed the bed shear velocities measured in this study to equivalent flow speeds one metre above the sediment bed (Muschenheim et al. 1986). I found that over a range of 5.1 to 21.4 cm s^{-1} all biodeposits would be eroded. The mean current velocity at the mussel farm falls within this range and hence could initiate the erosion of a large fraction of the material. The observed maximum current speed of 33 cm s^{-1} would be strong enough to completely erode all material.

These estimates show that the initial dispersal of biodeposits from the farm is not far but that it could increase significantly during algae blooms. The initial dispersal of biodeposits from natural mussel beds would be lower since

biodeposits are released into the boundary layer and therefore only exposed to lower current velocities. Pseudofaeces initially disperse further than faeces due to their lower sinking velocities. Depending on the hydrodynamic conditions, secondary dispersal potentially plays a more important role in the dispersal of biodeposits from mussel farms than initial dispersal and almost certainly serves as the major means of transport of biodeposits from natural mussel beds. Because pseudofaeces partly break down during erosion they will most likely create a layer of organic material in the vicinity of their initial point of contact with the sediment.

I have shown that biodeposit dispersal depends on the available diet and mussel size and conclude that it could vary considerably as a function of site and environmental conditions. Further research should address the effects of biodeposit repackaging and age on dispersal characteristics. Due to the commonly shallow habitats of mussels and their fast biodeposit sinking rates age has probably only a minor effect on the initial dispersal, however, because of the high potential for redistribution and modification by the benthos it could significantly alter further dispersal.

Chapter 3

Effects of mussel (*Perna canaliculus*) biodeposit decomposition on benthic respiration and nutrient fluxes

3.1 Introduction

Suspension-feeding bivalves filter particles from the water column which are either bound in mucus and rejected as pseudofaeces, or ingested and ultimately defecated. Faeces and pseudofaeces have higher sinking velocities than their constituent particles and therefore increase sedimentation. Once reaching the seabed they are collectively called biodeposits. Biodeposits have a high nutritional value (Kautsky and Evans 1987, Chapter 2) and show high bacterial activity (Kaspar et al. 1985, Grenz et al. 1990). Biodeposition increases the flux of organic matter to the sediment and the remineralisation of biodeposits increases sediment oxygen demand and supplies regenerated nutrients to the overlying water. Furthermore biodeposition can alter denitrification (Newell et al. 2002, Christensen et al. 2003) and burial rates (Hatcher et al. 1994, Newell 2004) leading to the removal of nutrients from the water column. Due to the tight coupling between benthic and pelagic systems in nearshore ecosystems, these modified sediment fluxes can have significant impacts on the nutrient dynamics of the whole ecosystem and affect primary production (Tenore et al. 1982, Porter et al. 2004).

In addition to their often high natural abundance, bivalves are also cultivated on longlines or racks in the upper water column, and biodeposition from these dense aggregations can affect sediment texture, chemistry and benthic community composition (Dahlbaeck and Gunnarsson 1981, Kaspar et al. 1985, Mirto et al. 2000, Norkko et al. 2001). Several numerical models have been developed to describe energy flow in coastal food webs where bivalve culture is important (e.g. Bacher et al. 1995, Chapelle et al. 2000, Dowd 2005). These models focus on bivalve growth and food supply but there is a need for a more accurate

representation of the effects of biodeposition on sediment nutrient fluxes and habitat degradation since these processes can influence ecosystem productivity (Henderson et al. 2001). In the few models that describe the benthic remineralisation of biodeposits and consequently sediment oxygen demand and nutrient release (Bacher et al. 1995, Chapelle et al. 2000, Dowd 2005) no distinction is made between biodeposits and other organic particles. For example, Chapelle et al. (2000) and Bacher et al. (1995) used published decay rates derived for sediments without additional organic input. Models that do not account for different sources of organic detritus by considering different decay rates may poorly predict sediment oxygen demand and nutrient release in areas affected by biodeposition.

Previous studies have conducted *in situ* and laboratory measurements to examine oxygen and nutrient fluxes beneath bivalve cultures (e.g. Kaspar et al. 1985, Hatcher et al. 1994, Christensen et al. 2003) and in all instances benthic respiration and ammonium release in these sediments were elevated compared to reference sites. Some studies have examined the biochemical and bacterial variation of incubated biodeposits in sediments or seawater (Stuart et al. 1982, Grenz et al. 1990, Fabiano et al. 1994) but did not provide decay rates. The only three publications of faecal pellet decay rates I could find were for the periwinkle *Littorina littorea* (Hargrave 1976) and for copepod faecal pellets decomposing in seawater (Hansen et al. 1996, Urban-Rich 1999). These decay rates are higher compared to those obtained by incubating sediment cores with and without additions of phytoplankton (e.g. Kristensen and Blackburn 1987, Sun et al. 1993, Kristensen and Holmer 2001) and suggest that not using specific decay rates will lead to an underestimation of benthic oxygen and nutrient fluxes following biodeposit sedimentation.

The objective of this study was to assess and quantify sediment biogeochemical changes as bivalve biodeposits age and to calculate biodeposit decay rates in sediments. I incubated coastal sediments to which I added fresh *Perna canaliculus* biodeposits and tracked changes in oxygen and nutrient fluxes as well as sediment characteristics during an 11 d period. The green-lipped mussel *P. canaliculus* is endemic to New Zealand and was chosen for this study because of its high natural

abundance (Morton and Miller 1973) and its intensive cultivation (Jeffs et al. 1999). Our experimental approach allowed us to estimate biodeposit decay rates that will help improve models of sediment biogeochemistry leading to better assessments of the impacts of bivalve aquaculture and the contribution of natural bivalve beds to nutrient cycling in coastal ecosystems.

3.2 Materials and methods

3.2.1 Core collection and incubation

Sixteen sediment cores were collected by SCUBA from a 13 m deep site (T = 20°C, S = 34 PSU) in the Firth of Thames, New Zealand (175°18' E, 36°59' S), a large shallow coastal embayment. This site is situated about one km from a commercial mussel farm and is not affected by any debris originating from the farm. The cores (ID = 9.5 cm, area = 71 cm^2, height = 30 cm) were inserted into the sediment to a depth of 12 cm retaining about 1.1 l of water overlying the sediment (3/5 of total volume) and sealed with o-ring fitted lids. The cores were removed from the sediment without disturbing the sediment-water interface, placed on ice in the dark and carefully transported to the laboratory. Upon arrival (~3 h after collection) they were immediately connected to a recirculating continuous flow system. At this stage two cores were discarded because the sediment had collapsed due to large burrows.

Incubations were set up in a constant temperature room at 20°C, the same as the water temperature at the collection site. Magnetically driven stirring bars fitted to the inside of the lids mixed the water in the sealed cores at a speed of 60 – 70 rpm that ensured that the sediment was not resuspended. Water was circulated from the cores to a 200 l aerated and stirred reservoir tank containing artificial seawater (S = 31.3 ± 1.0 PSU) and back again using peristaltic pumps that drew water through an outlet hose out of the top of the cores with a flow rate of ~12 ml min^{-1}. The water was replaced through an inlet hose at mid water height. A dye test confirmed that this procedure ensured a well-mixed water column in the cores. To avoid a build-up of nutrients in the reservoir tank an activated biological filter was installed. The filter volume was 0.018 m^3 and comprised of aged broken shell material that was activated in a stocked marine aquarium for 60 d. In addition, 10

% of the reservoir water was replaced daily with fresh artificial seawater. Incubations were kept in the dark to exclude activity from microphytobenthos that can absorb inorganic nitrogen released from the biodeposits and therefore limit nutrient release to the water column (Newell et al. 2002, Lohrer et al. 2004).

The cores were allowed to stabilise for 7 d in this recirculating continuous flow system before the addition of biodeposits on d 0. On d -2 and d -1 oxygen and nutrient fluxes were measured in all cores to ensure pre-treatment similarities. Two of the cores had irregular oxygen and nutrient fluxes most probably due to large burrows and together with another two randomly selected cores were disconnected from the peristaltic pumps on d 0 to determine the initial sediment characteristics (I-cores). Each core was sub-sampled with 3 ID = 2.8 cm syringe cores of which one was immediately sectioned at 0 – 0.2, 0.2 – 0.5, 0.5 – 1 cm then 1 cm intervals to 5 cm and analysed for porosity, water and organic matter (OM) content. The remaining syringe cores were frozen and analysed later for sediment grain size, chlorophyll *a* (chl *a*), phaeophytin (phaeo), organic carbon (OC) and total nitrogen (N) concentrations. Sediment remaining in the cores was sieved (0.5 mm) and the macrofauna preserved in 80 % isopropyl alcohol. Of the remaining ten cores five were randomly selected for biodeposit addition (B-cores) by inverting one biodeposit storage container into the overlying water allowing the biodeposits to settle onto the sediment surface. The remaining five cores served as controls (C-cores) and did not receive any biodeposit additions. After 1 h the cores were reconnected to the peristaltic pumps and 5 h later oxygen and nutrient fluxes were determined in all ten cores. These flux measurements were repeated daily until d 2 and on alternate days thereafter until d 10. At the end of the experiment three syringe cores were taken from each core and sectioned as described above.

3.2.2 Biodeposit production

Rope-cultured *Perna canaliculus* (80 – 100 mm shell length) were collected by SCUBA from the mussel farm. Mussels were scraped clear of epibionts, transported to the laboratory and allowed to acclimatise to laboratory conditions for 4 d in an aerated recirculating sea water system at 17 ± 2°C on a 12 h light :12 h dark cycle. Light was supplied by fluorescent tubes with an intensity of 400

µmol m^{-2} s^{-1}. During this time no food was added to the system and mussels completely emptied their guts. After the acclimatisation period 16 mussels were distributed among eight flow-through feeding chambers (length = 15.5 cm, width = 13 cm, vol. = 1.4 l, flow rate = 200 ml min^{-1}). They were fed natural seawater (suspended particulate material [SPM] = 100 ± 8 mg l^{-1}, OM = 11.7 ± 0.9 %, chl *a* = 2.8 ± 0.9 µg l^{-1}, phaeo = 2.6 ± 1.1 µg l^{-1} [± SD, n = 3]) freshly collected from Raglan Harbour (174°57' E, 37°48' S). The mussels were placed in the feeding chambers for 10 h on two consecutive days, in between they were returned to the recirculating seawater system. Biodeposits were collected approximately every 2 h from each feeding chamber and randomly assigned to one of nine storage containers which were kept on ice in the dark. I ensured that by the end of the second 10 h feeding period each container had received an equal quantity of biodeposits. Biodeposits from five of the storage containers were added to the B-cores and the remainder were analysed for chl *a*, phaeo, OM, OC and N content. The mean (± SD) amount of biodeposits in these four containers was 2.35 ± 0.37 g dry wt.

3.2.3 Flux measurements

Fluxes across the sediment-water interface were determined by sealing off the cores and measuring the concentration changes in the overlying water during a 5.5 – 8.5 h incubation period. Water samples (50 ml) for nutrient analysis (NH_4^+, NO_3^-, NO_2^-, PO_4^{3-}) were taken at the beginning and the end of the incubation with a syringe from a three-way valve attached to the outlet hose of each core. While a sample was being taken, the stirrer was temporally turned off (< 1 min) and the inlet hose opened so that the sample volume was replaced with reservoir water. Samples were immediately filtered (Whatman GF/C) and frozen for later analysis on a Lachat CQ8000 FIA system. Oxygen saturation in the cores was measured at the beginning and approximately every hour thereafter with a PreSens Microx I oxygen meter and a fiber-optic oxygen probe through taps in the core lids to obtain a total of five measurements over the incubation period. The oxygen concentration in the seawater of all cores at the beginning of the incubations was 97.6 ± 2.5 % saturation. Once the oxygen saturation had decreased by 15 – 20 % the second nutrient sample was taken and the cores were reconnected to the peristaltic pumps. Sediment oxygen consumption (SOC) was calculated by linear

regression of concentration with time after accounting for slight differences in the volume of water in each core. Nutrient fluxes were calculated in a similar way assuming a linear decline from the initial to the final concentration.

The NH_4^+ and PO_4^{3-} concentrations in the reservoir tank showed no variation over time and ranged from below detection limit to 0.0173 mg l^{-1} and 0.0026 to 0.0090 mg l^{-1}, respectively, which were lower than bottom water concentration measured *in situ* at the site where the cores were collected (Giles unpublished data). NO_3^- concentrations measured in the reservoir tank until d 4 were also lower than those measured *in situ* (<0.0068 mg l^{-1}), however, they increased from d 6 onward and reached 0.0334 mg l^{-1} by d 10.

3.2.4 Sediment and biodeposit analyses

Chl *a* and phaeo content of sediment and biodeposit samples were determined by extracting freeze-dried material in 90 % acetone and measuring fluorescence before and after acidification on a Turner Designs 10-AU Fluorometer (Arar and Collins 1997). Water content, porosity and OM were determined from dried and ashed sediment samples and corrected for salinity. Carbonate carbon was removed from samples by acidification with sulphurous acid (Verardo et al. 1990) before OC measurements and OC and N analyses were done using a Europa Scientific 20/20 isotope analyser. Sediment grain-size was measured with a Malvern Mastersizer-S after preparing the samples with 10 % hydrogen peroxide in water (v/v) to remove organic matter, and with calgon to disperse the particles and remove the >1 mm fraction (Singer et al. 1988).

3.2.5 Statistical analysis

I expected differences in sediment characteristics among treatments, i.e. B-, C- and I-cores, to occur primarily in the top sediment layers due to the addition of biodeposits to the sediment surface. Hence I conducted a one-way ANOVA (α = 0.05) for each sediment depth layer and all measured sediment characteristics. Post-hoc Tukey tests were used where differences among treatments were significant. The assumptions of homogeneity of variances and normality were confirmed using Levene and Kolmogorov-Smirnov tests. To examine SOC and nutrient fluxes in the B- and C-cores I conducted repeated measures ANOVA

analyses ($\alpha = 0.05$) with day of the experiment as repeated measures factor and core type as between-groups factor. I expected differences between treatments to commence only after biodeposit addition and differences among consecutive days only in the B-cores while biodeposits were decomposing. Therefore I conducted planned comparisons of the least squares means (contrast analysis). This allows the analysis of these more specific hypotheses than simple post-hoc analysis of main effects or interactions. All statistical analyses were conducted using Statistica 6.

3.3 Results

3.3.1 Biodeposit and sediment characteristics

Sediment water content and porosity did not differ significantly among the I-cores on d 0 and the B- and C-cores on d 10 (one-way ANOVA, $p > 0.355$). Water content ranged from 67.4 to 71.2 % in the top 1 cm and 62.9 to 68.0 % in the 1 – 5 cm interval. Porosity in these two intervals was 0.86 to 0.88 and 0.83 to 0.86, respectively. The >1 mm grain size fraction made up 2.9 – 8.5 % of the sediment dry weight and consisted primarily of broken shell material. The remaining sediment was very fine to fine silt with a median grain size of 3.1 to 8.5 µm. No consistent variation with depth or between treatments was observed. Macrofauna consisted of bivalves, polychaetes, oligochaetes, decapods and echinoids but were found only in low abundance (total ≤ 5 per core). Mean biomass in the B- and C-cores was similar (0.31 ± 0.23 and 0.52 ± 0.51 g dw m^{-2} respectively) but not surprisingly was higher in the I-cores (5.96 ± 3.94 dw g m^{-2}) because a few large individuals were present.

The amount of biodeposits added to each B-core was 2.35 ± 0.37 g dw (mean ± SD, n = 4) or 331 ± 52 g dw m^{-2}. Biodeposits had higher chl *a*, phaeo, OM, OC and N contents and a lower OC:N ratio compared to the sediments (Table 3.1). After 10 d incubation, the highest chl *a*, phaeo, OM, OC, N contents and molar OC:N ratio in the B-cores were found in the surface (0 – 0.2 cm) sediment layer (Fig. 1). These parameters were 5 to 38 % higher compared to the I-cores, i.e. the pre-treatment values, although the difference was only significant for OM (Tukey post-hoc test, $p = 0.006$). As expected, after 10 d incubation the chl *a*, phaeo, OC

and N contents in the 0 – 0.2 cm interval of the C-cores were 2 – 15 % lower compared to the I-cores. The OM content was elevated by 17 %, however, this difference was non-significant (p = 0.078). The differences between treatments were non-significant for all other parameters in all depth layers (one-way ANOVA, p > 0.086).

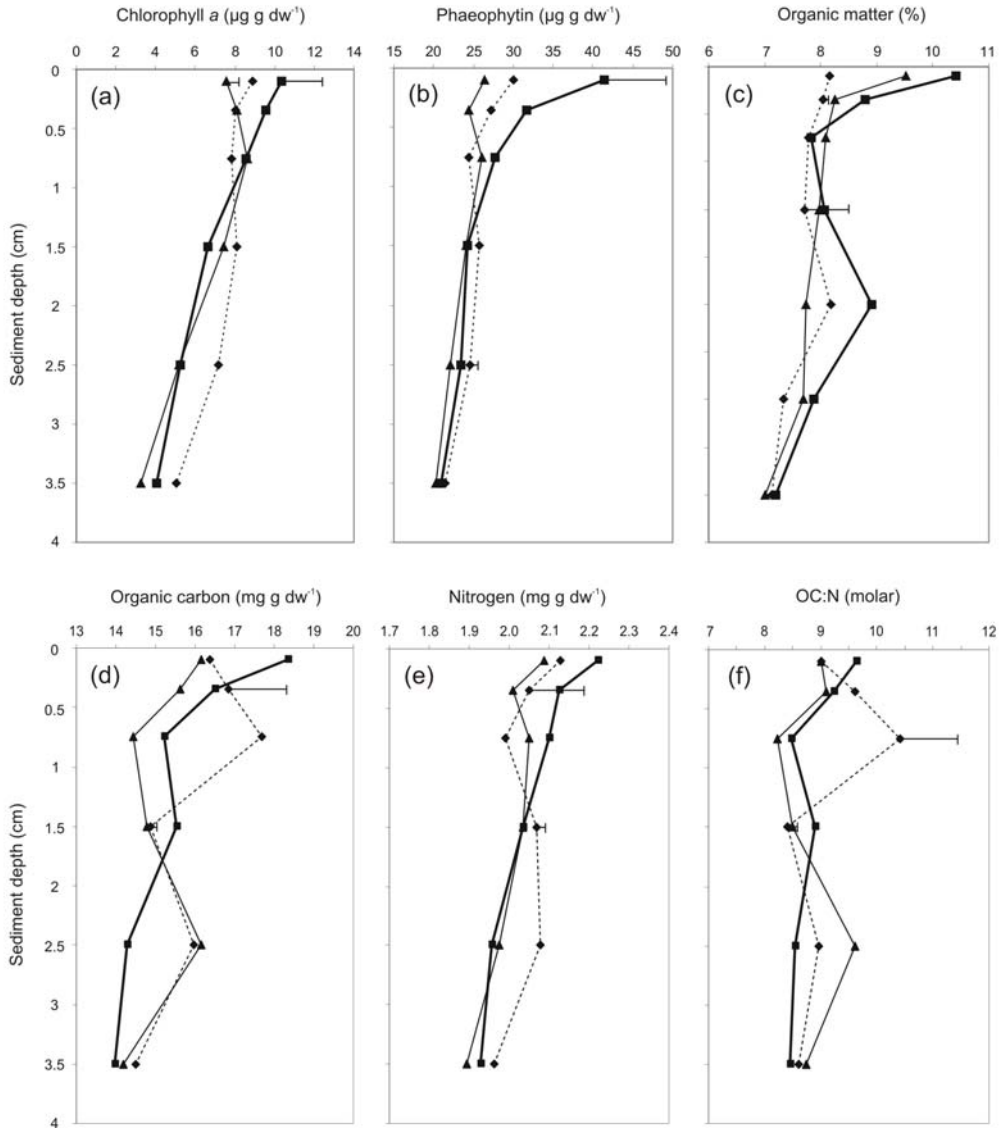

Figure 3.1. Depth distribution of (a) chlorophyll *a*, (b) phaeophytin, (c) organic matter, (d) organic carbon, (e) nitrogen and (f) organic carbon : nitrogen ratio in sediments from biodeposit (—■—) and control (—▲—) cores on d 10 and initial sediment characteristics (···◆···) cores on d 0. Data represent the means from the biodeposit and control (n = 5) and initial sediment characteristics cores (n = 4) in the 0 – 0.2, 0.2 – 0.5, 0.5 – 1, 1 – 2, 2 – 3 and 3 – 4 depth intervals. Error bars indicate the lowest and highest standard errors of all means.

Table 3.1. Biodeposit and pre-treatment surface sediment (I-cores, 0 – 0.2 cm) characteristics. Data represent the means and standard deviations in parentheses (n = 4).

	Biodeposits	I-cores (0-2 cm)
Organic matter (%)	10.3 (0.3)	8.2 (0.6)
Chlorophyll *a* (µg g dw^{-1})	29.9 (2.3)	8.9 (3.0)
Phaeophytin (µg g dw^{-1})	91.0 (8.0)	30.0 (9.6)
Organic carbon (mg g dw^{-1})	25.0 (0.1)	16.4 (2.5)
Nitrogen (mg g dw^{-1})	3.4 (0.03)	2.1 (0.2)
Organic carbon : nitrogen (molar)	8.6 (0.1)	9.0 (1.3)

3.3.2 Sediment oxygen consumption

The repeated measures ANOVA of SOC indicated significant effects of time ($p < 0.001$) and treatment ($p = 0.049$) as well as a significant interaction term for these two main effects ($p = 0.005$). On d -2 and d -1 SOC in the B- and C-cores ranged from 612 to 708 µmol m^{-2} h^{-1} and did not differ significantly between the treatments (planned comparisons, $p > 0.661$), indicating pre-treatment similarity in the cores (Fig. 3.2). After biodeposit addition the mean SOC rate in the B-cores increased significantly ($p = 0.016$) from 708 µmol m^{-2} h^{-1} on d -1 to a maximum of 1010 µmol m^{-2} h^{-1} on d 0. SOC decreased significantly ($p < 0.024$) during the following two days and after a slight increase on d 4 and d 6, declined to 640 µmol m^{-2} h^{-1} by d 10. In the C-cores SOC did not show any consistent pattern during the incubation period and ranged from 535 to 697 µmol m^{-2} h^{-1}. Differences were significant only between d 0 and d 1, and d 6 and d 8 ($p = 0.048$ and 0.001). After biodeposit addition SOC was always higher in the B-cores compared to the C-cores and differences were significant on d 0 to d 2 and again on d 6 ($p < 0.027$).

SOC rates of C-core 1 were unusually high from d -2 to d 0 (Fig. 3.2). At the beginning of the incubation on d 8 the oxygen saturation in this core was only 18 % and therefore the core was disconnected from the recirculating continuous flow system. Macrofauna analysis revealed a large crab in this core which would have

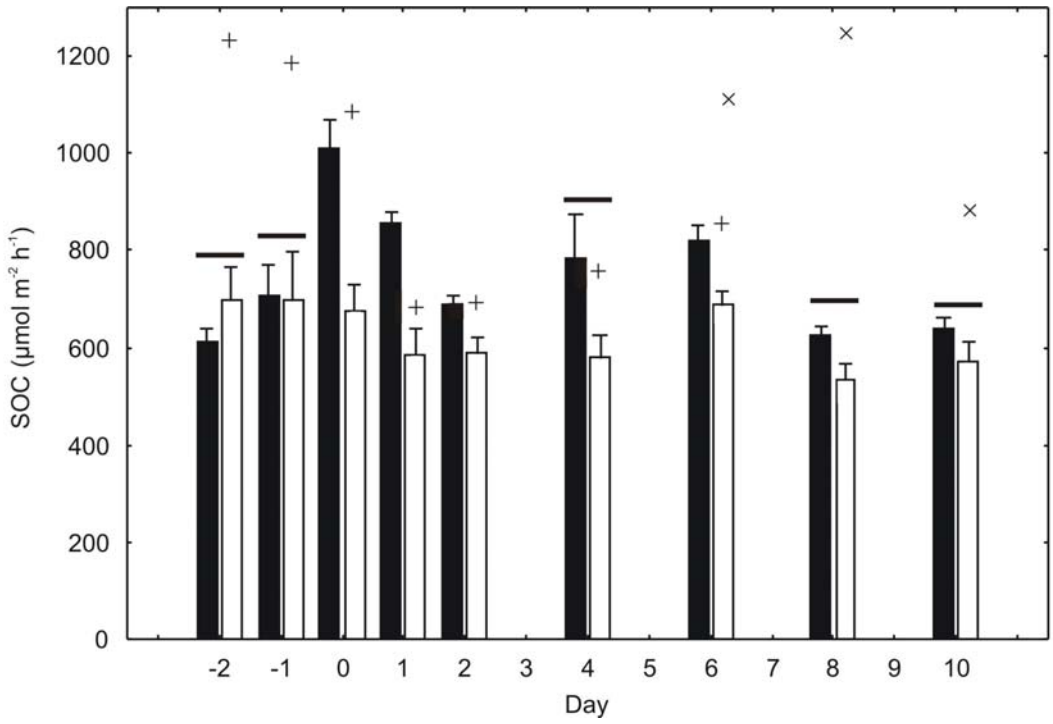

Figure 3.2. Sediment oxygen consumption (SOC) rates in biodeposit (black) and control (white) cores. Rates are given as mean +SE of 3 – 5 replicate cores. Crosses indicate measurements from control cores 1 (+, d -2 to d 6) and 4 (×, d 6 to d 8) that were excluded from the statistical analysis (see text for details). Horizontal lines above columns indicate that there was no significant difference between SOC in the biodeposit and control cores on those days (planned comparisons following repeated measures ANOVA, $p > 0.05$).

increased the biological activity and therefore caused the high SOC. For this reason I excluded C-core 1 from the statistical analysis. The SOC rates of C-core 4 were within the range of the other C-cores until d 4. From d 6 onwards they were very high and were excluded from the statistical analysis. This core contained one polychaete and two oligochaetes which may have died during the experiment and commenced to decompose prior to the measurements on d 6.

To examine the impact of the added biodeposits on SOC I subtracted the mean SOC measured in the C-cores from that of the B-cores (SOC_{B-C}). This difference was assumed to approximate the metabolism of the communities of microorganisms involved in the decomposition of the added biodeposits (see Discussion). The same approach was taken by Enokssen (1993) and Kristensen and Holmer (2001) to examine the difference in oxygen fluxes due to the addition

of plant material to incubation cores. The change of SOC_{B-C} over time (Fig. 3.3) suggests a first-order decomposition reaction of the biodeposits and to quantify this process I fitted a first-order G model using least squares estimation (Westrich and Berner 1984). Because of the constantly high oxygen saturation in the cores, the moderate amount of biodeposits added and the oxygenated surface layer of the sediments I assumed that decomposition was mainly mediated by aerobic microbial processes (i.e. $CH_2O + O_2 \rightarrow CO_2 + H_2O$; Chapelle et al., 2000). In this situation the first-order G model can be expressed as $SOC_{B-C}(t) = SOC_{B-C_0} e^{-k\,t}$ (Westrich and Berner 1984) where k is the first-order decay rate of organic matter in the biodeposits. The model fit ($SOC_{B-C}(t) = 297.5 e^{-0.16t}$) was significant (p = 0.001) and explained 72 % of

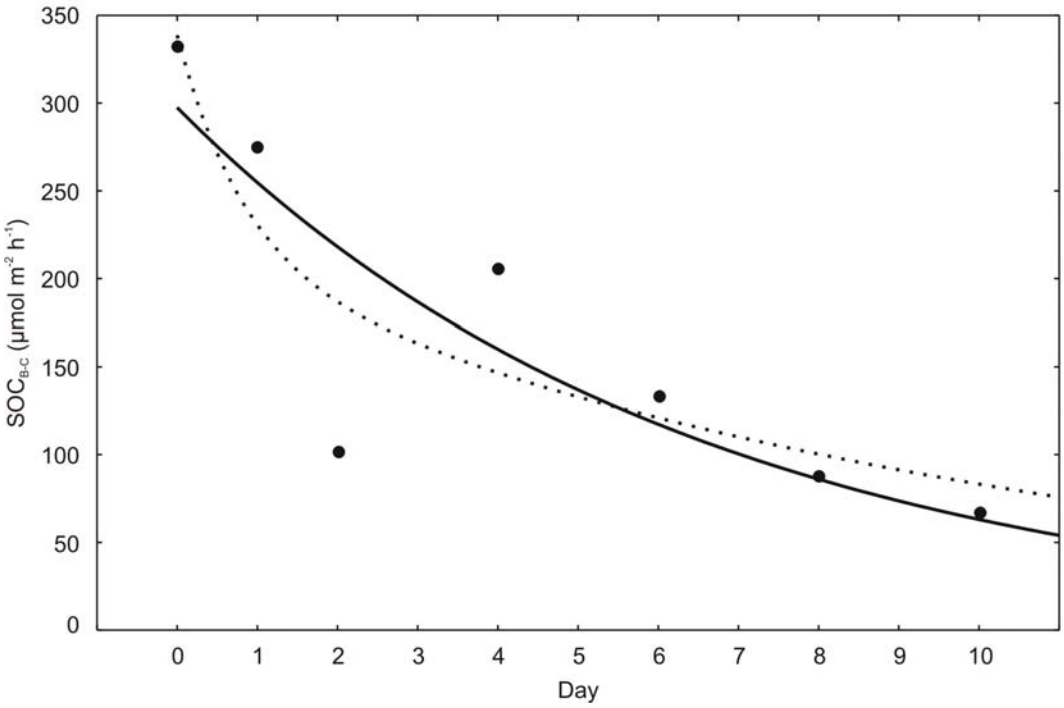

Figure 3.3. Changes in the difference between mean sediment oxygen consumption in B-cores and C-cores (SOC_{B-C}) during the 11 d experiment. The solid line represents the fit of a first-order G model ($SOC_{B-C}(t) = 297.5 e^{-0.16t}$, p = 0.001, $r^2 = 0.72$) and the dashed line that of a 2-G model ($SOC_{B-C}(t) = 211.6\, e^{-0.09\,t} + 127.1\, e^{-1.21\,t}$, p = 0.0266, $r^2 = 0.78$).

the variation in the data. Both fitted parameters were significant (SOC_{B-C_0} : p = 0.001, k: p = 0.033) and standard errors were 44.9 for SOC_{B-C_0} and 0.05 for k. The decay rate of 0.16 d^{-1} corresponds to a half-life time of 4.3 d for the degrading material.

SOC_{B-C} was unusually low on d 2 (Fig. 3.3). Oxygen consumption was consistently low in all B-cores and because the C-cores showed no abnormalities on this day I do not think that d 2 was an outlier, but is perhaps indicative of a more complex decomposition process than simple first-order decay. Decomposition occurs in two stages if the decomposing material consists of a rapidly and a slowly decomposing fraction (Westrich and Berner 1984). To examine if the low rates on d 2 indicate a two stage decomposition of the added biodeposits I fitted a two-G model (Westrich and Berner 1984) of the form $SOC_{B-C}(t) = SOC_{B-C_{01}} e^{-k_1 t} + SOC_{B-C_{02}} e^{-k_2 t}$. The model fit ($SOC_{B-C}(t) = 211.6 e^{-0.09 t} + 127.1 e^{-1.21 t}$) was significant (p = 0.027) and explained 78 % of the data, however, the individual parameters were non-significant (p = 0.35 to 0.75). The decay rates were 1.21 d^{-1} for the rapidly decomposing and 0.09 d^{-1} for the slowly decomposing fraction. These rates correspond to half-life times of 0.57 d and 7.4 d, respectively.

3.3.3 Nutrient fluxes

NH_4^+ fluxes varied significantly with time (repeated measures ANOVA, p < 0.001) and treatment (p = 0.027) but the interaction term was non significant (p = 0.054). On d -2 and d -1 NH_4^+ fluxes from the sediments in the B- and C-cores were not significantly different (planned comparisons, p > 0.111) demonstrating pre-treatment similarity (Fig. 3.4a). In the B-cores, NH_4^+ release was low before biodeposit addition (22.8 and 25.3 µmol m^{-2} h^{-1}), increased significantly (p = 0.013) from d -1 to d 0 and then continued to increase until reaching a maximum of 143.8 µmol m^{-2} h^{-1} on d 4. From d 4 to d 10 the fluxes in the B-cores gradually decreased (non-significant, p > 0.165). NH_4^+ fluxes in the C-cores remained relatively constant from d -2 to d 4 (-11.2 to 40.0 µmol m^{-2} h^{-1}) but started to increase on d 6 to a maximum of 78.8 µmol m^{-2} h^{-1} on d 8 (non-significant, p > 0.530). After biodeposit addition NH_4^+ release rates from the sediments in the B-

Figure 3.4. Sediment (a) ammonium (NH_4^+), (b) nitrate (NO_3^-) and (c) phosphate (PO_4^{3-}) fluxes (positive = flux from sediment to water column) and (d) N:P molar ratios of fluxes in biodeposit (black) and control (white) cores. Rates are given as mean +SE of 3 – 5 replicate cores. Crosses indicate measurements from control cores 1 (+, d -2 to d 6) and 4 (×, d 6 to d 8) that were excluded from the statistical analysis. Horizontal lines above columns indicate that there was no significant difference between the flux in the biodeposit and control cores on those days (planned comparisons following repeated measures ANOVA, $p > 0.05$). N:P ratios are given as mean $(NH_4^+ + NO_3^-)/PO_4^{3-}$ flux +SE of 3 – 5 replicate cores.

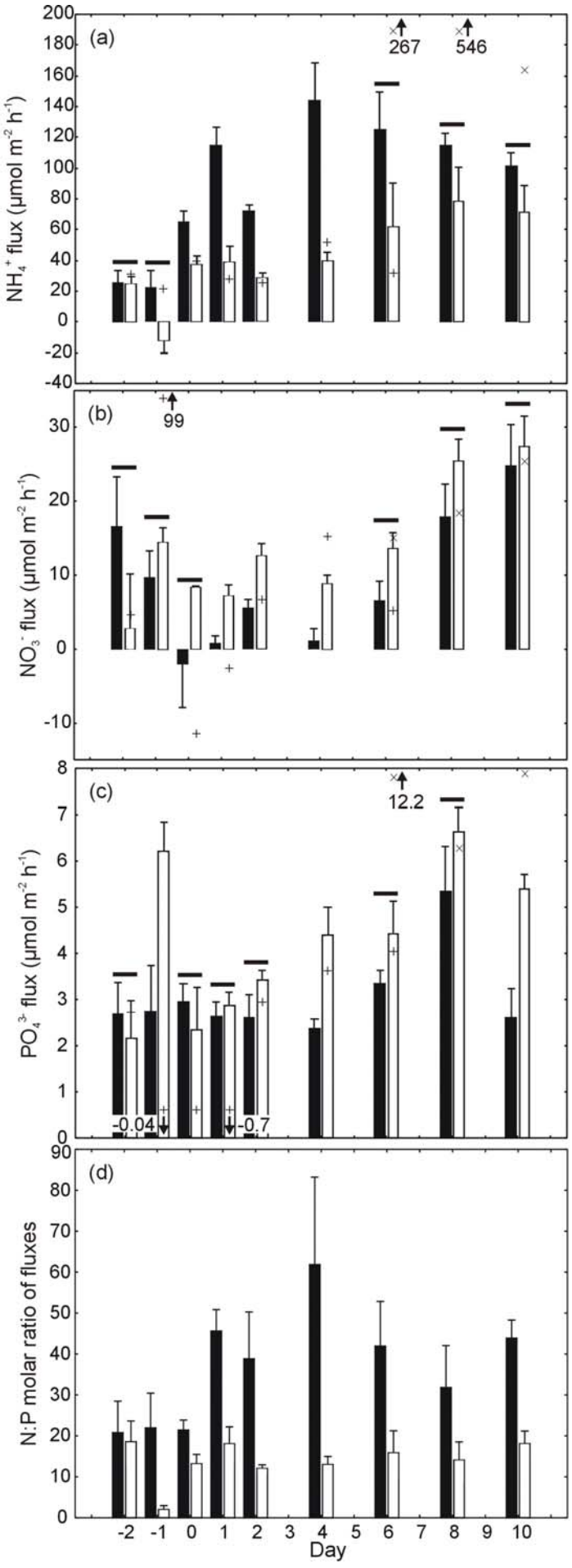
(a)
267
546
NH_4^+ flux (µmol m^{-2} h^{-1})
(b)
99
NO_3^- flux (µmol m^{-2} h^{-1})
(c)
12.2
-0.04
-0.7
PO_4^{3-} flux (µmol m^{-2} h^{-1})
(d)
N:P molar ratio of fluxes
Day

cores were always higher compared to the C-cores and these differences were significant ($p < 0.001$ to 0.043) from d 0 to d 4.

For NO_3^- and PO_4^{3-} flux only time was a significant factor (repeated measures ANOVA, $p = 0.007$ and 0.027). NO_3^- fluxes showed a complex pattern in both the B- and C-cores (Fig. 3.4b) and all differences between consecutive days within a treatment were non-significant (planned comparisons, $p > 0.089$). Differences between treatments were significant only on d 4 (planned comparisons, $p = 0.027$). During d -2 and d -1 fluxes ranged from 2.7 to 16.6 µmol m^{-2} h^{-1}. On d 0 the mean NO_3^- flux in the B-cores was directed into the sediment (-2.1 µmol m^{-2} h^{-1}) but reverted to a release on all following days. The NO_3^- release increased from 0.8 µmol m^{-2} h^{-1} on d 1 to 5.5 µmol m^{-2} h^{-1} on d 2 and from 1.1 µmol m^{-2} h^{-1} on d 4 to 24.7 µmol m^{-2} h^{-1} on d 10. After d -2, NO_3^- fluxes in the C-cores were consistently higher compared to those in the B-cores and increased gradually from d 4 onwards to 27.5 µmol m^{-2} h^{-1} on d 10. In almost all samples the NO_2^- concentration was below detection limit (0.001 mg l^{-1}) and accordingly NO_2^- data have not been presented.

PO_4^{3-} release rates did not indicate any response to the biodeposit addition in the B-cores and seemed to vary haphazardly in the C-cores (Fig. 3.4c). Fluxes in the B-cores varied only marginally between d -2 to d 4 and d 10 (2.4 to 3.0 µmol m^{-2} h^{-1}) with slightly higher rates on d 6 and d 8 (3.3 and 5.4 µmol m^{-2} h^{-1}). PO_4^{3-} fluxes in the C-cores were significantly (planned comparisons, $p < 0.014$) higher than those in the B-cores on d -1 and d 4. This confirmed the lack of a consistent pattern. The fluxes ranged from 2.2 to 6.6 µmol m^{-2} h^{-1}, and with the exception of d -2 and d 0, were higher compared to fluxes in the B-cores. The only significant time differences in both the B- and C-cores were the changes between d 4 and d 6 ($p < 0.047$).

The molar N:P ratios in the sediment-water fluxes were calculated as (NH_4^+ flux + NO_3^- flux)/PO_4^{3-} flux (Fig. 3.4d). Before biodeposit addition to the B-cores the N:P flux ratios were very similar in the B- and C-cores, except for the very low ratio in the C-cores on d -1 which was caused by a flux of NH_4^+ into the sediment and a high PO_4^{3-} release on this day. The N:P flux ratio in the C-cores remained

close to the ratio observed on d -2 over the 13 d incubation period with an average of 13.9 (SE = 1.7). The mean N:P flux ratio in the B-cores on d -2 to d 0 was 21.4 (SE = 0.3) but increased on d 1 to 45.6. It remained elevated for the rest of the incubation period. The mean N:P flux ratio after biodeposit addition was 40.8 (SE = 4.7).

3.4 Discussion

3.4.1 Sediment and biodeposit characteristics

The 331 g dw m^{-2} of biodeposits added to the B cores is equivalent to ~3 d of the additional deposition under the mussel farm from which the mussels were collected (106 g dw m^{-2} d^{-1}) compared to a nearby reference site (Chapter 4). If I assume that this additional deposition is made up of biodeposits and apply the first-order biodeposit decay rate I obtain an approximate stable biodeposit concentration in the sediments under the mussel farm of 628 g dw m^{-2}, about twice at much as I added to the B-cores. Hatcher et al. (1994) observed enhanced sedimentation rates under a mussel farm of 52.3 g dw m^{-2} d^{-1} and biodeposit deposition from farms has been estimated as 151.4 g dw m^{-2} d^{-1} (Dankers and Zuidema 1995) and 252.5 g dw m^{-2} d^{-1} (Jaramillo et al. 1992), indicating that the sedimentation rates measured under the farm of this study are within the range of those measured at other mussel culture sites. The material accumulating under the farm will be the less reactive fraction of the total deposited material. Therefore, I consider the amount of biodeposits added to the B-cores representative of the amount of labile biodeposits available to the benthos underneath a mussel farm.

The added biodeposits could be traced in the B-cores through elevated chl *a*, phaeo, OM, OC and N concentrations in the top 0.2 cm sediment layer compared to the C- and I-cores. Sediment characteristics of the B- and C-cores were measured only at the end of the experiment and therefore a large fraction of the biodeposits would have already been remineralised. This probably explains why the concentrations in the B-cores were elevated as expected but not significantly different to the other treatments.

In our study, mussels had only a limited acclimatisation period to the diet before biodeposit production. This may have influenced their chemical composition. However, as far as I could tell the composition of biodeposits is consistent with previously published studies for *Perna canaliculus* feeding on natural seston (Hawkins et al. 1999, Giles and Pilditch 2004). Moreover, the seston concentration and composition used to produce the biodeposits was representative of conditions at the mussel collection site (Giles unpublished data). Therefore, the proportion of faeces to pseudofaeces in the biodeposits should be similar to that produced *in situ*.

3.4.2 SOC and decay rates

Immediately after biodeposit addition to the B-cores, SOC was increased by ~1.5×, which is in the range of observed *in situ* SOC rate enhancements of 1.2 – 3× under mussel farms compared to reference sites (Grant et al. 1995, Mazouni et al. 1996, Christensen et al. 2003). An immediate SOC increase is a common response to the addition of OM (Kelly and Nixon 1984, Enoksson 1993, Kristensen and Holmer 2001) and is associated with the increase in electron transport system activity of benthic microorganisms (Graf et al. 1982). Following the rapid increase, SOC slowly declined to initial levels because the decomposing biodeposits were becoming limiting. Enhanced microbial activity associated with mussel faeces and pseudofaeces in sediments has been found under mussel lines (Grant et al. 1995). In a study of sediments enriched with mussel biodeposits this response had a duration of about 10 d (Grenz et al. 1990) which is very similar to the timeframe observed in this study.

No previous studies have compared degradation rates of pseudofaeces and faeces. Pseudofaeces are fragile and break up easily (Giles and Pilditch 2004) thus providing a large area for microorganisms and may result in faster degradation rates compared to the more compact faecal pellets. Therefore the two fractions of the two-G model fitted in this study may represent rapidly decomposing pseudofaeces and slowly decomposing faeces. However, because the individual model parameters were non-significant the two-G model should be interpreted with caution and experiments designed to examine the decay rates of the two

biodeposit components are needed. For these reasons I used below the decay rate derived from the first-order G model for comparisons with published decay rates.

Decomposition can be described as a concentration change of a particular component of the decomposing material over time, e.g. chl *a*, OC, N, OM, or as a change in fluxes from the decomposing material, e.g. SOC, dissolved organic carbon, dissolved organic nitrogen and CO_2. Several studies have examined the decomposition of organic material in coastal sediments and applied first-order or two-G models (e.g. Kelly and Nixon 1984, Sun et al. 1993, Kristensen and Mikkelsen 2003). However, because the decomposition rates have been characterised using different components of the decomposing material, published measurements were made at different temperatures and the amount and quality of the decomposing material are not always readily available, comparisons are difficult. Despite these problems, I compared the results of this study to published decay rates derived from first-order G models based on measurements made at 15 – 22°C, to determine how rapidly mussel biodeposits decompose compared to other organic material in coastal sediments.

Decay rates for sediments without additions of OM range from 0.0005 d^{-1} (Kristensen and Blackburn 1987) to 0.024 – 0.044 d^{-1} (Sun et al. 1993, Ingalls et al. 2000) and as expected these rates are substantially lower than the biodeposit decay rate derived in this study. Many studies have calculated decay rates for plant material added to coastal sediments and values range from 0.0073 – 0.1 d^{-1} for phytoplankton (Kelly and Nixon 1984, Sun et al. 1993) and 0.018-0.046 d^{-1} for macroalgae (Ingalls et al. 2000, Kristensen and Mikkelsen 2003). These plant decay rates are 1.6 to 22× lower compared to those calculated in this study. A two-G model applied to the decomposition of fresh diatoms in sand and silt resulted in decay rates of 0.490 – 1.214 d^{-1} for the rapidly decomposing and 0.015 – 0.026 d^{-1} for the slowly decomposing fraction (Kristensen and Holmer 2001). These rates are also slightly lower than those obtained from the two-G model used in this study. The only faecal material decay rates I could find that were derived from a G-model approach were rates of copepod faecal pellets decomposing in seawater. Hansen et al. (1996) examined the change of copepod faecal pellet volume over time and calculated decay rates between 0.024 and 0.288 d^{-1}. Urban-

Rich (1999) observed a half-life time of 2.4 d for copepod faecal pellets decomposing in -1°C seawater. This corresponds to a decay rate of 0.29 d^{-1}. Although these experiments were conducted in seawater, different parameters were measured and copepod faecal pellets have a very different morphology to mussel biodeposits, their decay rates are surprisingly similar.

Aquatic animals ingest transient bacteria with their food and also contain resident bacteria in their guts (Harris 1993). Many transient bacteria survive the passage through the gut and are egested with the faeces and some residential bacteria may also be passed out of the guts. Therefore faecal pellets are already colonised by large populations of microorganisms when they are expelled and this promotes their decomposition, leading to high decay rates. In addition, faecal pellets consist to a large extent of already broken down material which makes them more labile compared to fresh plant material. It is important to note that biodeposit mineralisation commences immediately after egestion into the water column. The extent of water column mineralisation depends on the transit time to the seabed, a function of biodeposit settling velocity, water depth and currents. Biodeposits sink rapidly and in natural mussel beds they settle within a few seconds (Miller et al. 2002, Giles and Pilditch 2004). Biodeposits originating from aquaculture structures take longer to settle but at our study site, faeces reach the sediment surface within approximately 7 min. Pseudofaeces sink up to 70 % slower than faeces (Giles and Pilditch, 2004) and may therefore undergo more mineralisation in the water column. Nevertheless, compared to the biodeposit half-life of 4.3 d calculated in this study, mineralisation in the water column is likely to play only a minor role compared to that in the sediments. These comparisons of mussel biodeposit decay rates to those of non-treated sediments, decomposing plant material and copepod faecal pellets, confirm the important role biodeposits play as substrate in the remineralisation of OM and hence the benthic-pelagic coupling of nutrient cycling in coastal sediments.

In calculating decay rates, I assumed that biodeposit decomposition was conducted by aerobic microorganisms, but it is possible that the addition of biodeposits to the cores also stimulated anaerobic decomposition. If so, then some of the additional SOC in the B-cores would have been used for the oxidation of reduced inorganic compounds at the oxic/anoxic interface (Sun et al. 1993, Aller

1994, Kristensen and Holmer 2001) leading to an overestimation of the decay rates. In addition, anaerobic microclimates may have developed on the sediment surface or around the biodeposits if the diffusive boundary layer constituted sufficient resistance for oxygen flux across the solid-water interface (Joergensen and Revsbech 1985). However, the surface sediments of all cores appeared well oxygenated throughout the experiment. Visual observations of the redox potential discontinuity layer showed a layer depth of at least several mm and the oxygen saturation in our cores during the incubations never fell below 80 %. The amount of biodeposits I added was representative of that found under mussel farms and created only a very thin layer on top of the sediment surface of the cores (Fig. 3.1). Mussel faecal pellets are very thin open cylinders with a high surface area to volume ratio and pseudofaeces are amorphous in shape and break down easily (Chapter 2). Hence I assume that biodeposit shape and their distribution on the sediment surface did not promote the development of a thick boundary layer and therefore did not create significant anaerobic microclimates. As a result, I conclude that aerobic mineralisation accounted for most of the additional benthic respiration in the B-cores and that our decay rates represent a reasonable value for the decomposition of biodeposits in coastal sediments.

3.4.3 Nutrient fluxes

NH_4^+ showed the largest response to biodeposit addition reaching a maximum on d 4 when fluxes were 3.6× higher than in control cores. Similarly, an increase in sediment NH_4^+ release is commonly observed beneath mussel farms and enhancements of up to 14× have been recorded (e.g. Hatcher et al. 1994, Mazouni et al. 1996, Christensen et al. 2003). The increased NH_4^+ flux was not as immediate as the increase in SOC. Several studies have shown a similar gradual increase of the NH_4^+ release over a few days following the enrichment of sediments with plant material (e.g. Garber 1984, Enoksson 1993). This is most likely caused by a temporary uptake of nitrogen from the water to build microbial protein (Garber 1984, van Duyl et al. 1993, Wotton and Malmqvist 2001) and therefore resulted in a lower initial net NH_4^+ flux than expected from the remineralisation activity alone.

A change to a NO_3^- uptake by the sediments as a response to organic additions has been observed *in situ* (Jensen et al. 1990) and in laboratory enrichments (Hansen and Blackburn 1992, Enoksson 1993). The influx of NO_3^- into the sediments on d 0 compared to an efflux on all other days could indicate an inhibition of nitrification (the oxidation of NH_4^+ to NO_3^-) by a temporary limitation of oxygen in the sediment which was used up by the aerobic microorganisms decomposing the added biodeposits or a stimulation of anaerobic decomposition via denitrification (the reduction of NO_3^- to N_2) initiated by the increased amount of OM available in the sediments. The reduced availability of OM after a few days of decomposition and associated decline in microorganism activity would have reversed these effects and may have lead to a gradual increase in the NO_3^- flux from the sediment.

NO_3^- release rates rose sharply in all cores from d 8 onwards and the NH_4^+ flux in the C-cores increased on d 6 which indicates some fundamental changes in the nitrogen cycling in the cores that cannot be explained with the data available. The increase in NO_3^- release may have been responsible for the elevated NO_3^- concentrations in the reservoir tank during the last days of the incubation period. The key focus of this study was to assess and quantify how sediment oxygen and nutrient fluxes respond to biodeposit deposition. To obtain information on more detailed processes in the sediments future studies should include the measurements of sediment oxygen and nutrient profiles, microbial activity, burial rates as well as nitrification and denitrification.

Compared to the nitrogen cycle the role of bivalve biodeposits in the sediment phosphorus cycle is less clear (Newell 2004). The increased N:P flux ratios in the B-cores following biodeposit addition could have been caused by either a proportionally higher bacterial assimilation of PO_4^{3-} compared to nitrogen or the adsorption of PO_4^{3-} on the oxidised sediment surface layer. Bacteria involved in the mineralisation of organic material in the sediments assimilate a considerable part of the released nutrients to meet their own demands, particularly during the rapid bacterial growth following the addition of organic material to the sediments (van Duyl et al. 1993). Bacteria have a N:P ratio of about 9 (van Duyl et al. 1993). To maintain this N:P ratio bacteria need to assimilate proportionally more

phosphorus than nitrogen from detritus of phytoplankton origin, which has a Redfield ratio of about 16:1, and this could have caused the increased N:P flux ratios observed in this study. In all sediments the flux of PO_4^{3-} to the overlying sediment is greatly influenced by the adsorption on the oxidised surface layer and under oxic conditions the formation of iron-manganese phosphate complexes. Adsorption to oxyhydroxides can remove PO_4^{3-} from the sediment-water interface (e.g. Bray et al. 1973, Eyre and Ferguson 2002) and the lack of a PO_4^{3-} flux response to biodeposit addition and the consequentially increased N:P flux ratio in the B-cores could also be explained by this process. An enhanced N:P flux ratio under a mussel farm compared to a reference site was also measured by Hatcher et al. (1994). An altered stoichiometry of the benthic nutrient regeneration could affect primary producers (Nixon 1981) and may potentially be more significant than the changes of the individual fluxes (Hatcher et al. 1994).

3.4.4 Biodeposit nitrogen and carbon budget

The fate of biodeposit N and OC in the cores was examined by calculating the proportion of each element that was remineralised from the first-order G model and the proportion of N that was released in inorganic forms. The N and OC contents of biodeposits was 0.34 and 2.50 %, respectively, hence 80 mmol N m^{-2} and 689 mmol OC m^{-2} were added to the B-cores on d 0. Between d 0 and d 10 an additional 277 mmol O_2 m^{-2} were consumed in the B-cores and applying a C:O_2 ratio of 1 for aerobic decomposition showed that 40 % of the added OC was decomposed during this period. Using an O_2:N ratio of 6.625 (Redfield 1934, Newell et al. 2002) I calculated an aerobic mineralisation of 42 mmol N m^{-2} or 52 % of the added biodeposit N. Thus approximately half of the OC and N was decomposed during the 11 d incubation. I assumed that a large proportion of the remaining material was less reactive compared to the decomposed fraction. This concludes that substrate availability became limiting for microorganisms involved in the decomposition of biodeposits. The mean additional NH_4^+ flux from the sediments in the B-cores between d 0 and d 10 was 54 μmol m^{-2} h^{-1}, which shows that only 34 % of the mineralised N was released as NH_4^+. Some of the mineralised N would have been assimilated into bacterial biomass (van Duyl et al. 1993) but the removal of NH_4^+ could also be attributed to nitrification and potentially subsequent denitrification. A review of nitrification rates measured in

11 different coastal marine and estuarine sediments showed they are remarkably similar with an average of 2.4 mmol N m^{-2} d^{-1} (Herbert 1999). Over the incubation period of this study this would represent 64 % of the mineralised N. Because I could not detect an increased NO_3^- flux in the B-cores, NO_3^- may have been denitrified, however, the data from this study are not sufficient to support this argument.

Several factors must be considered before extrapolating the decay rates derived in this study to other situations. The annual temperature variation at our site is only 7 deg. (Giles unpublished data) and I assume that the decay rates I calculated will not vary much over this temperature range. However, the temperature dependence of biodeposit decay rates needs to be examined for applications in other climates. By using relatively small incubation cores and discarding those containing large macrofauna I obtained fluxes and decay rates representative of sediments with little macrofauna irrigation. However, coastal sediments may contain large communities of macrofauna that via particle reworking and transport, grazing and excretion can have significant impacts on the remineralisation of OM, SOC and nutrient fluxes (Aller 1994, Lohrer et al. 2004). In addition, our experiments did not consider the impact of microphytobenthos on nutrient and oxygen fluxes.

Chapter 4

Sedimentation from mussel (*Perna canaliculus*) culture in the Firth of Thames, New Zealand: Impacts on sediment oxygen and nutrient fluxes

4.1 Introduction

Shellfish aquaculture is growing worldwide and previous studies on the environmental effects of shellfish farming have shown a variety of impact levels ranging from low (e.g. Crawford et al. 2003, Danovaro et al. 2004) to significant (review by Newell 2004) including the development of anoxic sediments (Dahlbaeck and Gunnarsson 1981, Christensen et al. 2003), changes in macrofauna communities (Tenore et al. 1982, Stenton-Dozey et al. 2001) and major transformations in carbon, oxygen and nitrogen metabolism in the sediments underlying farms (e.g. Christensen et al. 2003). Many studies have indicated that the primary environmental impact of shellfish culture is increased sedimentation. This occurs because cultured shellfish usually grow suspended on longlines in the upper water column and feed on natural phytoplankton which they repackage into rapidly settling biodeposits (faeces and pseudofaeces). In addition detritus originating from epibiota attached to culture structures contribute to the increased sedimentation (Kaiser et al. 1998).

The mineralisation of sedimented organic matter consumes oxygen and releases nutrients into the water column. In estuaries nutrients regenerated from the decomposition of organic matter in the sediments play an important role and can supply up to 100 % of the nutrient requirements of primary producers in the overlying water (e.g. Nixon 1981, Herbert 1999, Gibbs et al. 2005). The increased organic input from shellfish culture has been shown to increase sediment oxygen consumption (e.g. Christensen et al. 2003), nitrogen regeneration rates (e.g. Hatcher et al. 1994) and affect denitrification (e.g. Kaspar et al. 1985) and therefore may accelerate nutrient turnover and redistribute

nutrients in the whole ecosystem. The rates of these principally bacterially-mediated processes depend on temperature and are subject to complex interactions in marine sediments involving both physico-chemical and biological factors (e.g. Hatcher et al. 1994, Mazouni et al. 1996, Herbert 1999) and seasonal measurements are necessary to develop a comprehensive description of their induced impacts. In addition sedimenting material can be dispersed by currents and so impacts depend on hydrodynamic conditions at the site as well as the scale of the cultivation process (Kaiser et al. 1998, Chamberlain et al. 2001).

In New Zealand the cultivation of the Greenshell^{TM} mussel *Perna canaliculus* has increased dramatically over the last 25 years and more major expansions are planned (Jeffs et al. 1999, Christensen et al. 2003). Most mussel farms are located in the Marlborough Sounds, South Island, but currently there are also more than 2000 ha of existing and approved farm area in the Firth of Thames, North Island, with applications pending for approximately another 6000 ha (Broekhuizen et al. 2004). This would increase the area allocated to mussel farming in the Firth of Thames to 7.3 % of the total area. Two previous studies have examined the environmental impacts of mussel culture in the Marlborough Sounds (Kaspar et al. 1985, Christensen et al. 2003). These studies showed significant effects on sediment characteristics and nutrient dynamics and concluded that the introduction of mussel farms may affect the nitrogen dynamics in the ecosystem, and that local conditions should be taken into account when considering new areas for mussel farming. The study by Christensen et al. (2003) was conducted in summer and Kaspar et al. (1985) measured benthic respiration in summer and autumn only. No previous studies have examined the impacts of mussel culture in the Firth of Thames. The aim of this study was to assess the effects of a mussel farm in the Firth of Thames on sedimentation, sediment characteristics, oxygen and nutrient fluxes, and how these effects differ between seasons. It also provides important data for models of shellfish aquaculture, which do not yet adequately describe the effects of aquaculture on benthic nutrient fluxes (Henderson et al. 2001).

4.2 Methods

4.2.1 Study sites and sampling times

This study was conducted at a small (40 ha) mussel farm in the Western Firth of Thames, New Zealand (Fig. 4.1), that has been operating in its current size since 1994. Mussels (*Perna canaliculus*) are cultured in the upper 6 m of the water column on longlines parallel to shore that are arranged in three blocks. These blocks are ~1000 m long in east-west direction and 114 m, 108 m and 186 m wide with 240 m and 127 m wide gaps between them. The farm comprises 145 longlines that each support ~2000 m of dropper line with stocking densities of ~5000 seed (<40 mm) per m and ~1700 adults per m. The harvest cycle is approximately 15 months and the farm produces about 1680 T per harvest. At any time cultured mussels have a range of sizes because seeding and harvesting is done at different times in different parts of the farm. Prior to sampling site selection, tidal currents in the area were assessed by deploying an InterOcean Systems S4 Current Meter (V. 5.153) under the farm 1 m above the sea bed for 8 d. Current speeds ranged from 3.1 to 32.8 cm s^{-1} during flood and 3.7 to 31.7 cm s^{-1} during ebb tide and the predominant current direction ranged from 83 to 163 degrees (magnetic) and 270 to 339 degrees, respectively. Accordingly, three sampling sites were chosen, one directly beneath the farm (farm site), another ~50 m outside the farm but within the influence of water flowing through the farm during ebb flow (edge site) and finally a reference site was chosen outside the

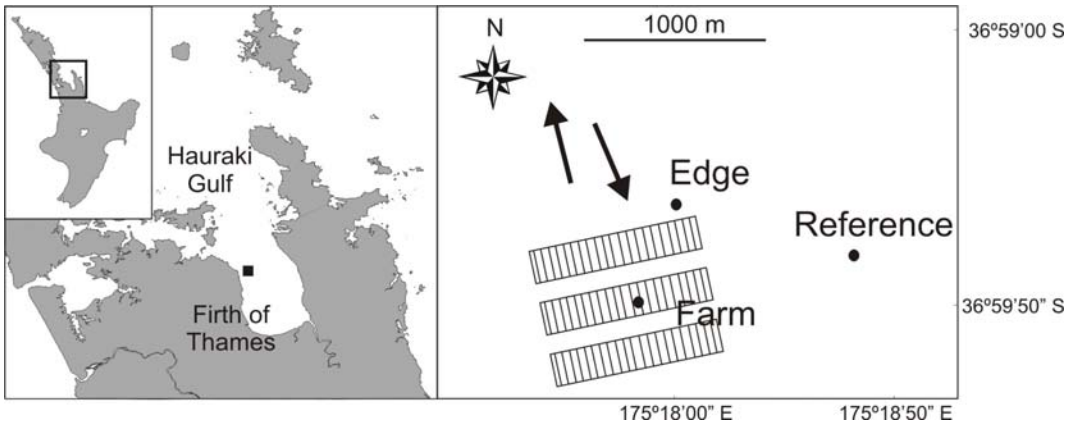

Figure 4.1. Location of mussel farm and sampling sites in the Western Firth of Thames, New Zealand. Arrows indicate the predominant current directions during flood (SSE) and ebb (NNW) tide.

Table 4.1. Sampling sites characteristics. Data represent the annual mean or range of seasonal means. Standard deviations given in parentheses where n > 2. ND = not determined.

	Farm	Edge	Reference
Water depth (m)	11	13	16
Currents			
Velocity range (cm s^{-1})	3.1 – 32.8	ND	1.46 – 53.4
Mean flow (cm s^{-1})	19.0	ND	22.1
Temperature (°C)[a]			
Winter 03	14.4 (1.1)	13.7	13.7 (0.6)
Spring 03	15.0 (0.4)	14.8	14.7 (0.5)
Summer 04	21.4 (0.8)	21.1	21.4 (0.9)
Autumn 04	17.5 (0.6)	17.0	16.9 (0.2)
Winter 04	12.6 (0.6)	12.0	12.0
Salinity (PSU)[b]	33.1	34.3	34.1
Bottom water:			
O_2 (µM)	150 – 191	ND	131 – 175
NO_3^- (µM)	0.25 – 0.37	ND	0.25 – 0.75
NH_4^+ (µM)	0.61 – 1.72	ND	0.86 – 1.26
Surficial sediment (0 – 0.5 cm):			
Median grain size (µm)[c]	8.5 (1.3)	8.4 (3.8)	8.0 (1.7)
Silt/clay fraction (vol %)[c]	76 – 90	87 – 95	81 – 92
Porosity	0.60 – 0.74	0.85 – 0.87	0.87 – 0.90
Water content (%)	36 – 51	66 – 69	70 – 74
Shell fraction (%)	36 – 61	0 – 5	4 – 8
OM content (%)	7 – 10	8 – 9	8

[a] average of surface and bottom water (difference of season means always <0.9°C)
[b] average of surface and bottom water in all seasons (difference always <4 PSU)
[c] 0 – 1 cm

farm and lateral to the predominant N-S flow through the farm (Fig. 4.1, Table 4.1). After choosing the sites currents were also measured at the reference site to confirm that it was outside the influence of the farm.

The mean water depth was 11 m at the farm, 13 m at the edge and 16 m at the reference site. Water temperature at the three sampling sites was vertically homogenous and ranged from 12 °C in winter to 21.4 °C in summer (Table 4.1). Average salinity was between 33.1 and 34.1 PSU. Mean seasonal suspended particulate material concentrations in surface (sw) and bottom water (bw) were generally higher at the farm (sw: 3.9 – 9.7, bw: 4.4 – 19.6) compared to the edge and reference sites (sw: 3.1 – 5.7, bw: 5.6 – 10.2) and always higher in the bottom water compared to the surface water. The percentage of particulate organic matter

was almost identical at all sites (15 – 37 %) and annual means were about 7 % lower in the bottom water compared to the surface water (Giles unpublished data). Sediments under the farm contained shell fragments and burrows as well as some epifauna (e.g. mussels and starfish).

Sampling was carried out once per season between June 2003 and August 2004. Sediment oxygen consumption (SOC) and nutrient fluxes were measured in winter (June 2003), spring (October 2003), summer (February 2004) and autumn (May 2004). Sediment characteristics and sedimentation rate measurements commenced in October 2003 and the winter samples were collected in August 2004. Due to bad weather conditions sedimentation rates could not be determined at the reference site in spring and winter and SOC and nutrient fluxes could not be measured in winter.

4.2.2 Benthic chambers

Sediment oxygen and nutrient fluxes were measured *in situ* at the farm and reference sites using clear acrylic (light) and PVC (dark) cylindrical benthic chambers (volume = 20 l, surface area = 0.115 m^2) that were deployed by SCUBA. A recirculating pump (flow rate = 0.95 ± 0.05 l min^{-1}) drew water from inside the chamber (8 cm above the sediment surface) and replaced it through a cross valve in the centre of the chamber top. A dye test confirmed that this procedure created a homogeneously mixed water volume and diver observation ensured that it did not cause resuspension inside the chamber. Between three and four replicates of each chamber type were deployed at each site, under the farm approximately 2 m away from the longlines. An area of sediment was selected trying to avoid benthic mussels or other obvious fauna or burrow openings. The visibility at all sites was very poor due to high turbidity and occasionally chambers were accidentally placed on top of mussel clumps. This was only noticed during retrieval and in these instances the chamber data were discarded.

Water samples from inside the chambers were taken from a boat with a vacuum pump via tubes (ID = 3.2 mm) that withdrew water from mid-water height near the centre of the chamber. Water removed from the chamber was replaced with ambient water that entered the chamber through a one-way valve in the lid. The

chambers were deployed for 3.3 to 6.7 h and between three and six samples were taken during each deployment period. Sampling commenced approximately one hour after deployment to allow any disturbed sediment to settle. The tube connecting the chamber to the vacuum pump was flushed (250 – 300 ml) prior to taking a 50 ml water sample with a syringe from a 3-way valve attached to the tube without allowing any air bubbles to enter the sample. The sample was mixed using a magnetic stirrer and the oxygen concentration measured with a YSI Model 55 system with attached YSI dissolved oxygen probe. Another 60 ml was collected and immediately filtered through a 25 mm Whatman GF/C filter, stored on ice and frozen once ashore for later analysis of NH_4^+, NO_3^-, NO_2^- and PO_4^{3-} on a Lachat CQ8000 FIA system. During each sampling occasion one ambient water sample was taken and analysed in the same way as the samples from the benthic chambers. Once the oxygen saturation inside the benthic chambers had decreased by 15 – 20 % the incubation ended.

To account for potential water column effects (i.e. in the enclosed water above the sediments) I incubated water samples and measured changes in oxygen and nutrient concentrations over time. Three bottom water samples were taken just after the chamber deployments and one of these was immediately sampled for oxygen and nutrient concentrations. The remaining two water samples were placed in 1-l bottles (one clear, one dark) without air gaps, attached to a line and incubated just above the sediment surface. After a deployment time identical to the benthic chambers both were sampled for oxygen and nutrient concentrations. Water column effects were negligible and sediment oxygen and nutrient fluxes were defined as the slope of the regression (r^2 = 0.32 – 0.96) between concentration and incubation time corrected for the dilution of the water inside the chamber with ambient water from the volume replacements.

4.2.3 Sediment sample collection

At each study site twelve sediment samples were collected by SCUBA and stored on ice in the dark until being processed or frozen. Three types of cores (one each for sediment characteristics, pigments, macrofauna) were used and four replicate cores of each type were collected. Two of the four sediment characteristic cores (ID = 5.1 cm, length = 30 cm) were sectioned (0 – 0.5, 0.5 – 1 cm then 1 cm

intervals to 5 cm) within 6 h of collection and the individual sections frozen for later analysis of porosity, water content, organic matter (OM) and shell content. The remaining two cores were frozen for later analysis of sediment grain size at the same sectioning intervals as described above. Pigment cores were syringe cores (ID = 2.8 cm, length = 12 cm) that were frozen and later sectioned (as above) and analysed for chl *a*, phaeo, OC and N. Macrofauna cores (ID = 13 cm, length = 30 cm) were inserted approximately 15 cm into the sediment. Once ashore the sediment was immediately sieved (0.5 mm) and the >0.5 mm fraction preserved in 80 % isopropyl alcohol for later identification of macrofauna.

4.2.4 Sediment traps

To estimate quantity and quality of the sedimenting material four cylindrical acrylic sediment traps (aspect ratio = 8.6, height = 60 cm, ID = 7 cm) were deployed between 3 and 8 d at each study site. The four traps were attached to a cross-frame 2 m above the seafloor with an inter-trap spacing of >7-trap diameters, which was sufficient to ensure minimised inter-trap interaction and maintain trapping efficiency (Nodder and Alexander 1999), and baffles (height = 7.5 cm, ID = 12 mm) were used to diminish turbulence and to create a calm layer in the traps (Bloesch and Burns 1980). The traps were filled to 7 cm with high-density (50 ‰ excess) salt brine solution to minimise sample wash-out and preserve the collected material and the overlying trap volume was filled with filtered (4.5 µm) seawater.

Traps were deployed and recovered by SCUBA and opened and closed using plastic bags. After recovery the sediment traps were stored on ice in the dark and within 24 h the seawater overlying the brine solution was siphoned off and the collected material processed. The content of one of the four replicate sediment traps was preserved in 80 % isopropyl alcohol and that of the remaining three traps was gently sieved through a 200 µm mesh. Mussel faecal pellets are significantly larger than 200 µm (Chapter 2) and they were sorted with pipettes, counted, rinsed with distilled water to remove salts and for each replicate sediment trap analysed separately for total dry weight, OM, chl *a*, phaeo, organic carbon (OC) and nitrogen (N). The remainder of the >200 µm fraction consisted mainly of zooplankton which were not included in further analyses. The <200 µm

fraction was analysed as described above for faecal pellets. The results of the two fractions were combined to calculate total sedimentation rates for each trap.

4.2.5 Laboratory analyses

Chl *a* and phaeo content of sediment, sediment trap and water samples were determined using the 90 % acetone extraction method on a Turner Designs 10-AU Fluorometer (Arar and Collins 1997). OC and N analyses of sediments and sediment trap material were done using a Europa Scientific 20/20 isotope analyser after treating OC samples with sulphurous acid to remove carbonate carbon (Verardo et al. 1990). Water content, porosity and OM were determined from dried and ashed sediment samples and corrected for salinity. Sediment grain size was measured with a Malvern Mastersizer-S after preparing the samples with 10 % hydrogen peroxide to remove organic matter, calgon to disperse the particles and removal of the >1 mm fraction (Singer et al. 1988). The sediment shell fraction was calculated as the loss of dry sediment weight after acidification with 10 % HCL. OM, chl *a*, phaeo, OC and N concentrations were expressed as value per non-shell fraction of sediment dry weight.

4.2.6 Data analysis

Sediment characteristics, sedimentation rates and sediment oxygen and nutrient fluxes were compared between sites, seasons and benthic chamber types (for oxygen and nutrient fluxes) using a full factorial General Linear Model (GLM) Analysis of Variance (ANOVA). Any non-significant interaction terms of the highest order were removed and the analysis repeated. For significant GLM results I performed Tukey post-hoc tests. The assumptions of homogeneity of variances and normality were confirmed using Levene's and Kolmogorov-Smirnov tests.

4.3 Results

4.3.1 Sedimentation rates

Sedimentation rates were measured as total mass, OM, OC, N, chl *a* and phaeo fluxes and were generally highest at the farm followed by the edge and reference sites (Fig. 4.2). Total mass fluxes at the farm and edge sites were highest in spring

(548 and 453 g dw m^{-2} d^{-1}, respectively) and decreased significantly ($p < 0.004$) during the following seasons to 242 and 318 g dw m^{-2} d^{-1}, respectively, in winter (Fig. 4.2a, Table 4.2). From spring to autumn rates were 10 to 22 % lower at the edge compared to the farm site but in winter they were 24 % higher. Mussel faecal pellets represented 3.4 to 4.4 % of the flux at the farm and 0 to 2.1 % at the edge

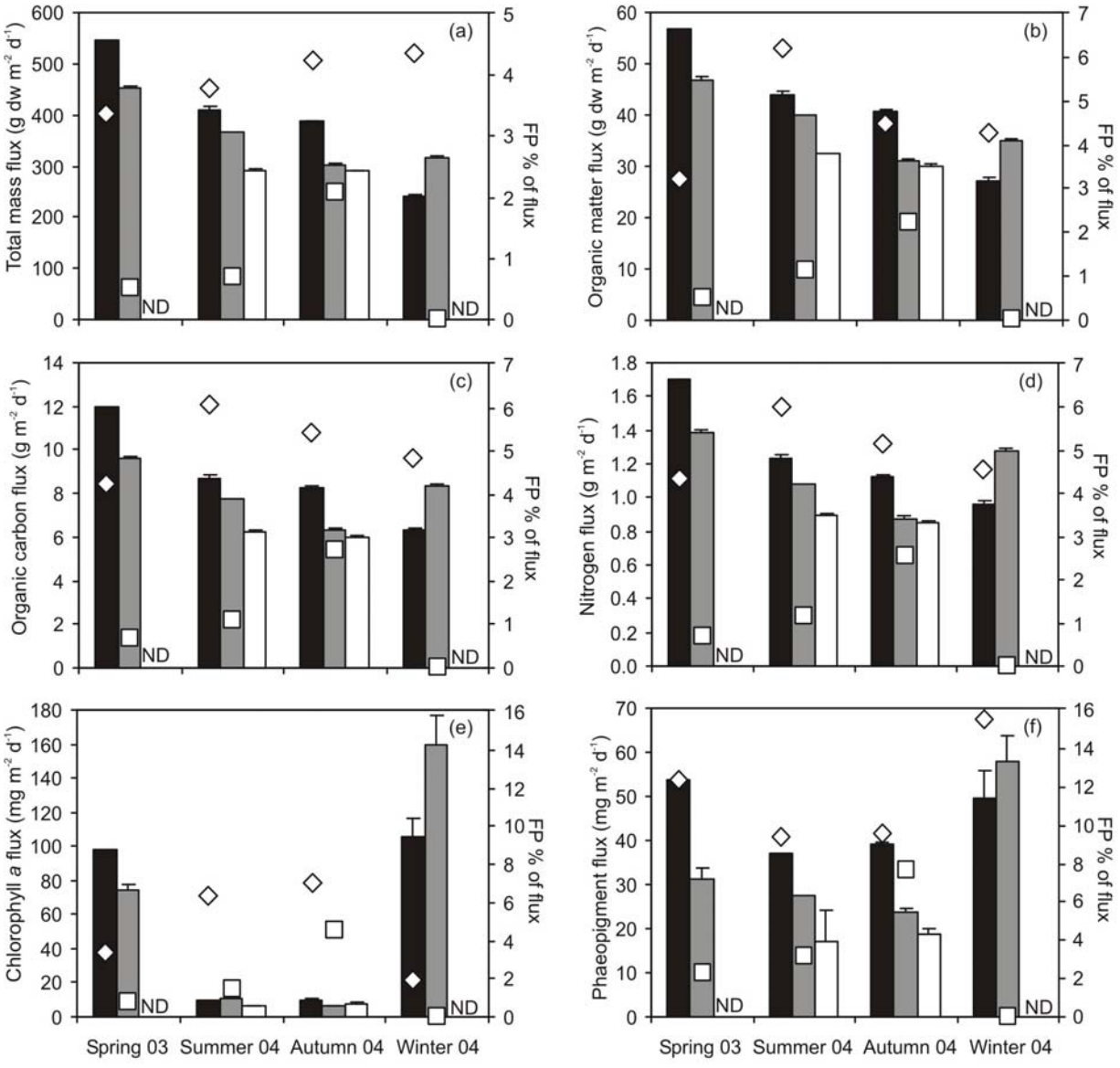

Figure 4.2. Sedimentation rates as (a) total mass flux, (b) organic matter flux, (c) organic carbon flux, (d) nitrogen flux, (e) chlorophyll *a* flux and (f) phaeopigment flux at farm (black bars), edge (grey bars) and reference (white bars) sites. The percentage contribution of mussel faecal pellets (FP) to the flux is represented by diamonds (farm site) and squares (edge site). No mussel faecal pellets were found at the reference site. Error bars indicate the standard deviation where n > 2. ND = not determined.

Table 4.2. GLM analysis of variance of total dry weight, organic matter, chlorophyll *a*, phaeopigment, organic carbon and nitrogen sedimentation with factors site (F = Farm, E = Edge, R = Reference) and season (Wi = Winter (no data at reference site), Sp = Spring (no data at reference site), Su = Summer, Au = Autumn).

Variable	Source of variability	df	Mean squares	F-ratio	P	Significant Tukey post-hoc test	
						Site	Season
Total dry weight flux	Site	1	0.102	18.38	**<0.001**		
	Season	1	0.054	9.81	**0.006**		
	Site × Season	4	0.104	18.76	**<0.001**	Wi: E > F	F: Sp > Su = Au > Wi
	Error	18	0.006			Sp: F > E	E: Sp > Su > Au, Sp > Wi
						Su: F > R, E > R	
						Au: F > R, F > E	R: –
Organic matter flux	Site	1	0.001	6.96	**0.017**		
	Season	1	0.001	10.96	**0.004**		
	Site × Season	4	0.001	8.44	**<0.001**	Wi: –	F: Sp > Su = Au > Wi
	Error	18	0.0001			Sp: –	E: Sp > Su = Au = Wi
						Su: F > R	R: –
						Au: F > R, F > E	
Chloro-phyll *a* flux	Site	1	3481	4.57	**0.047**		
	Season	1	105	0.14	0.715		
	Site × Season	4	16543	21.71	**<0.001**	Wi: E > F	F: Wi = Sp > Su = Au
	Error	17	762			Sp: F > E	E: Wi > Sp > Su = Au
						Su: –	R: –
						Au: –	
Phaeo-pigment flux	Site	1	7287.1	15.72	**<0.001**		
	Season	1	1.1	0.002	0.962		
	Site × Season	4	2713.5	5.85	**0.004**	Wi: –	F: –
	Error	17	463.5			Sp: F > E	E: Wi > Sp = Su = Au
						Su: F > R	R: –
						Au: F > R	
Organic carbon flux	Site	1	49.33	19.86	**0.002**		
	Season	1	31.80	12.80	**<0.001**		
	Site × Season	4	64.50	25.96	**<0.001**	Wi: E > F	F: Sp > Su = Au > Wi
	Error	18	2.49			Sp: F > E	E: Sp > Wi = Su > Au
						Su: F > R, E > R	R: –
						Au: F > R, F > E	
Nitrogen flux	Site	1	0.861	17.98	**<0.001**		
	Season	1	0.771	16.12	**<0.001**		
	Site × Season	4	1.343	28.06	**<0.001**	Wi: E > F	F: Sp > Su > Wi, Sp > Au
	Error	18	0.048			Sp: F > E	
						Su: F > R	E: Sp > Su > Au, Wi > Su > Au
						Au: F > R, F > E	
							R: –

Values in bold are significant at $p < 0.05$. Tukey post-hoc test results for significant differences between treatments are shown for Site and Season at $p < 0.05$.

site. Sedimentation at the reference site in summer and autumn was lower compared to the other two sites (about 290 g dw m^{-2} d^{-1}) and no faecal pellets were found.

The OM flux followed a pattern similar to that observed for total mass flux because of the similar OM contents (~10 – 12 %) of the trap material collected at the three sampling sites (Fig. 4.2b). Mussel faecal pellet contribution was also similar, except for a higher contribution (6.2 %) in summer under the farm. OC and N fluxes also showed the same pattern as the total mass flux, however, faecal pellets constituted higher proportions of the fluxes at the farm (4.3 to 6.1 %) and edge (0 to 2.7 %) sites (Fig. 4.2c and d). The molar C:N ratio of the sedimenting material without faecal pellets ranged from 7.6 to 8.5 with no significant ($p = 0.185$) differences between sites but significantly ($p = 0.006$) lower values in winter than in the other seasons. Faecal pellet C:N ratios were 8.1 to 8.9 but I did not analyse sufficient samples for statistical analysis. The fluxes of chl *a* at the farm and edge sites were significantly higher in spring and winter (74.2 – 159.0 mg m^{-2} d^{-1}) compared to summer and autumn (6.5 – 11.3 mg m^{-2} d^{-1}) and there was no consistent pattern between the sampling sites (Fig. 4.2e). Mussel faecal pellets made up 1.9 to 7 % of the chl *a* flux at the farm and 0 to 4.5 % at the edge site. With the exception of winter the phaeo flux at the farm site was 26 to 42 % higher than at the edge of the farm and 53 % higher compared to the reference site (Fig. 4.2f). In winter it was 14 % lower than at the edge site. The proportion of the phaeo flux comprised of mussel faecal pellets was 9.4 to 15.5 % at the farm and 0 to 8 % at the edge site, at both sites the highest of all measured sedimentation fluxes.

4.3.2 Sediment characteristics

The surficial sediments at the three sampling sites were mainly composed of silt and clay (Table 4.1). Porosity and water content were significantly ($p < 0.001$) lower under the farm compared to the edge and reference sites but sediments under the farm contained significantly ($p < 0.001$) higher levels of shell material. The OM content was similar at all sampling sites ($p = 0.855$) and showed no significant seasonal pattern ($p = 0.127$).

Macrofauna was composed of six main taxonomic groups: polychaetes, ophiuroidea, bivalves, crustaceans, gastropods and echinoidea (Fig. 4.3). Abundance under the farm (2.1 g 0.01 m^{-2}) was 2.3× and 3.2× higher than that at the edge and reference site, respectively, and at all three sites it was dominated by polychaetes and ophiuroidea. Under the farm the total biomass was 0.052 g

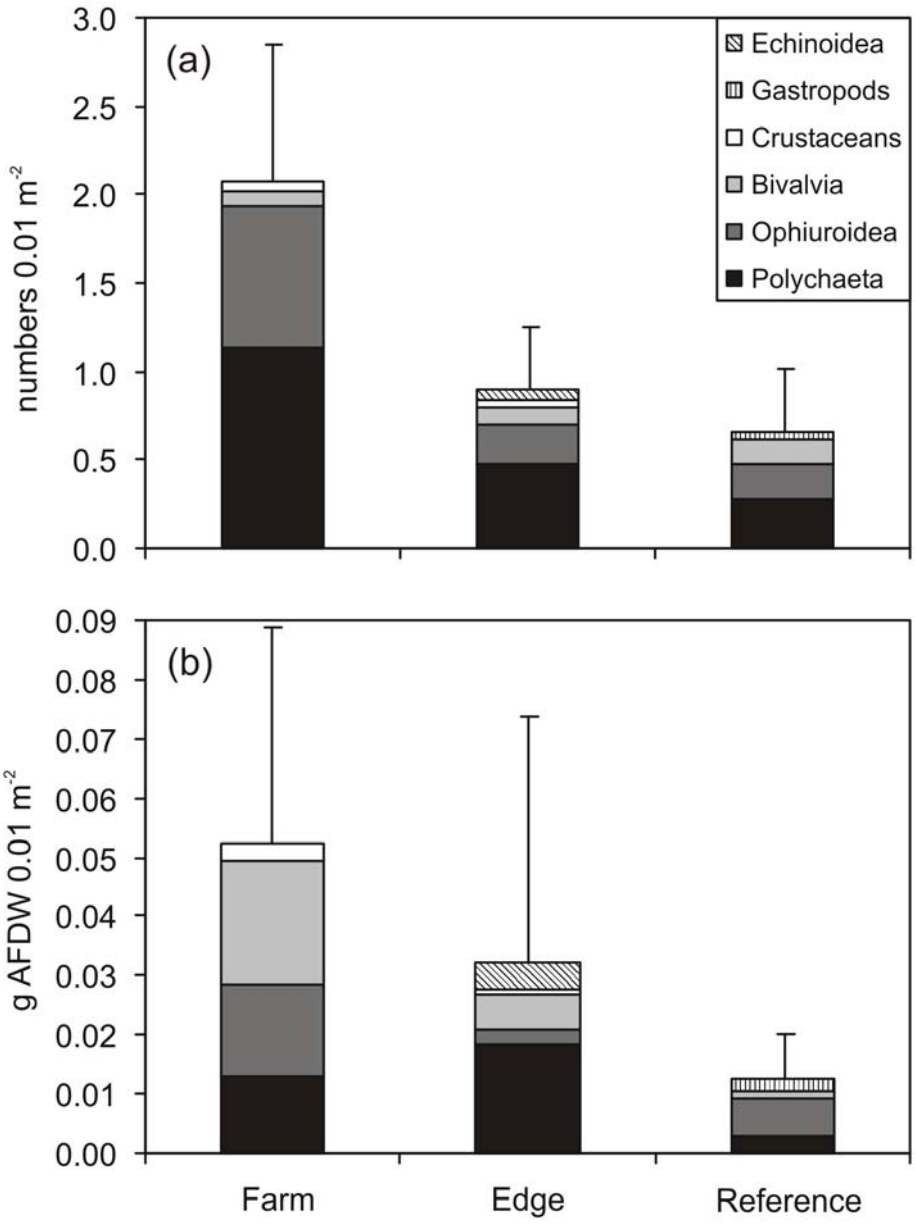

Figure 4.3. Macrofauna (a) abundance and (b) biomass at the three sampling sites showing contributions of the different taxonomic groups. Error bars indicate total standard deviation.

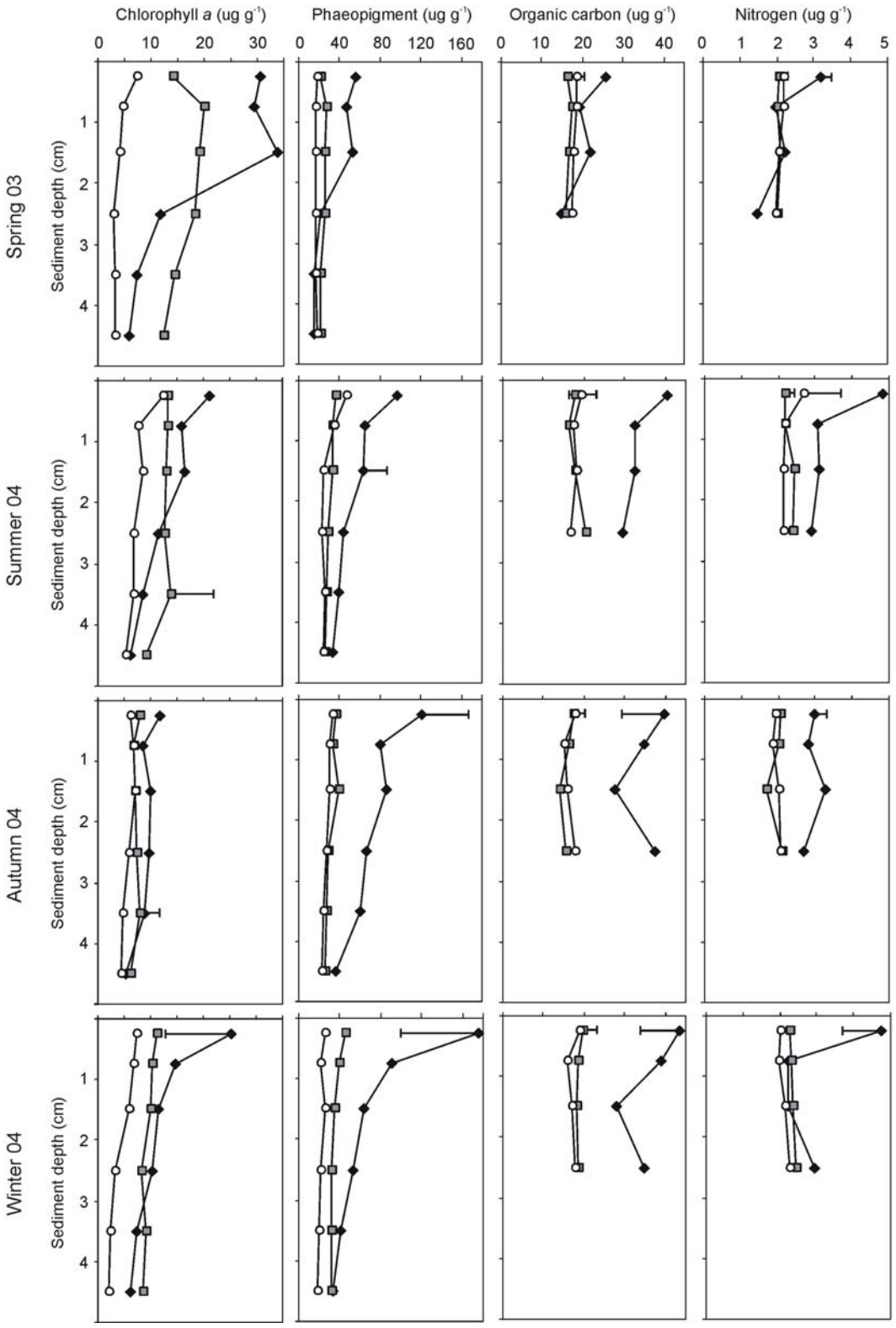

Figure 4.4. Sediment profiles of chlorophyll *a*, phaeopigment, organic carbon and nitrogen during the four seasons at the farm (◆), edge (■) and reference (○) sites. Error bars indicate the lowest and highest standard deviations of all means where n > 2. For chlorophyll *a* and phaeopigment n = 2 in spring and n = 3 in all other seasons. For organic carbon and nitrogen n = 4 in the top sediment layer and n = 1 below. In some instances error bars indicating the lowest standard deviations are covered by the marker. ND = not determined.

Table 4.3. GLM analysis of variance of surficial (0 – 0.5 cm) sediment characteristics with factors site (F = Farm, E = Edge, R = Reference) and season (Wi = Winter, Sp = Spring, Su = Summer, Au = Autumn).

Variable	Source of variability	df	Mean squares	F-ratio	P	Significant Tukey post-hoc test	
						Site	Season
Chloro-phyll *a*	Site	2	662.8	32.25	**<0.001**		
	Season	3	145.5	7.08	**0.001**		
	Site × Season	6	54.8	2.67	**0.035**	Wi: F > E = R	F: Sp = Wi > Au
	Error	29	20.6			Sp: F > E = R	E: –
						Su: –	R: –
						Au: –	
Phaeo-pigment	Site	2	24260	26.77	**<0.001**		
	Season	3	2943	3.25	**0.037**		
	Site × Season	6	2424	2.67	**0.035**	Wi: F > R, F > E	F: Wi > Sp
	Error	28	906			Sp: –	E: –
						Su: –	R: –
						Au: F > R	
Organic carbon	Site	2	1914.0	82.83	**<0.001**		
	Season	3	110.6	4.79	**0.007**		
	Site × Season	6	71.9	3.11	**0.015**	Wi: F > E = R	F: Sp < Su = Au = Wi
	Error	35	23.1			Sp: –	E: –
						Su: F > E = R	R: –
						Au: F > E = R	
Nitrogen	Site	2	16.67	64.16	**<0.001**		
	Season	3	2.31	8.88	**<0.001**		
	Site × Season	6	1.10	4.24	**0.003**	Wi: F > E = R	F: Su = Wi > Sp = Au
	Error	36	0.26			Sp: –	E: –
						Su: F > E = R	R: –
						Au: –	
OC:N	Site	2	16.16	2.61	0.086		
	Season	3	20.13	3.25	**0.031**		Au > Su
	Error	41	6.20				

Values in bold are significant at $p < 0.05$. Tukey post-hoc test results for significant differences between treatments are shown for Site and Season at $p < 0.05$.

AFDW 0.01m^{-2} of which bivalves made up the largest proportion (0.021 g AFDW 0.01 m^{-2}), followed by ophiuroidea, polychaetes and crustaceans. At the edge of the farm polychaetes had the highest biomass (0.019 g AFDW 0.01 m^{-2}) comprising more than half of the total macrofauna biomass. Biomass at the reference site was very low (0.013 g AFDW 0.01 m^{-2}) and consisted of polychaetes, ophiuroidea, bivalves and gastropods.

The chl *a* concentration in the surficial (0 – 0.5 cm) sediments under the farm was highest in spring (30.5 µg g^{-1}) and lowest in autumn (11.7 µg g^{-1}, Fig. 4.4) and the concentrations in the top 2 cm were higher compared to those at the edge of the farm and at the reference site. The difference in the top 0.5 cm was significant in

spring and winter (p = <0.001 – 0.041) but non-significant during summer and autumn (Table 4.3). The chl *a* concentrations in the surficial sediments at the edge (7.8 – 14.0 μg g^{-1}) were moderately higher compared to those at the reference site (6.3 – 12.5 μg g^{-1}) in all seasons. Phaeo concentrations under the farm were highest in the surficial layer (56 – 176 μg g^{-1}) and showed a distinct elevation in the sediments under the farm compared to the reference (significant in autumn and winter, p = <0.001 – 0.014) and edge (significant in winter, p < 0.001) sites. The phaeo concentrations were generally slightly higher at the edge of the farm compared to the reference site. OC and N concentrations were always higher in the surficial sediments under the farm (26 – 44 and 3.2 – 4.8 μg mg^{-1}, respectively) compared to the other two sites (16 – 20 and 1.9 – 2.7 μg mg^{-1}, respectively, (Fig. 4.4). The OC elevation was significant in summer, autumn and winter (p < 0.001) and that of N in summer and winter (p < 0.001). The mean annual molar OC:N ratio under the farm was 11.3 compared to 9.7 at the edge and 10.0 at the reference site but this site difference was non-significant (p = 0.086) and showed no consistent seasonal trend.

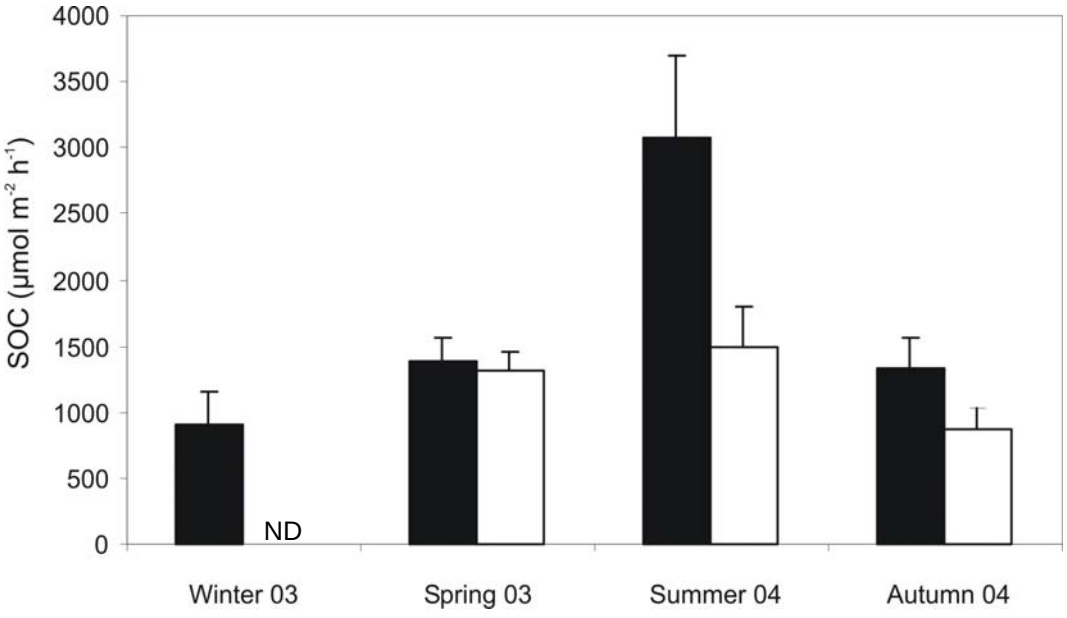

Figure 4.5. Sediment oxygen consumption (SOC) rates at the farm (F, black bars) and reference (R, white bars) sites. Error bars indicate standard deviation where n > 2. ND = not determined.

Table 4.4. GLM analysis of variance of sediment oxygen consumption (SOC) and sediment ammonium (NH_4^+), phosphate (PO_4^{3-}), nitrate (NO_3^-) and nitrite (NO_2^-) fluxes with factors site (F = Farm, R = Reference), season (Wi = Winter (no data at reference site), Sp = Spring, Su = Summer, Au = Autumn) and chamber type (light, dark).

Variable	Source of variability	df	Mean squares	F-ratio	P	Significant Tukey post-hoc test	
						Site	Season
SOC	Site	0					
	Season	2	4199673	44.43	**<0.001**		
	Chamber	1	63208	0.67	0.420		
	Site × Season	2	1534208	16.23	**<0.001**	Sp: –	F: Su > Sp = Au = Wi
	Error	30	94534			Su: F > R	R: Su > Au
						Au: –	
NH_4^+ flux	Site	0					
	Season	2	4311	0.56	0.577		
	Chamber	1	1187	0.15	0.697		
	Site × Season	2	57566	7.48	**0.002**	Sp: –	F: Wi < Sp = Au
	Error	30	7698			Su: –	R: Su > Au
						Au: F > R	
NO_3^- flux	Site	1	1194.5	13.03	**0.001**	F > R	
	Season	3	299.6	3.27	**0.034**	no significant differences	
	Chamber	1	15.5	0.17	0.684		
	Season × Chamber	3	305.8	3.34	**0.032**	no significant differences	
	Error	31	91.7				
NO_2^- flux	Site	0					
	Season	2	98.5	6.96	**0.004**		
	Light	0					
	Site × Season	2	104.3	7.38	**0.003**		
	Season × Light	2	15.0	1.06	0.361		
	Site × Light	0					
	Season × Site × Light	2	100.6	7.12	**0.003**	see text	see text
	Error	26	14.1				
PO_4^{3-} flux	Site	1	937.1	9.32	**0.004**	F > R	
	Season	3	276.7	2.75	0.058		
	Chamber	1	25.0	0.25	0.621		
	Error	34	100.5				

Values in bold are significant at $p < 0.05$. Tukey post-hoc test results for significant differences between treatments are shown for Site and Season at $p < 0.05$.

4.3.3 Sediment oxygen and nutrient fluxes

The differences in SOC, NH_4^+ and PO_4^{3-} fluxes between light and dark chambers showed no consistent patterns and were non-significant ($p = 0.420$, $p = 0.697$ and $p = 0.621$, respectively, Table 4.4, Fig. 4.5 and Fig. 4.6). The season × chamber interaction term was significant ($p = 0.032$) for NO_3^- flux but the Tukey post-hoc test revealed no significant differences and the chamber factor was non-significant ($p = 0.684$). Therefore light and dark chamber data were combined and all flux rates presented are means of light and dark chambers.

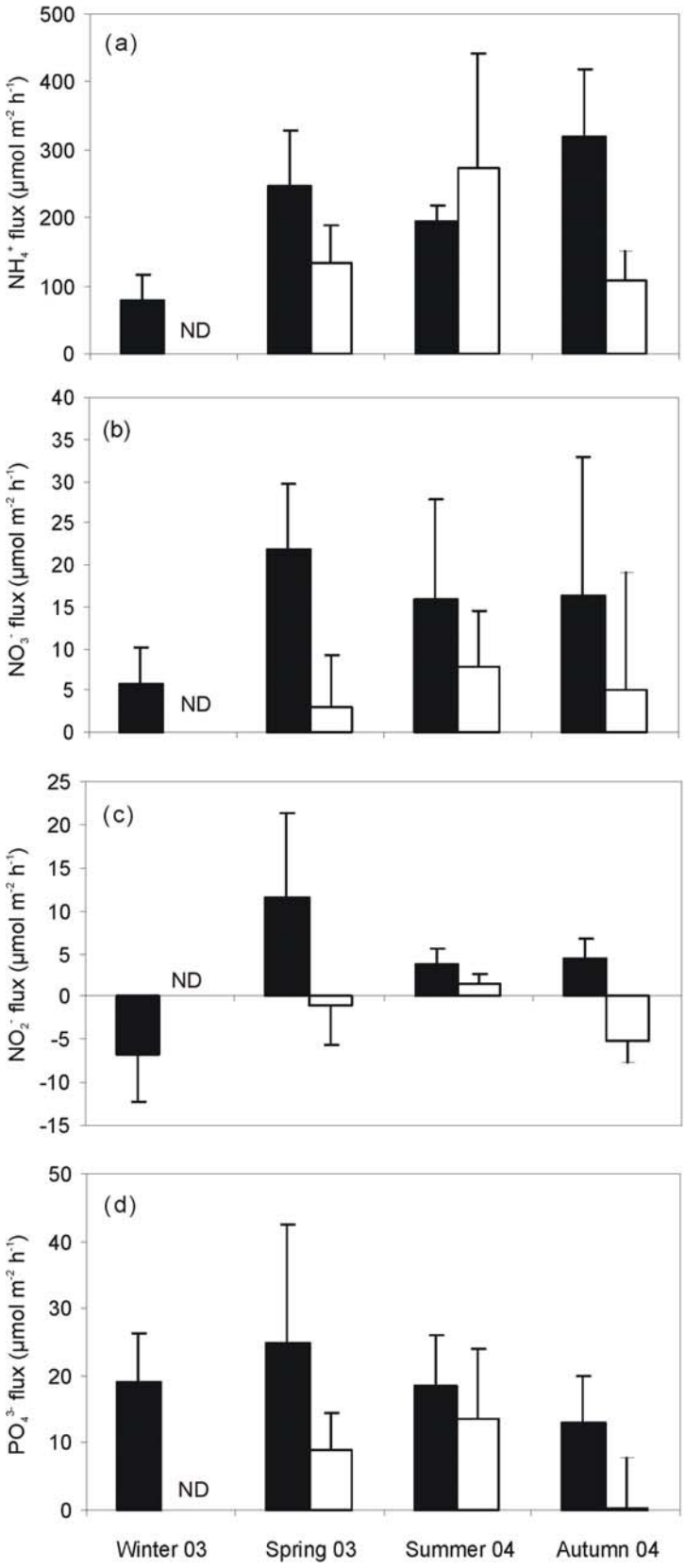

Figure 4.6. Sediment (a) ammonium (NH_4^+), (b) nitrate (NO_3^-), (c) nitrite (NO_2^-) and (d) phosphate (PO_4^{3-}) fluxes at the farm (F, black bars) and reference (R, white bars) sites (positive = flux from sediment to water column). Error bars indicate standard deviation where n > 2. ND = not determined.

The highest SOC (3083 µmol m^{-2} h^{-1}) was measured in summer at the farm site and the lowest (864 µmol m^{-2} h^{-1}) in autumn at the reference site (Fig. 4.5). Under the farm SOC was significantly ($p < 0.001$) higher in summer compared to the other three seasons during which rates did not differ significantly (907 µmol m^{-2} h^{-1} in winter to 1378 µmol m^{-2} h^{-1} in spring, Table 4.4). At the reference site sediment respiration was also highest in summer (1489 µmol m^{-2} h^{-1}) but differences between the sampled seasons (spring, summer, autumn) were less compared to the farm site and were only significantly ($p = 0.020$) different between summer and autumn. SOC was higher under the farm compared to the reference site during all seasons but only significantly ($p < 0.001$) in summer.

NH_4^+ was released from the sediments at both sites in all seasons with highest rates measured in autumn (319 µmol m^{-2} h^{-1}) and lowest in winter (80 µmol m^{-2} h^{-1}) under the farm (Fig. 4.6a). NH_4^+ fluxes under the farm were significantly ($p = <0.001$ and 0.030, Table 4) higher in autumn and spring than in winter. At the reference site NH_4^+ release was maximal in summer (275 µmol m^{-2} h^{-1}), significantly higher (2.5×, $p = 0.033$) than rates observed in autumn and 2× higher ($p = 0.285$) than those in spring. In spring and autumn the NH_4^+ fluxes were 1.8 and 3.0× higher under the farm compared to the reference site but in summer the flux was 1.4× lower under the farm. The increased NH_4^+ release under the farm was significant ($p = 0.006$) in autumn.

NO_3^- fluxes were also always directed out of the sediments (Fig. 4.6b) and were significantly higher at the farm site compared to the reference site ($p = 0.001$, Table 4.4). NO_3^- release at the farm site was highest in spring (21.8 µmol m^{-2} h^{-1}), did not vary significantly between summer and autumn and was lowest in winter (5.8 µmol m^{-2} h^{-1}). There was less seasonal variation at the reference site and NO_3^- fluxes ranged from 3.1 µmol m^{-2} h^{-1} in spring to 7.8 µmol m^{-2} h^{-1} in summer.

NO_2^- fluxes showed no consistent patterns between sites, seasons and chamber types (Fig. 4.6c) which was confirmed by a significant season × site × chamber interaction term ($p = 0.003$, Table 4.4). In spring, summer and autumn NO_2^- was released from the sediments under the farm with highest rates observed in spring (11.5 µmol m^{-2} h^{-1}) but in winter the flux was directed into the sediment (-6.8

µmol m^{-2} h^{-1}). At the reference site fluxes were generally lower and except for summer NO_2^- was taken up by the sediment.

All PO_4^{3-} fluxes show a release from the sediments at both sites (Fig. 4.6d) and fluxes were significantly higher at the farm compared to the reference site ($p = 0.004$, Table 4.4). Under the farm the highest PO_4^{3-} release occurred in spring (24.9 µmol m^{-2} h^{-1}) and lowest in autumn (13.1 µmol m^{-2} h^{-1}). The fluxes measured in winter and summer were very similar. At the reference site PO_4^{3-} release ranged from 0.2 µmol m^{-2} h^{-1} in autumn to 13.5 µmol m^{-2} h^{-1} in summer.

4.4 Discussion

4.4.1 Sedimentation

The annual mean sedimentation rates measured under the farm and at the reference site were 1.4 – 57× higher than previously published rates for shellfish farms (Table 4.5). A combination of sediment derived from two rivers draining farm land plus high current speeds and wind generated waves that resuspend sediment on nearby extensive intertidal mudflats contributed to the high rates measured in this study. Sediment traps measure gross sedimentation which may include a significant proportion of material that was resuspended either locally or at some distance away from the sampling site and transported with the currents (Horppila and Nurminen 2005). To estimate resuspension in the sediment traps I used the method of Gasith (1975) which is based on differences between the organic fraction of settleable particulate matter in the water column and that of resuspended sediment. Under the farm resuspension estimates ranged from 71 % of total sedimentation in spring to 87 % in autumn. Due to an absence of data I could only estimate resuspension at the edge site for two and at the reference site for one season. At the edge of the farm resuspension was also lowest in spring (56 %), 77 % in summer and at the reference site in summer it was 82 %. These estimates confirmed that resuspension plays an important role at our sampling sites and the adjusted sedimentation rates are very similar to those measured by Hatcher et al. (1994, Table 4.5). Current speed was high at both the farm and reference site, and the estimated resuspension rates are consistent among sites. Therefore I suggest that resuspension and hence the overestimate of

Table 4.5. Sedimentation rates and site characteristics reported under shellfish farms (F) and at reference sites (R). Sedimentation rates are given as total dry weight (total dw), organic matter (OM), organic carbon (OC), chlorophyll *a* (chl *a*) and phaeopigment (phaeo). Also shown are molar OC:N and chl *a*:phaeo ratios.

Authors	Species	Location	Farm (F) / Ref (R)	Depth m	Currents cm s^{-1}	Total dw g m^{-2} d^{-1}	OM g m^{-2} d^{-1}	OC g m^{-2} d^{-1}	OC:N molar	Chl *a* mg m^{-2} d^{-1}	Phaeo mg m^{-2} d^{-1}	Chl *a*: phaeo
This study	*Perna canaliculus*	New Zealand	F[a]	11	2.1 – 35.2	396 78[×]	40	8.8	8.15	55.9 9.8[b]	45.0 38.1[b]	1.24 0.26[b]
			R[b]	16	1.5 – 53.4	290 53[×]	31	6.2	8.35	6.9	17.9	0.39
Crawford et al. 2003	*Crassostrea gigas, Mytilus planulatis*	Australia	F[c] R[c]	8 – 12	3.4 – 18.5	7 – 15[*] 7 – 17[*]						
Dahlbaeck and Gunnarson 1981	*Mytilus edulis*	Sweden	F[d]	8 – 13	3	20.9		2.4 – 3.1	12.7	2.1	13.8	0.15
			R[d]	8 – 13	3	12.1		1.7	14	0.7	1.3	0.53
Danovaro et al. 2004	mussel species not known	Italy	F[a]	11		4.5 – 17	1.0 – 1.2				0.91 – 5.97[+]	
			R[a]	11		6.9 – 9.4					0.32 – 4.06[+]	
Hatcher et al. 1994	*Mytilus edulis*	Canada	F[a]	7		88.7		7.4	9.0			
			R[a]	7	4 – 7	36.4		2.1	10.9			
Hayakawa et al. 2001	*Crassostrea gigas*	Japan	F[a]	25[*]	<5 – 15	11		0.77				
Stenton-Dozey et al. 2001	*Mytilus galloprovincialis*	South Africa	F[e]	12 – 15	1.25			845				
			R[e]	12 – 15	7.5			281				

[a]annual average or range
[b]summer and autumn
[c]summer
[d]autumn
[e]summer and winter
[*]estimated from a figure
[+]chloroplastic pigment equivalents (chl *a* + phaeo)
[×]adjusted for resuspension

sedimentation from our sediment trap measurements affected all three sampling sites to a similar extent and that comparisons between these sites are accurate. Because of the high estimated resuspension rates I focus this discussion on the additional sedimentation measured under the farm and at the edge of the farm compared to the reference site rather than on absolute sedimentation rates.

Several authors equate the additional sedimentation measured under a mussel farm with mussel biodeposition (e.g. Dahlbaeck and Gunnarsson 1981, Baudinet et al. 1990, Chamberlain et al. 2001, Danovaro et al. 2004). However, mussel farm structures provide substratum on which epibiota can settle (e.g. Kaiser et al. 1998). In addition mussels excrete NH_4^+ and thereby promote high levels of productivity in algae attached to the mussel lines (e.g. Kaiser et al. 1998). Detritus other than mussel biodeposits originating from the farm structures, including biodeposits produced by the biofouling communities, can therefore significantly contribute to sedimentation (e.g. Stenton-Dozey et al. 2001) but no previous studies have quantified these different components of sedimenting material under mussel farms. The annual mean additional deposition I measured under the farm compared to the reference site was 106 g m^{-2} d^{-1} of which only 15.2 g m^{-2} d^{-1} comprised of mussel faeces. At the edge of the farm 2.8 of the 44 g m^{-2} d^{-1} additional flux was made up of faeces. This indicates that 86 % of the additional material settling under the farm and 94 % of that sedimenting at the edge of the farm was not due to mussel faeces deposition. Based on seston SPM and OM concentrations I estimate that mussel pseudofaeces production is similar to faeces production (Hawkins et al. 1999). Pseudofaeces break up and disperse easily (Chapter 2) and therefore only a fraction of all produced pseudofaeces may accumulate on the sediments below the mussels. Future studies should examine the composition of sedimenting material more closely and investigate possible sources.

The chl *a* sedimentation rates measured under and at the edge of the farm in spring and winter were about 10× higher than those measured during summer and autumn. This corresponds to high water column chl *a* concentrations during these seasons (14.2 and 7.2 µg l^{-1} in winter and spring, respectively) compared to only 2.0 µg l^{-1} in summer (not measured in autumn), a pattern that has previously been

observed (Keeley 2001). I suggest that most of the collected material in winter and spring was phytoplankton which is also supported by the lower contribution of mussel faeces to the total flux during these seasons. In summer and autumn the chl *a*:phaeo ratio of the sedimenting material was lower under the farm compared to the reference site (Table 4.5) which is in accordance with observations by Dahlbaeck and Gunnarson (1981), who regarded this as a result of mussel grazing on phytoplankton.

4.4.2 Sediment characteristics

Sediment characteristics as well as sediment-water oxygen and nutrient fluxes under the farm show a range of attributes commonly associated with enhanced organic flux under shellfish culture as well as biodeposition, despite the low contribution of mussel biodeposits to total sedimentation. This could indicate that the predominant part of the fine non-faecal material is dispersed from the sediment trap sampling site either while settling or via erosion on the sediment surface while a higher proportion of the larger and heavier faecal pellets remain in the vicinity of the trap and therefore may contribute more to the material actually accumulating in the sediment than estimated from the material collected in the traps 2 m above the sediment surface.

The elevated OC, N, chl *a* and phaeo concentrations in the sediments under the farm are consistent with measurements made in other farm-affected areas (Table 4.6) and are indicative of the additional organic input due to bivalve biodeposition (Chapter 3). An increased C:N ratio in the surficial sediments is also commonly found under farms and could be due to a faster degradation of nitrogen compared to carbon in biodeposits (Dahlbaeck and Gunnarsson 1981) or the accumulation of refractory OC (Stenton-Dozey et al. 2001) which would also explain the increased OC concentration in the deeper farm sediments (Fig. 4.4). The elevated OC concentration at depth could also indicate the transport of organic material by macrofauna (Stenton-Dozey et al. 2001). I found an increased abundance of macrofauna under the farm where animals were possibly attracted by the increased organic material and may have enhanced burial rates. However, I found no considerable change in macrofauna diversity and abundance was low

Table 4.6. Surficial sediment and site characteristics reported under shellfish farms (F) and at reference sites (R). Sedimentation characteristics shown are organic matter (OM), organic carbon (OC), organic carbon : nitrogen ration (OC:N), chlorophyll *a* (chl *a*) and chl *a* : phaeopigment ratio (chl *a*:phaeo).

Authors	Species	Location	Farm (F) / Ref (R)	Depth m	Currents cm s^{-1}	OM %	OC %	OC:N molar	Chl *a* ug g^{-1}	Phaeo ug g^{-1}	Chl *a*: phaeo
This study	*Perna canaliculus*	New Zealand	F[a]	11	2.1 – 35.2	7 – 10	2.6 – 4.4	11.3	12 – 30	56 – 176	0.10 – 0.55
			R[a]	16	1.5 – 53.4	8 – 9	1.8 – 1.9	10.0	6 – 12	18 – 48	0.19 – 0.41
Barranguet et al. 1994	*Mytilus galloprovincialis*	France	F[a]	4		16.6	4.9	14.4	>R	>R	
			R[a]	4		12.1	3.3	24.6			
Christensen et al. 2003	*Perna canaliculus*	New Zealand	F[b]	19	6 – 12		12	16.9	3.5× <R	2.5 – 3.1× >R	0.011
			R[b]	19	6 – 12		7	13.2			0.12
Crawford et al. 2003	*Crassostrea gigas, Mytilus planulatis*	Australia	F[b]	8 – 12	3.4 – 18.5	2 – 4					
			R[b]			1.2 – 4					
Dahlbaeck and Gunnarson 1981	*Mytilus edulis*	Sweden	F[c]	8 – 13	3	24	10	6 – 9.2[×]			
			R[c]	8 – 13	3	11	5.8				
Danovaro et al. 2004	mussel species not known	Italy	F[a]	11		1.2 – 6.1			1 – 11.2	2.5 – 35.1	
			R[a]	11		1.7 – 7.8			1.4 – 8.3	2.6 – 26.2	
Grant et al. 1995	*Mytilus edulis*	Canada	F[a]	7	<15		7.5	10.1	57.8		
			R[a]	7	<15		7.13	10.3	30.9		
Kaspar et al. 1985	*Perna canaliculus*	New Zealand	F[d]	11	111	8	0.7 – 1.4[°]	6.2 – 7.2	same as R	2.6× R	0.54
			R[d]	11	111	7	0.7 – 1.4[°]	7.9 – 10			1.5
Mirto et al. 2000	mussel species not known	Italy	F[a]	10					9 – 54	86.8[+]	
			R[a]	10					2.3 – 21.9	13.5[+]	
Stenton-Dozey et al. 2001	*Mytilus galloprovincialis*	South Africa	F[e]	12 – 15	1.25		7.5	12 – 15			
			R[e]	12 – 15	7.5		0.4	5 – 7			

[a]annual average or range
[b]summer
[c]autumn
[d]spring, summer, autumn
[e]summer and winter
[+]chloroplastic pigment equivalents (chl *a* + phaeo)
[×]increase with depth
[°]not separately specified

at all three sites so I cannot confirm that the observed differences are solely due to the influence of the farm. Reported impacts of bivalve cultures on macrofauna abundance and biomass vary. Some studies report a reduction in macrofauna biomass and diversity under bivalve cultures (e.g. Kaspar et al. 1985, Stenton-Dozey et al. 2001) whereas others found the opposite trend (e.g. Grant et al. 1995) or inconclusive results (Chamberlain et al. 2001).

All studies that measured the impact of bivalve culture on photosynthetic pigments in the sediments found a strong increase in the phaeo concentration compared to reference sites (Table 4.6) suggesting that this chl *a* degradation product is derived from the deposition of biodeposits. I measured the highest surficial sediment chl *a* concentrations in spring and winter, reflecting the high phytoplankton sedimentation during these seasons, but did not observe correlations with season for the other parameters. Mussel biodeposits in coastal sediments have a degradation rate of 0.16 d^{-1} which is 1.6 to 22× faster than that of plant material and 1 to 2 orders of magnitude faster compared to sediments without additional organic input (Chapter 3). Once mussel biodeposits reach the sediments they are mineralised rapidly and do not change sediment characteristics as much as slower decomposing material does. Thus I suggest that this rapid mineralisation may cause the decoupling of sedimentation and sediment characteristics.

4.4.3 Sediment respiration and nutrient fluxes

Sediment respiration and nutrient flux rates can be affected by microphytobenthos (MPB) primary production that is dependent on several factors (e.g. light, temperature, nutrients) with light being most important (MacIntyre et al. 1996). It is commonly assumed that the euphotic depth for MPB is reached where the photosynthetically active radiation (PAR) is approximately 1 % of the water surface value (e.g. Masini and McComb 2001). At both, the farm and reference sites, 1 % of the surface water light intensity (measured using a Sea-Bird Electronics SEACAT CTD profiler) was reached 2 – 3 m above the sediment and I found no significant differences between the light and dark chambers that would indicate an active MPB community. Therefore I suggest that MPB activity did not substantially affect SOC and nutrient dynamics at our sampling sites. Sediment

oxygen and nutrient fluxes showed no consistent correlations with sedimentation rates or surficial sediment characteristics during the four seasons. I suggest that this was due to a combination of the fast mineralisation of mussel biodeposits and the fact that a large proportion of the material collected in the traps was probably exported from the sampling sites as tidally driven horizontal flux (Hatcher et al. 1994). The general coupling between oxygen and nutrient fluxes and water temperature represents the temperature dependent bacterial activity associated with the decomposition of OM in the sediments (e.g. Zeitzschel 1980) and the mostly elevated fluxes from the sediments under the farm show the expected response to increased organic input (e.g. Grant and Hargrave 1987).

SOC is affected by a range of factors and by itself may therefore not be a sensitive indicator of bivalve culture impact (Hatcher et al. 1994). Macrofauna may significantly contribute to sediment respiration (Hatcher et al. 1994, Stenton-Dozey et al. 2001) but because of the very low biomass at all sampling sites I do not consider its impact significant. Our SOC rates also include oxygen used for the oxidisation of reduced inorganic compounds related to anaerobic mineralisation (Pamatmat 1975) and the elevated OC concentrations in the deeper sediments under the farm could represent organic matter available for anaerobic degradation via denitrification, sulphate, iron or manganese reduction (Canfield et al. 1993). Because the bottom water at the three sampling sites was well oxygenated and the surficial sediments of all analysed cores displayed an oxic layer of several mm throughout the year I do not think that anaerobic mineralisation activity was significantly elevated in the sediments at the farm site. However, the strong increase in SOC, and the low NH_4^+ and NO_3^- release in summer could indicate an increase in anaerobic microbial activity due to the elevated temperatures. The low nitrogen flux rates could indicate an increase of denitrification (the reduction of NO_3^- to N_2) under the farm since NO_3^- bottom water concentrations were very low throughout the year (Table 4.1) and any NO_3^- required for denitrification would have to be supplied by nitrification (the oxidation of NH_4^+ to NO_3^-) in the sediments which reduces the amount of NH_4^+ being released into the overlying water (Christensen et al. 2003). Increased nitrification rates in summer would also enhance SOC and hence contribute to the high SOC elevation measured during this season. In temperate coastal waters

denitrification is usually lowest during summer because it is limited by low nitrate concentrations in the bottom water and sediment (Rysgaard et al. 1995, Sundback and Miles 2000). However, when nitrate is available (in the overlying water or through nitrification) good correlations have been observed between denitrification activity and ambient temperature (Herbert 1999). Burrowing macrofauna may have led to a better irrigation of the sediment with oxygenated bottom-water creating aerobic microsites in the anaerobic sediment layer that could have enhanced nitrification (Kaspar et al. 1985). The high OM concentration in the sediments under the farm compared to the reference site could have fuelled denitrification explaining why NH_4^+ flux was only reduced at the farm site.

PO_4^{3-} fluxes are affected by a range of chemical reactions and sediment characteristics (Sundby et al. 1992, Mazouni et al. 1996). Regenerated PO_4^{3-} can be adsorbed on oxidised surface sediments which reduces the PO_4^{3-} flux into the overlying water (Sundby et al. 1992) but I found no relationship between bottom water oxygen concentrations and PO_4^{3-} flux under the farm. Therefore I suggest that the high PO_4^{3-} release rates in winter and spring under the farm were more likely a response to the increased phytoplankton sedimentation.

4.4.4 Comparison of sediment-water fluxes under shellfish farms

To compare our results to those measured at other locations and to obtain a range of observed impacts of shellfish farming on sediment-water fluxes I summarised previously published fluxes below farms and at corresponding reference sites (Table 4.7). Published SOC rates under shellfish farms range from 0 to 4188 µmol m^{-2} h^{-1} and those measured in this study were well within this range. All reference sites had lower SOC (83 – 1563 µmol m^{-2} h^{-1}) compared to farm sites, except for sites examined by Stenton-Dozey et al. (2001). However, sediments under their mussel farm were anoxic and despite lower SOC under the farm they could not conclusively separate these rates from the reference site. Mazouni et al. (1996) measured a net oxygen production in winter which was related to the activity of benthic microphytes.

Table 4.7. Oxygen, ammonia (NH_4^+) and nitrate (NO_3^-) sediment-water fluxes (positive = flux from sediment to water column), nitrogen mineralisation (N min) and sediment denitrification rates reported under shellfish farms (F) and at reference sites (R).

Authors	Species	Location	Farm (F) / Ref (R)	Depth m	SOC µmol m^{-2} h^{-1}	NH_4^+ flux µmol m^{-2} h^{-1}	NO_3^- flux µmol m^{-2} h^{-1}	N min µmol m^{-2} h^{-1}	Denitrification µmol m^{-2} h^{-1}
This study	*Perna canaliculus*	New Zealand	F[a]	11	1676 907 – 3083	210 80 – 320	15.0 6 – 22		
			R[b]	16	1221 864 – 1489	173 108 – 275	5.3 3 – 8		
Barranguet et al. 1994	*Mytilus galloprovincialis*	France	F[a]	4	875 – 4188*	85 – 540*			
			R[a]	4	938 – 1563*	20 – 80*			
Baudinet et al. 1990	*Mytilus galloprovincialis*	France	F[a]	5		100 – 366	-18 – -4*		
			R[a]	5		20 – 70*	-59 – 5		
Christensen et al. 2003	*Perna canaliculus*	New Zealand	F[c]	19	1657	275*	-8*		8.3
			R[c]	19	1039	20*	9*		15.3
Hatcher et al. 1994	*Mytilus edulis*	Canada	F[a]	7	170 – 1670*	75 – 645*	-65 – 95*		
			R[a]	7	83 – 1380*	-20 – 290*	-110 – 25*		
Kaspar et al. 1985	*Perna canaliculus*	New Zealand	F[b]	11	404[d]			1217	142
			R[b]	11	252[d]			629	21
Mazouni 2004	*Crassostrea gigas*	France	F[a]	5		25 – 600*	-158 – 50+*		
			R[a]	5		-100 – 360*	-200 – 0+*		
Mazouni et al. 1996	*Crassostrea gigas*	France	F[a]	5	0 – 2208	32.6 – 660	-158 – 17+		
			R[a]	5	617 – 1250*	-30 – 359	-100 – 23.8+		
Stenton-Dozey et al. 2001	*Mytilus galloprovincialis*	South Africa	F[e]	12-15	1100	690*	<5		
			R[e]	12-15	1500*	180*	<5		

[a]annual average or range
[b]spring, summer and autumn
[c]summer
[d]summer and autumn
[e]summer and winter
*estimated from a figure
+NO_3^- + NO_2^-

An increase in sediment NH_4^+ release is commonly the largest response to organic enrichment due to shellfish culture and the rates measured in this study were within the published range of 25 – 690 µmol m^{-2} h^{-1}. At some reference sites NH_4^+ was taken up by the sediment during some times of the year but as at our site the fluxes were mainly directed out of the sediment (-100 – 290 µmol m^{-2} h^{-1}). NO_3^- fluxes were more variable between locations. At some farm and reference sites NO_3^- was always taken up by the sediments, others showed a consistent release or seasonally variable flux directions. Overall fluxes ranged from -158 – 95 µmol m^{-2} h^{-1} under farms and -200 – 25 µmol m^{-2} h^{-1} at the reference sites. NO_3^- flux rates measured at our sampling sites were in the range of those measured elsewhere but were always directed out of the sediment. The one study I could find that measured N mineralisation rates under a mussel farm (Kaspar et al. 1985) showed that this process is about 2× higher under the farm compared to the reference site which is in accordance with the elevated NH_4^+ release rates measured under all farms. Two studies examined the impact of increased sedimentation from mussel culture on denitrification rates and obtained contradicting results. Christensen et al. (2003) measured lower denitrification rates under the farm whereas Kaspar et al. (1985) observed an increase. These comparisons show that despite the very different local conditions the observed impacts of mussel culture on SOC and NH_4^+ fluxes are remarkably consistent.

4.4.5 Implications for ecosystem nitrogen dynamics

To assess the impact of mussel culture on the nitrogen dynamics in the Firth of Thames I examined the contribution of benthic DIN (NH_4^+ + NO_3^-) release to the nitrogen requirements of primary producers. The annual mean primary production estimate for the Firth of Thames has been estimated as 5.8 mmol N m^{-2} d^{-1} (Zeldis 2005). At the reference site sediment DIN release could supply 74 % of the nitrogen requirements of primary producers confirming the importance of benthic nutrient regeneration in maintaining primary production in this region. These findings are consistent with the LOICZ budget of Zeldis (2005) that suggested extensive recycling of nitrogen in the Firth of Thames. Under the farm DIN release made up 94 % of primary production requirements which demonstrates that the mussel culture can lead to a redistribution of nutrients and hence may affect the nutrient dynamics at least in the vicinity of farms. The supply of new

and regenerated nutrients on the northeastern New Zealand continental shelf and adjacent Hauraki Gulf (Fig. 4.1) is strongly affected by hydrodynamic forcing (Zeldis 2004). Wind-driven upwelling causes extensive loading of the Hauraki Gulf water column with nitrate and can change the ratios of new to regenerated nitrogen in the ecosystem. However, at our study sites further inshore in the Firth of Thames nitrate bottom water concentrations were low during all four sampling periods suggesting either low effects of upwelling on the nitrate concentrations or a lack of upwelling events during this study. To obtain a more complete estimate of the contribution of benthic remineralisation to the nutrient dynamics in the water column and modifications due to mussel culture development, measurements should be repeated and related to hydrodynamic conditions such as upwelling and downwelling as well as the impacts of land based activities.

The LOICZ budget analysis of Zeldis (2005) demonstrated active denitrification in the Firth of Thames (1.9 mmol m^{-2} d^{-1}), potentially buffering the system against excessive N loading and potential eutrophication. The influence of bivalve culture on denitrification rates have not yet been fully characterised (Newell 2004) and previous studies on the impacts of mussel farms on denitrification rates have been inconsistent, showing both increase (Kaspar et al. 1985) and decrease (Christensen et al. 2003) in farm-affected sediments. Gilbert et al. (1997) measured an increase in natural denitrification but a decrease in potential denitrification under shellfish cultures. This indicates the complex interactions of processes involved in sediment denitrification and their susceptibility to environmental parameters such as oxygen and nitrate availability and organic input (Herbert 1999). This study indicated a potential increase in denitrification under the farm in summer during times of increased microbial activity and associated nutrient regeneration which may prevent an increased retention of nitrogen in the system and hence limit eutrophication.

The farm I studied is very small and located in a high-energy environment and the degree and extent of impacts from bivalve cultures is expected to differ considerable between culture sites. These differences have been attributed to a range of factors, including farm age, stocking density, longline configuration and orientation, distance of dropper lines from the sediment, hydrodynamics and local

environmental conditions (e.g. Chamberlain et al. 2001, Newell 2004). An increase in stocking density enhances biodeposition and hence may intensify organic enrichment of the underlying sediments and the higher production over a longer period of time from older leases may cause a gradual habitat degradation (Crawford et al. 2003). In a previous study no strong relationships were found between husbandry practice (number of years of operation and stocking density) and benthic parameters such as OM, redox potential, sulphide content and macroinvertebrate diversity indices (Miron et al. 2005). Instead, differences in the level of impact are commonly linked to different current patterns (Chamberlain et al. 2001, Hartstein and Stevens 2005) that are considered to have more important effects on benthic characteristics than any effects of the mussel farmers' practices (Miron et al. 2005). Sedimentation from mussel farms in areas where biodeposit dispersal and water exchange are limited can result in severely reduced conditions (Dahlbaeck and Gunnarsson 1981, Stenton-Dozey et al. 2001, Christensen et al. 2003) which limit denitrification (Herbert 1999). The physical structure of cultures reduces the water flow through the farm and generates undercurrents beneath the farm (Plew et al. 2005). Therefore farm configuration and depth of the dropper lines are likely to influence the dispersal of sedimenting material and more research should be done to investigate how these parameters can be optimised to minimise benthic impacts. Consequently I suggest that site-specific hydrodynamic and biogeochemical conditions should be taken into account when planning new mussel farms and sediment-water nutrient fluxes should be monitored before and after farm development to prevent excessive modifications of nutrient dynamics.

Chapter 5

Modelling mussel biodeposit dispersal and remineralisation

5.1 Introduction

Cultured mussels modify mass and energy fluxes in coastal ecosystems by linking the upper water column in which they live, attached to suspended structures, to the benthos. They feed on phytoplankton and organic particles in the water column and produce faeces and pseudofaeces (biodeposits) which are rapidly deposited to the seabed. This organic matter biodeposition stimulates benthic metabolism and enhances the regeneration of nutrients (e.g. Christensen et al. 2003) and can lead to changes in sediment characteristics (e.g. Dahlbaeck and Gunnarsson 1981) and benthic community composition (Tenore et al. 1982, Stenton-Dozey et al. 2001). In some previous studies, these mussel farm impacts were confined to less than 50 m from the farm boundary (Mattsson and Linden 1983, Chamberlain et al. 2001, Hartstein and Stevens 2005). However, these farms were located in low energy environments and it has been shown that the degree of environmental impact is directly related to the system's ability to disperse biodeposits from the farm (Chamberlain et al. 2001, Newell 2004).

Mussel aquaculture is growing worldwide and in New Zealand major expansions of the cultivation of the Greenshell^{TM} mussel *Perna canaliculus* are planned (Jeffs et al. 1999, Christensen et al. 2003). Many of the proposed farms are much larger than existing farms, thus local impacts may become more severe and far-field impacts more likely (Broekhuizen et al. 2002); however, up to now far-field effects of aquaculture have received little attention (Grant et al. 2005). Numerical modelling is a useful tool to simulate the potential interactions of bivalve aquaculture and its supporting coastal marine ecosystem. Thus it improves our understanding and can support decision making processes when assessing the impacts of expanding bivalve cultivation. The most important potential effects of

suspended bivalve culture are biodeposition and seston depletion (Grant et al. 2005) and several mathematical models have been developed to assess their environmental impacts (e.g. Dowd 1997, Campbell and Newell 1998, Gangnery et al. 2001). Most models have been focused mainly on predicting bivalve growth and carrying capacity (Dowd 2005) and only few models specifically include biodeposition (Bacher et al. 1995, Chapelle et al. 2000, Dowd 2005, Grant et al. 2005, Hartstein and Stevens 2005). In some models biodeposits are included in a general benthic detritus compartment (Bacher et al. 1995, Dowd 2005). The model by Grant et al. (2005) assumes that the influence of mussels is homogenised throughout a whole bay but this assumption does not hold in our study area. Chapelle et al. (2000) developed their model for a lagoon ecosystem and Hartstein and Stevens (2005) simulated only biodeposit dispersal. Consequently there is a need for more models simulating the deposition and subsequent remineralisation of biodeposits from suspended bivalve culture (Henderson et al. 2001).

This chapter is divided into two major parts. The first part (Section 5.2) comprises a model of mussel faeces dispersal from a mussel farm and the second part (Section 5.3) a model of organic material remineralisation in the sediments below a mussel farm.

5.2 Modelling biodeposit dispersal

5.2.1 Introduction

Biodeposition from suspended bivalve culture enhanced the flux of organic material to the sediments. Numerical models can be used to predict the footprint of farms by simulating the dispersal of biodeposits through the water column as well as their redistribution on the sediment surface via resuspension, thus assessing the spatial extent of the environmental impact. Chapelle et al. (2000) and Bacher et al. (1995) simulate the impact of oyster culture on nitrogen dynamics in the Thau lagoon (France) and in their box models biodeposition drives sediment nutrient and oxygen fluxes but actual biodeposition rates are not presented. The ecosystem box model by Dowd (2005) simulates a benthic detrital pool that contains biodeposits as well as other detritus. The time evolution of this

pool shows high frequency fluctuations associated with resuspension and settling but this model does not have a spatial component. Grant et al. (2005) took a system-wide budget approach to assess the susceptibility of different sites to mussel culture impacts. The fate of egested biodeposits was portrayed as the balance between production and flushing by tides and most of the mechanics of deposition were avoided. Hartstein and Stevens (2005) modelled the dispersal of mussel biodeposits with a particle tracking model. Sinking trajectories were calculated from current magnitude and direction, sinking speed and eddy diffusion coefficients but resuspension was ignored. Rather than modelling the explicit hydrodynamics of their study sites (two sheltered and one exposed) they drove their model with the observed variability and conducted a sensitivity analysis of the controlling parameters. None of these studies explicitly modelled biodeposit dispersal and validated models with *in situ* biodeposition measurements.

The aim of this study was to simulate the initial deposition and assess the potential for subsequent resuspension of faeces produced by cultured mussels in the western Firth of Thames, New Zealand. My objective was to simulate mussel faeces dispersal by using a simple particle tracking model and parameterising and validating the model with data measured in Chapters 2 and 4. To my knowledge this is the first attempt to assess these two transport processes separately and to quantify the contribution of resuspension to the dispersal of mussel faeces. Mussel pseudofaeces are fragile and break up easily when exposed to water flow (Chapter 2). Therefore they have very different transport characteristics in comparison with the compact faecal pellets and some may never reach the sediment. In this study I examine the dispersal of mussel faeces because *in situ* data are available to validate model results. In addition faeces are produced continuously whereas pseudofaeces production is more intermittent, being strongly influenced by the concentration of suspended particulate material (Hawkins et al. 1999).

5.2.2 Methods

5.2.2.1. Study area and mussel farm description

This study was conducted in the Firth of Thames, New Zealand, a large (1100 km^2) shallow (maximum water depth = 30 m) estuary that opens onto the Hauraki Gulf (Fig. 5.1). I assessed the dispersal of mussel faeces from a small (40 ha) mussel farm in the Western Firth of Thames (Fig. 5.2) that has been operating at its current size since 1994. The average water depth around the farm is approximately 10 m with shallower areas in the south-west and deeper areas in the north-east. Mussels (*Perna canaliculus*) are cultured in three blocks perpendicular to the shore on longlines in the upper 6 m of the water column. These blocks are 1000 m long in east-west direction and cover areas of approximately 12, 11 and 19 ha each. The gaps between them are about 24 and 13 ha.

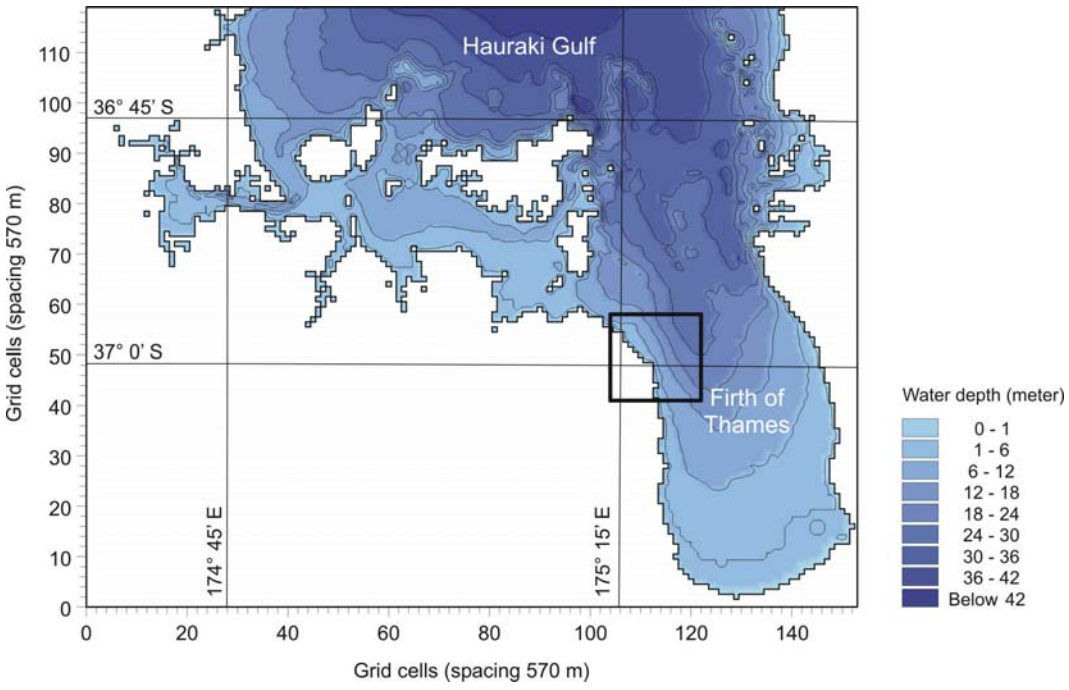

Figure 5.1. Hauraki Gulf grid comprised of 570 × 570 m^2 grid cells covering the Firth of Thames and lower and middle Hauraki Gulf. Black rectangle indicates the position of the mussel farm grid.

5.2.2.2. Bathymetry

Two bathymetry grids were used for this study. The first was a regular grid of 154 × 120 cells, each 570 × 570 m^2 that covered the middle Hauraki Gulf (Fig. 5.1), hereafter referred to as the Hauraki Gulf grid. This grid was provided by John Oldman (NIWA) and originally presented in Black et al. (2000). The second was a regular grid of 55 × 52 cells, each 190 × 190 m^2 that covered the area around the mussel farm in the Firth of Thames (Fig. 5.2), hereafter referred to as the mussel farm grid. The grids are orientated North/South. Due to the limited available depth data it was not possible to create a finer grid. Depths were digitised from RNZN Navigation charts NZ53, NZ532 and NZ533. Evenly spaced grids were created by interpolation with the Kriging method using the Golden Software 'Surfer' package and the ASCII files that were produced were imported into the Danish Hydraulic Institute (DHI) Water and Environment (http://www.dhi.dk) modelling software.

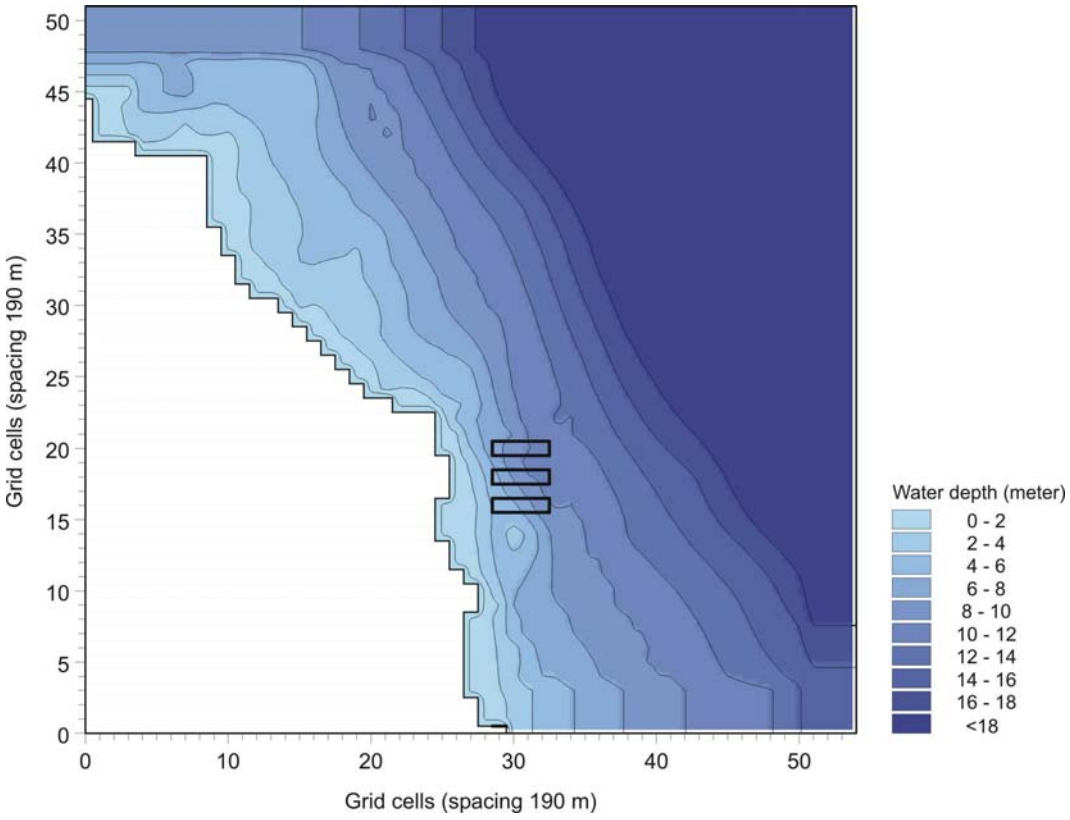

Figure 5.2. Mussel farm grid comprised of 190 × 190 m^2 grid cells. Enclosed grid cells indicate the cells representing the mussel farm.

5.2.2.3. Hydrodynamic model

Model description

The DHI two-dimensional MIKE 21 Flow Model was used to model currents in the mussel farm. This model is a general finite difference modelling system for the simulation of water levels and flows in estuaries, bays and coastal areas. It simulates unsteady two-dimensional flows in one vertically homogeneous layer. The water column around the farm is usually well mixed (Chapter 4) and I assumed that the water flow in this area could be simulated adequately by a two-dimensional model. In addition, I did not have sufficient data to calibrate and verify a three-dimensional model.

Two hydrodynamic models were implemented using the Hauraki Gulf grid and the mussel farm grid respectively (described above). The Hauraki Gulf model was forced with tidal elevations at the open boundary predicted from the 13 most dominant tidal constituents (M_2, S_2, N_2, K_2, K_1, O_1, P_1, Q_1, $2N_2$, MU_2, NU_2, L_2 and T_2) at the centre point of the open ocean boundary. Water flow information was extracted from the results of this simulation at the boundary locations of the smaller mussel farm grid (which was entirely enclosed by the larger grid). These results were used to force the mussel farm model at the four open boundaries. This approach enabled me to simulate the area of interest around the farm with a finer grid while maintaining the influence of current flows from the central Hauraki Gulf area.

Parameters

The parameters required for the hydrodynamic model were the Manning number ($m^{1/3}$ s^{-1}) and the wind friction coefficient (-). The former describes bed resistance and the latter determines how readily near-surface flows are influenced by the wind. Because no data were available to provide estimates of these parameters, the default values of 32 $m^{1/3}$ s^{-1} and 0.0026, respectively, were used. Wind data (hourly measurements) were obtained from a weather station at Paeroa, approximately 55 km south-east of the mussel farm (Fig. 5.3).

Table 5.1. List of symbols used in this section. Sources of parameter values are given in the text.

Symbol	Definition	Unit	Value
d	fall diameter	cm	0.042 – 0.136*
D	cylinder (faecal pellet) diameter	cm	0.022 – 0.186
D_l	longitudinal dispersion coefficient	$m^2\ s^{-1}$	0.02 – 0.5*
D_t	transversal dispersion coefficient	$m^2\ s^{-1}$	0.02 – 0.5*
D_v	vertical dispersion coefficient	$m^2\ s^{-1}$	0.0001 – 0.01*
g	acceleration due to gravity	$cm\ s^{-2}$	981
L	cylinder (faecal pellet) length	cm	0.10 – 6.52
S	relative particle density	-	1.025 – 1.252*
SV	faecal pellet sinking velocity	$cm\ s^{-1}$	0.9 – 4.3
u(z)	horizontal flow speed	$m\ s^{-1}$	simulated
u_*	bed shear velocity	$m\ s^{-1}$	simulated
u_{*C}	critical bed shear velocity	$cm\ s^{-1}$	0.48
z_0	bed roughness	m	0.0002 – 0.005*
θ_c	critical Shields parameter	-	0.07
κ	von Karman's constant	-	0.41
μ	viscosity	$g\ cm^{-1}\ s^{-1}$	0.01
ρ	faecal pellet density	$g\ cm^{-3}$	1.048 – 1.280*
ρ_f	fluid density	$g\ cm^{-3}$	1.022

* model parameters that were manipulated

Simulation period and model validation

The hydrodynamic model was validated by comparing simulated water depths, current speeds and directions to data measured with an InterOcean Systems S4 Current Meter (V. 5.153) and conducting a correlation analysis. The S4 was deployed from 13 December 2004 to 1 February 2005 approximately 50 m east and 20 m north of north-eastern corner of the farm to minimise effects of the farm structure on measured currents. Since the current meter was deployed 1 m above the sea bed, the depth-averaged current speeds were calculated by assuming a standard "law of the wall" velocity profile to estimate the free-stream currents (Nielsen 1992):

$$\mathrm{u(z)} = \frac{u_*}{\kappa} \ln\left(\frac{\mathrm{z}}{z_0}\right) \tag{5.1}$$

where u(z) is the horizontal flow speed (m s^{-1}) at height z above the sea bed (m), u_* the bed shear velocity (m s^{-1}), κ the von Karman's constant (taken to be 0.41) and z_0 the bed roughness length (m).

The simulation period for the Hauraki Gulf model was from 13 December 2004, 15:00, to 1 February 2005, 15:00, with a timestep of 20 s. The mussel farm model simulation commenced on 14 December 2004 at 12:00 to allow time for the water flows in the larger-scale Hauraki Gulf model to stabilise. The timestep for this model was 10 s and the simulation period was 49 d. Current direction, speed and water depth were saved in half-hour intervals.

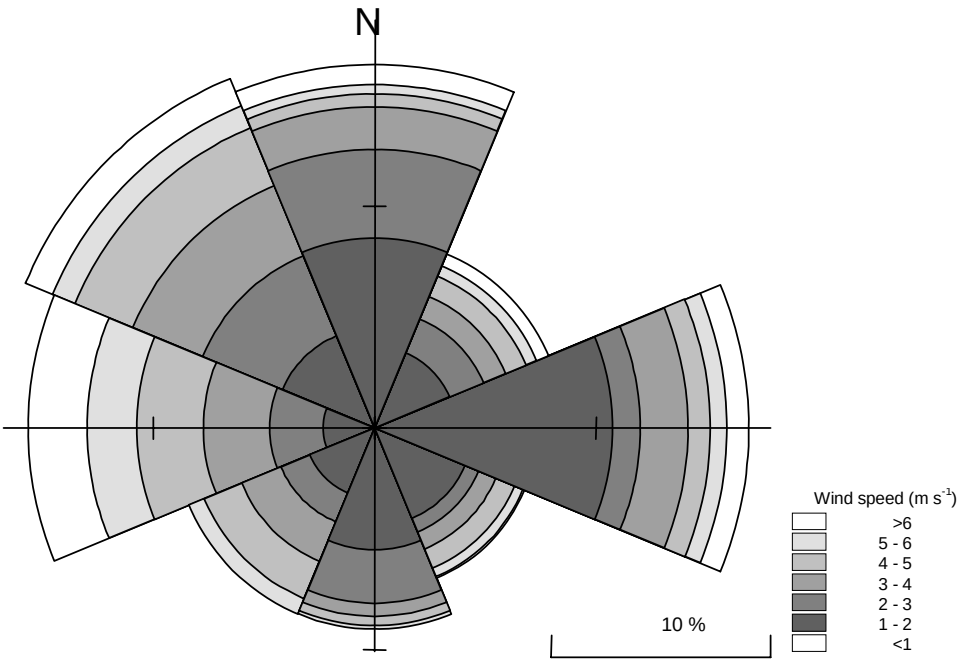

Figure 5.3. Wind rose for time period of Hauraki Gulf model simulation. Each sector projects in the direction from which the wind blew. Distance from centre represents percentage of time wind blew from the corresponding direction.

5.2.2.4. Particle tracking models

Model description

To examine the dispersal of particles, I used the DHI MIKE 21 & MIKE 3 particle analysis (PA) module in the mussel farm grid. The PA module is used to simulate the transport and fate of dissolved and suspended substances discharged in lakes, estuaries, coastal areas or in the open sea. It is based on the random walk technique where an ensemble of particles is followed instead of solving the Eularian advection-diffusion equation at each grid cell. The particles move due to the advective current and turbulent fluctuations. The advective velocities are obtained from the results of the mussel farm hydrodynamic model and turbulence is described by dispersion coefficients. The output of the PA module is control volume specific, e.g. given as kg m^{-2} for sedimentation and kg m^{-3} for suspended particle concentrations. These results were converted into a particle (faecal pellet) specific output using the average particle weight of 0.91 mg faecal $pellet^{-1}$ (mean of 20 measurements of faecal pellets collected in sediment traps over four seasons, see Chapter 4; standard deviation = 0.38, unpublished data). Two models were run: The first one ("initial dispersal model") was intended to simulate only the initial dispersal of mussel faeces from the farm. The second one ("resuspension model") was intended to simulate the initial dispersal as well as subsequent resuspension of these particles. By running the models separately I was able to assess the contribution of the two transport processes to the overall mussel faeces dispersal.

Farm representation

The mussel farm was represented by 12 grid cells (Fig. 5.2), each farm block being one grid cell wide and 4 cells long. Particles were released at each timestep 1, 3 and 6 m below the sea surface from the centre of each of these cells. In the time taken by particles to first reach the seafloor, they often travelled only a short horizontal distance (relative to the 190 × 190 m^2 cell size). Consequently a large proportion of the particles remained in their release cell and the resulting distribution failed to show a gradual dispersal pattern. In addition, simulating only one release point per 190 × 190 m^2 grid cell, i.e. 12 release points in total, was not sufficiently detailed to represent the deposition from the mussel farm well. To obtain a better spatial resolution the output frequency parameter, that defines the

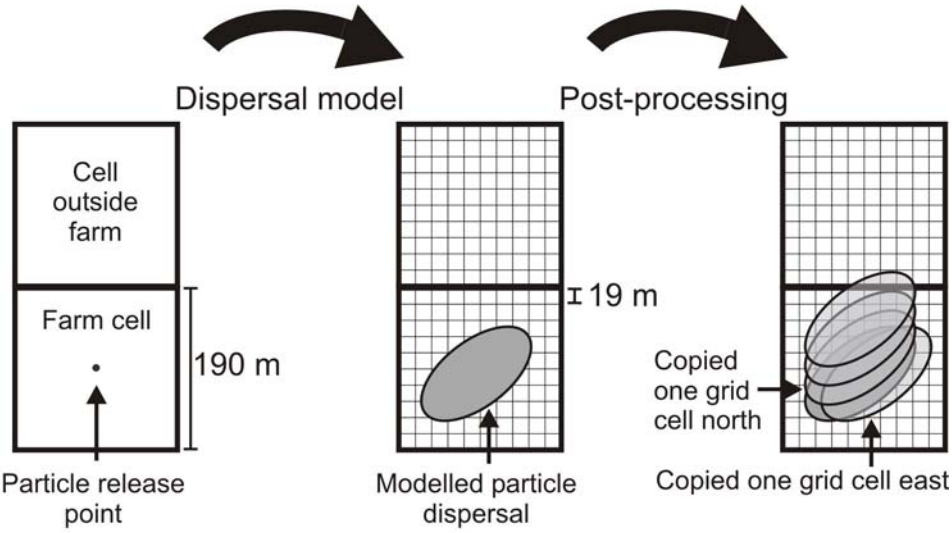

Figure 5.4. Illustration of post-processing of model results. In the dispersal model output each 190 × 190 m^2 grid cell was divided into 100 19 × 19 m^2 grid cells. Modelled particle distribution was copied from their initial position relative to each of the corresponding 100 19 × 19 m^2 grid cells to obtain a better spatial resolution of results.

resolution of the saved particle concentration relative to the cell size, was set to -10. Therefore each 190 × 190 m^2 cell of the mussel farm grid was represented by 100 cells in this finer grid of 541 × 511 cells each 19 × 19 m^2 (hereafter referred to as dispersal grid, Fig. 5.4). This is possible because the PA module stores individual particle positions and only converts them to concentrations after the simulation. To simulate additional release points (one per 19 × 19 m^2 dispersal grid cell) the particle concentrations obtained from the model runs were copied from their original position relative to each of the 100 dispersal grid cells that correspond to the original mussel farm grid cell (Fig. 5.4). This post-processing simulated a particle release from each of the dispersal grid cells, i.e. 1200 release points in total, and provided a more spatially even result.

Parameters

In the PA module, particles are characterised by their sinking velocity (m s^{-1}), relative density (-), fall diameter (m) and critical Shields parameter (-). Because I provided sinking velocities from measurements, relative density, fall diameter and critical Shields parameter were not used within the model to simulate the initial dispersal of particles but they were important in the resuspension model (see below).

Sinking velocity

Particle sinking velocities (0.9 – 4.3 cm s^{-1}) were obtained from *Perna canaliculus* faecal pellet sinking velocity measurements (Chapter 2). These measurements were done for faecal pellets produced by the wide size range of mussels (27 to 114 mm shell length) that can be found at the farm. These velocities were specified as probability distributions that were calculated from the measured settling rates using 0.2 cm s^{-1} intervals.

Density

No measurements of faecal pellet densities were available and therefore densities were indirectly calculated from the sinking velocities and faecal pellet size measurements (Chapter 2) using the semiempirical equation for sinking velocity SV (cm s^{-1}) of a cylinder, a modification of the Stokes settling equation (Komar et al. 1981):

$$SV = 0.079 \frac{1}{\mu}(\rho - \rho_f) g L^2 \left(\frac{L}{D}\right)^{-1.664} \quad (5.2)$$

where L and D are the cylinder (faecal pellet) length (cm) and diameter (cm), g the acceleration due to gravity (981 cm s^{-2}), ρ in the particle density (g cm^{-3}), and μ and ρ_f are the fluid viscosity (g cm^{-1} s^{-1}) and density (g cm^{-3}). The calculated faecal pellet density was 1.048 ± 0.013 g cm^{-3}. Faecal pellets have a cylindrical shape but with open edges that curl up and inwards creating a longitudinal groove (Chapter 2). Nevertheless, a cylinder was the most similar shape to *Perna canaliculus* faecal pellets for which an empirical equation exists for the calculation of densities. The application of equation 5.2 is limited to particles with $\rho_f \cdot SV \cdot L/\mu < 2$ but this condition was not met by the mussel faecal pellets ($\rho_f \cdot SV \cdot L/\mu$ = 10 – 177) due to their large size and high sinking velocities. Equation 5.2 has not been tested for $\rho_f \cdot SV \cdot L/\mu > 3$ and therefore the calculated density may not be correct. The only published measured faecal pellet densities I could find were those of copepod and polychaete pellets. They range from 1.07 to 1.28 g cm^{-3} (e.g. Taghon et al. 1984, Butler and Dam 1994, Feinberg and Dam 1998) and show that the value estimated in this study is somewhat low. I tested the sensitivity of the model to faecal pellet density by running the resuspension model using the maximum published density and comparing the results to the original resuspension model result.

Fall diameter

The fall diameter of a particle is the equivalent diameter of a sphere that has the same sinking velocity. I calculated the diameter of spheres that have the same sinking velocities as *Perna canaliculus* faecal pellets under the experimental conditions (Chapter 2) from the Stokes equation. The mean fall diameter calculated from all faecal pellet sizes is 0.136 ± 0.022 cm (n = 149).

Critical Shields parameter

Particles are redistributed after initial contact with the sediment when the bed shear velocity is higher than the critical shear velocity for the simulated particles, i.e.:

$$u_* > \sqrt{\theta_c (S-1) g d} \tag{5.3}$$

where θ_c the critical Shields parameter, S the relative particle density ($S = \rho/\rho_f$) and d the particle fall diameter (m). If the bed shear velocity is slightly above the critical shear velocity at the erosion threshold, particles jump along the bed. At higher shear velocities particles may be resuspended. The critical Shield's parameter is defined as:

$$\theta_c = \frac{{u_{*C}}^2}{(S-1) g d} \tag{5.4}$$

where u_{*C} is the critical bed shear velocity (cm s^{-1}) for the simulated particles. The critical Shield's parameter was calculated from measured bed shear velocities required to erode *Perna canaliculus* faecal pellets from sediments (Chapter 2) and the parameters estimated above. The obtained value of 0.07 represents the critical Shields parameter relating to the erosion of 50 % of all faecal pellets produced by mussels of all size classes used in the erosion experiment (Chapter 2).

Dispersion coefficients

Two horizontal (longitudinal, D_l, and transversal, D_t) and one vertical (D_v) dispersion coefficients were used in the MIKE 21 PA module. Because no measurements were available I applied dispersion coefficients (D_l, D_t = 0.1 m^2 s^{-1}; D_v = 0.001 m^2 s^{-1}) published by Cromey et al. (2002) who simulated the resuspension of fish farm waste using a 10 m resolution grid.

Bed roughness

A typical estuarine bed roughness of z_0 = 0.001 m was selected (Black and McShane 1990).

Simulation period and model validation

Because of the high particle sinking velocities and shallow water depth around the farm area, particles settle quickly (in a few minutes). A simulation period of 25 h was chosen to represent two tidal cycles and allow a small timestep of 10 s. These parameters ensured that a particle at most moves one grid cell during one timestep. Preliminary model runs showed that longer simulation periods did not change the initial dispersal pattern. The resuspension model result does depend on the simulation period (see discussion), but because this model did not include particle decay particles were continuously redistributed and a steady-state solution could not be achieved. The chosen simulation period was considered long enough to provide a good estimate of the potential for resuspension while keeping the model runtime acceptable.

The initial dispersal model was validated by converting simulated particle deposition rates to faecal pellet deposition rates and comparing these to measurements of initial deposition rates made under the farm, at the edge of the farm and at a reference as described in Chapter 4. I converted the model output to actual faecal pellet deposition rates by estimating the number of cultured mussels and applying faecal pellet production rates measured during laboratory experiments (unpublished data). The farm comprises 145 longlines that each support on average 2093 m of dropper line. The mussel density on the dropper lines depends on mussel age and farming practice and I used a value of 140 m^{-1} which was applied in a modelling study at a nearby mussel farm in Wilson's Bay in the eastern side of the Firth of Thames (Broekhuizen et al. 2002). I therefore estimate that the farm contains ~4.2×10^7 mussels. The average faecal pellet production rate measured in the laboratory during the biodeposit production experiment (Chapter 2) was 8.35 (± 2.7 SD, n = 32) faecal pellets $mussel^{-1}$ h^{-1} (unpublished data) and hence the total number of faecal pellets produced by mussels in the farm is estimated as ~3.5×10^8 h^{-1}. Over the 25 h particle tracking simulation period this amounts to ~8.9×10^9 faecal pellets and comparing this to

the ~3.2×10^5 particles released in the model produced a scaling parameter of 27371 that I use to convert the model output to a simulated faecal pellet deposition rate.

Sensitivity analysis

The initial dispersal model simulation period was between spring and neap tide so I expected the predicted dispersal distances to represent average patterns. To test the influence of tides on faecal pellet dispersal the initial dispersal model was also run during a spring ("spring tide dispersal model") and a neap tide ("neap tide dispersal model") and dispersal distances compared to those predicted by the original initial dispersal model.

A sensitivity analysis was conducted to test the sensitivity of the model to the dispersion coefficients and bottom roughness since published values were chosen for these parameters. The horizontal dispersion coefficients were set to 0.02 and 0.5 $m^2\ s^{-1}$, the vertical dispersion coefficient to 0.0001 and 0.01 $m^2\ s^{-1}$ and the bed roughness to 0.0002 and 0.005 m (Cromey et al. 2002) and the simulated initial dispersal patterns compared.

5.2.3 Results

5.2.3.1. Hydrodynamic model

Simulated flows in the Firth of Thames

The area of interest for this study is the western side of the Firth of Thames and therefore I present the model results for the Firth of Thames only rather than the whole Hauraki Gulf model domain. Currents in the Firth of Thames show a clear tidal pattern (Fig. 5.5). The model predicts strongest flows in the central southern Firth of Thames with current speeds up to 0.68 m s^{-1}. The residual (time-averaged) currents show the long-term water movements in the Firth of Thames were generally very low over the simulated period. Over the 25 h period of the particle tracking simulation current speeds in the area of the farm reached a maximum of 0.37 m s^{-1} and were on average 0.17 m s^{-1} (Fig. 5.6). Residual (time-averaged) currents were low (<0.02 m s^{-1}) and flowed southward through the farm (Fig. 5.7).

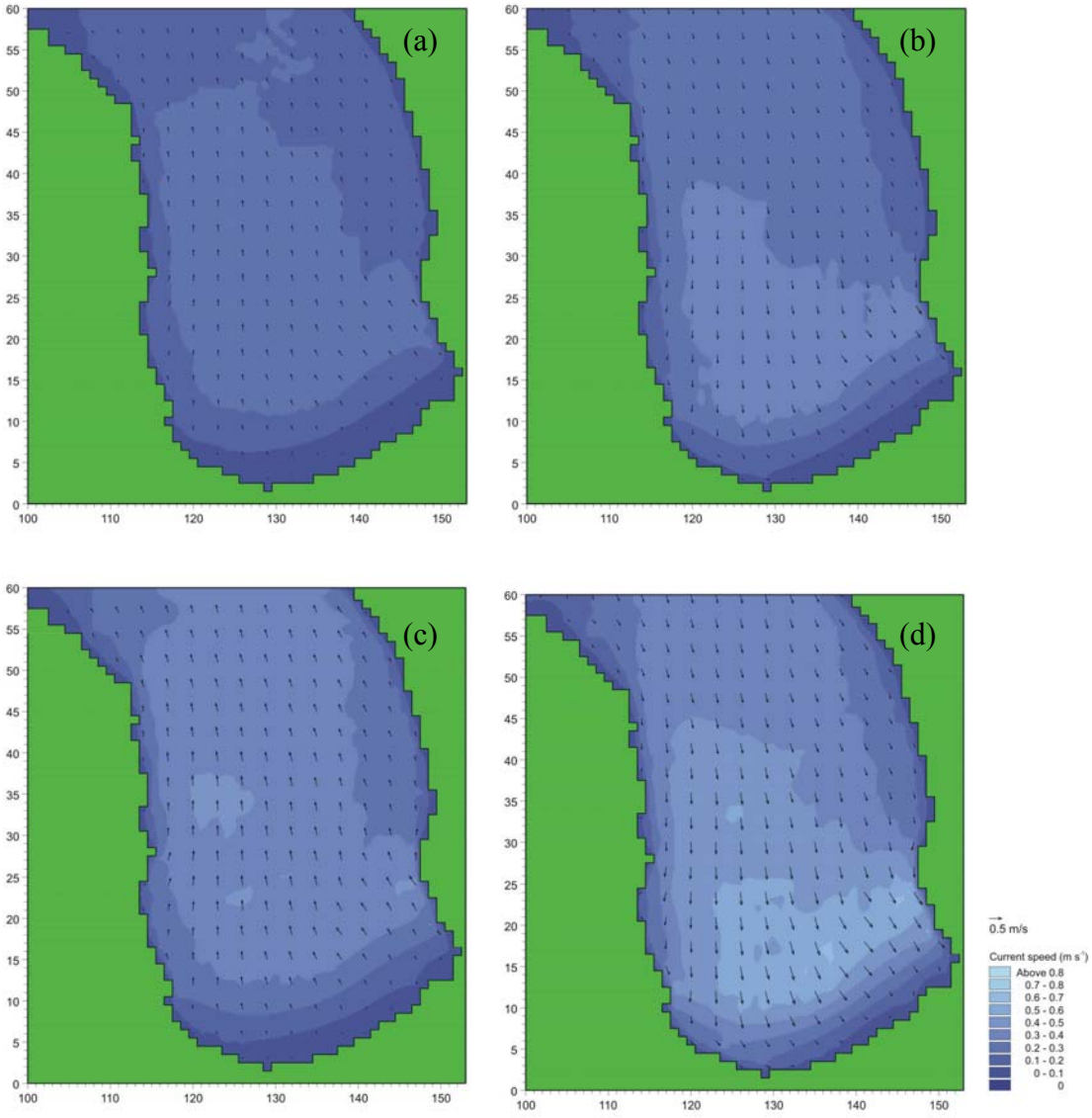

Figure 5.5. Predicted currents during peak (a) neap ebb, (b) neap flood, (c) spring ebb and (d) spring flood tide in the Firth of Thames during Hauraki Gulf model simulation period. Coordinate labels show grid cells.

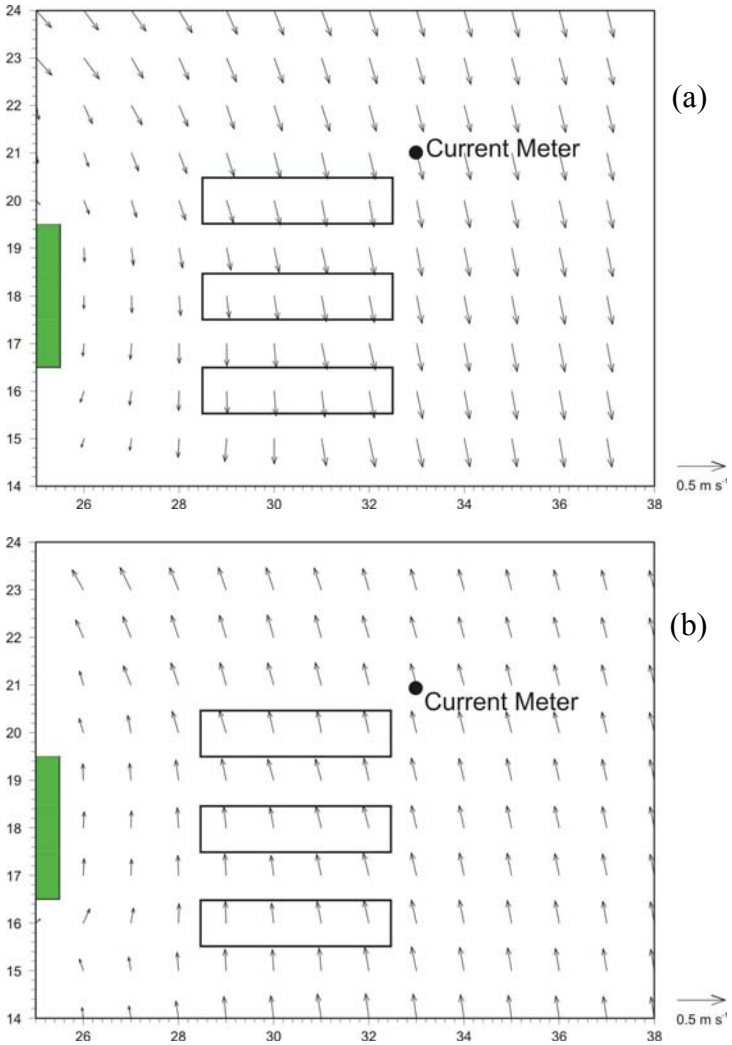

Figure 5.6. Predicted currents at peak (a) flood and (b) ebb tide during particle tracking model simulation period. Rectangles represent mussel farm blocks. Black dot represents position of current meter used to validate model results. Coordinate labels show grid cells.

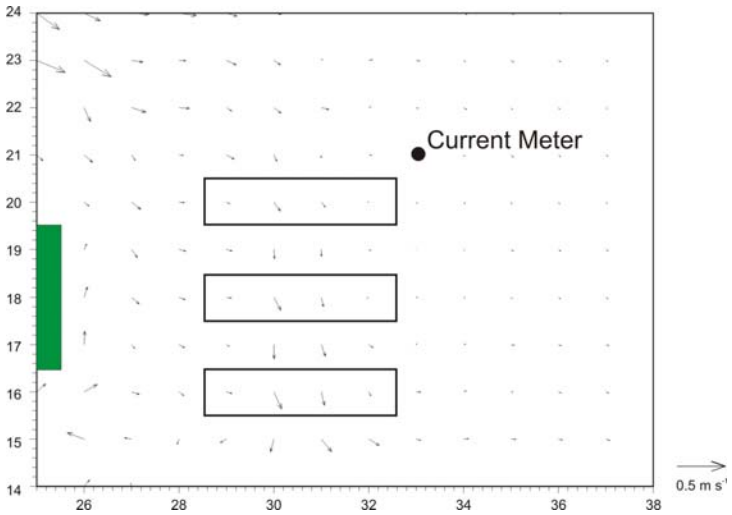

Figure 5.7. Residual currents during particle tracking model simulation period. Rectangles represent mussel farm blocks. Black dot represents position of current meter used to validate model results. Coordinate labels show grid cells.

Hydrodynamic model validation

Simulated currents had a lower maximum speed and narrower range of directions than those measured (Fig. 5.8). The correlation between observed and simulated water depth was strong ($r^2 = 0.98$), but the relationships of observed and simulated current speed and direction were very variable ($r^2 = 0.29$ and $r^2 = 0.61$, respectively) for the Hauraki Gulf model period.

There was no consistent pattern in the relationship of predicted and measured current speeds. The model generally underestimated current speed during the beginning of the simulation period and overestimated it towards the end. During the time of strong ebb and tidal flows the model predicted current direction adequately but it did not perform well during periods of low current speeds. I chose a 25 h period for the particle tracking model simulation during which simulated and measured current speed and direction were in relatively good agreement (Fig. 5.9).

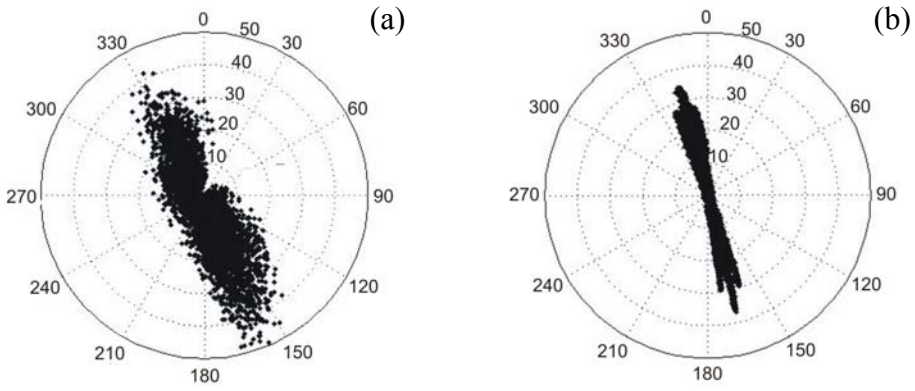

Figure 5.8. (a) Observed and (b) simulated current speed (cm s^{-1}, shown as distance from centre) and direction (° T, shown on outer circle) during Hauraki Gulf model period.

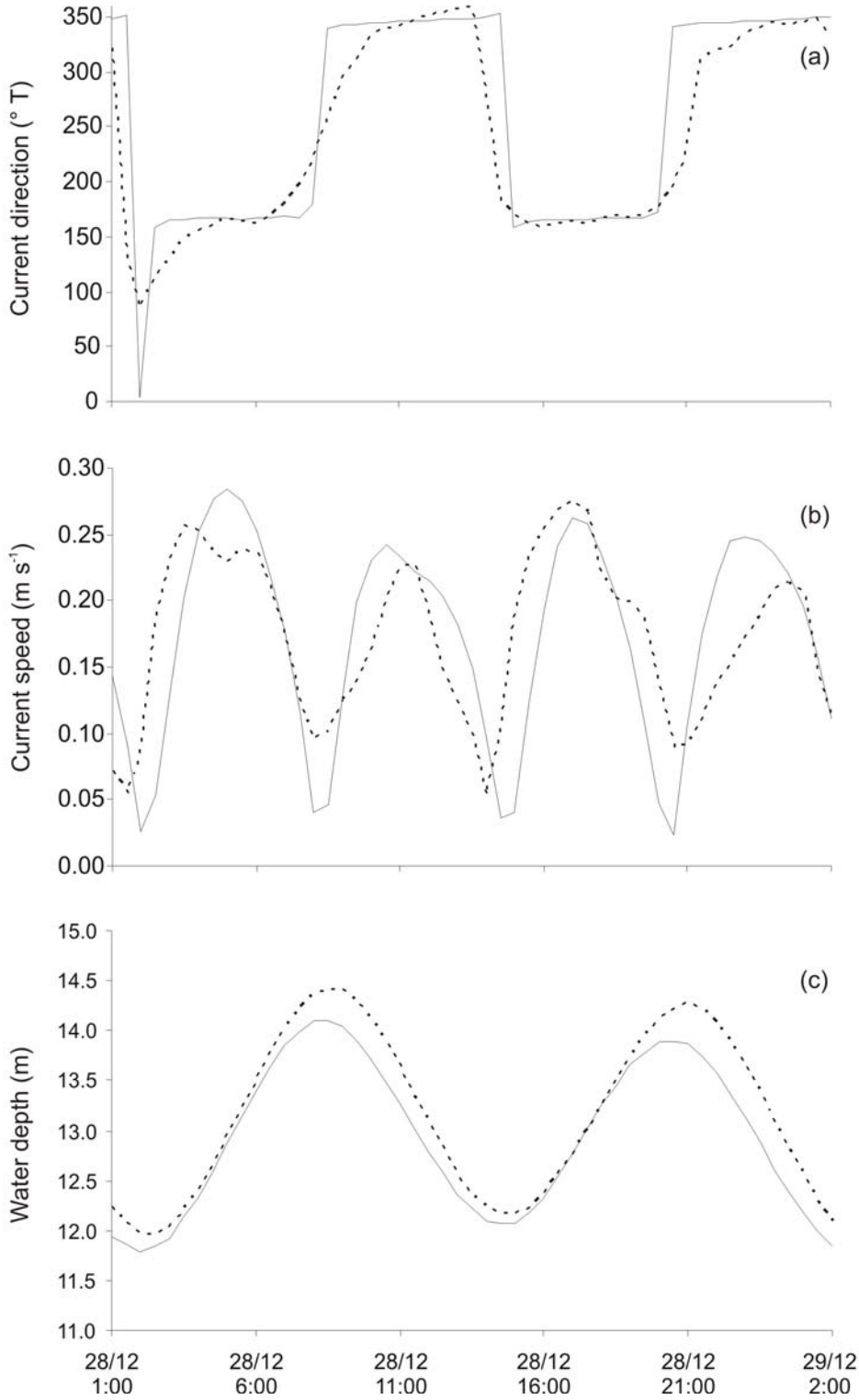

Figure 5.9. Simulated (solid line) and observed (dashed line) (a) current direction (˚ T), (b) current speed (m s^{-1}) and (c) water depth (m) during particle tracking model simulation period.

5.2.3.2. Initial dispersal model

Initial dispersal distances

Simulated faecal pellets dispersed primarily to the north with a maximum initial dispersal distance from the mussel farm of approximately 320 m (Fig. 5.10, Table 5.1). Particles could be found up to 57 m to the south, 95 m to the west and 38 m to the east of the farm, however, 88.3 % of all released particles were deposited beneath the three farm blocks and 95.7 % beneath the mussel farm (including the gaps between the three blocks). The maximum settling rate was 897 faecal pellets m^{-2} h^{-1} under the southern farm block. Areal settling rates decreased rapidly towards the edges and beyond the farm area. In addition to the maximum dispersal distance, I used the maximum distance from the farm edge to which settling rates higher than 100 faecal pellets m^{-2} h^{-1} were predicted to compare dispersal patterns among the different model runs. I chose 100 faecal pellets m^{-2} h^{-1} because this concentration is approximately one order of magnitude less than the maximum settling rate and therefore represents a concentration considerably lower than the maximum but still sufficiently high to cause changes in sediment characteristics (see measured rates below and Chapter 4). This distance was 57 m in this initial dispersal simulation.

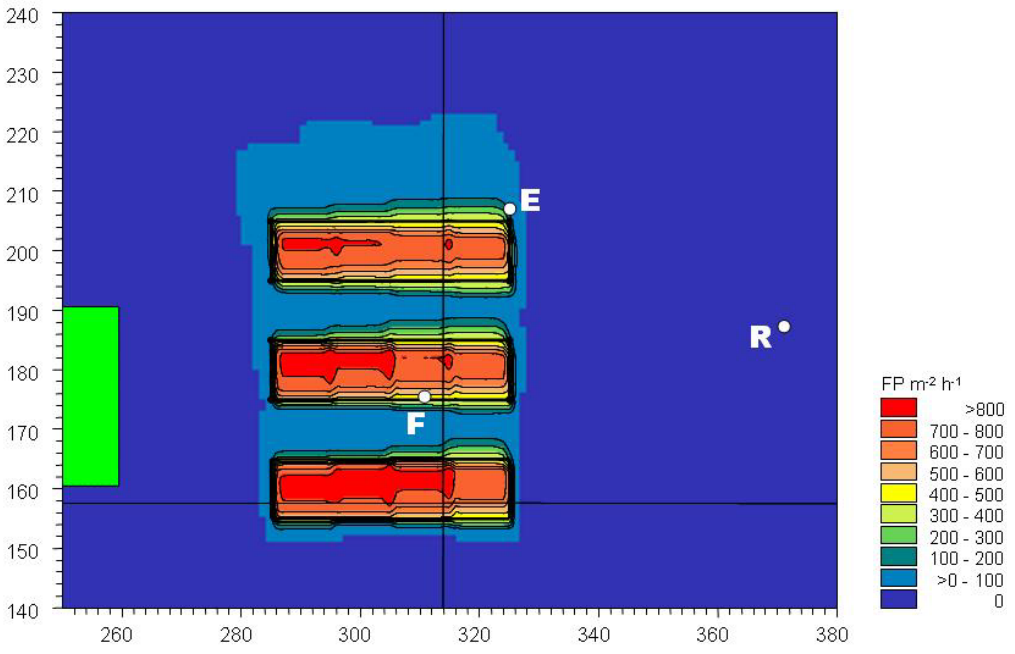

Figure 5.10. Faecal pellet (FP) sedimentation rates (FP m^{-2} h^{-1}) predicted by initial dispersal model. White dots represent study sites (F = Farm, E = Edge, R = Reference) where *in situ* faecal pellet sedimentation rates were used to validate model results. Coordinate labels show grid cells.

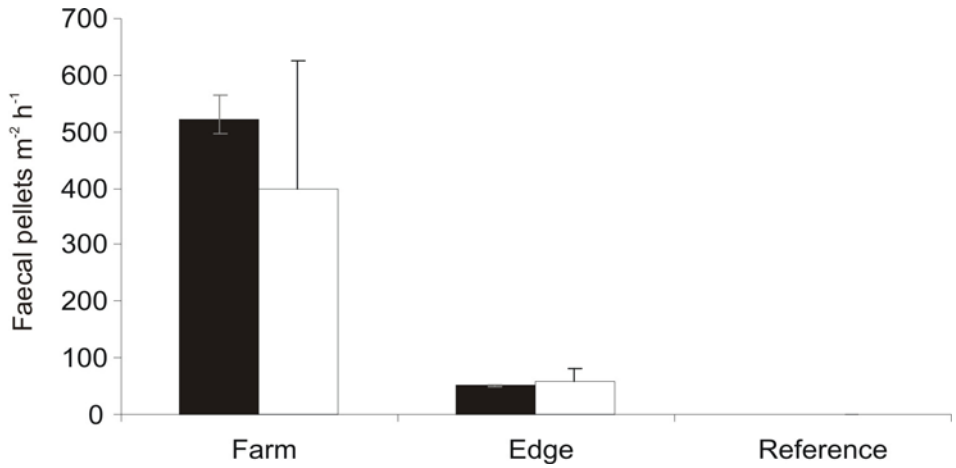

Figure 5.11. Comparison of faecal pellet (FP) sedimentation rates from model simulation (black bars) and *in situ* measurements (white bars, +SD) under the mussel farm (Farm), at the edge of the farm (Edge) and at a reference site (Reference). Error bars on model results indicate sedimentation rates obtained from neap (Farm: 565 FP m^{-2} h^{-1}, Edge: 48 FP m^{-2} h^{-1}) and spring tide (Farm: 495 FP m^{-2} h^{-1}, Edge: 52 FP m^{-2} h^{-1}) simulations. Site locations are shown in Fig. 5.10.

Initial dispersal model validation

The model predicted sedimentation rates of 521 faecal pellets m^{-2} h^{-1} at the farm site, 53 faecal pellets m^{-2} h^{-1} at the edge site and no sedimentation at the reference site (Fig. 5.11). The measured rates (mean of four seasons ± SD) were 399 ± 226 faecal pellets m^{-2} h^{-1} (farm), 57 ± 23 faecal pellets m^{-2} h^{-1} (edge) and 0 faecal pellets m^{-2} h^{-1} (reference; Giles, unpublished data).

Initial dispersal model sensitivity analysis

As expected faecal pellet dispersal was enhanced during the spring tide and reduced during the neap tide simulation (Table 5.2). During spring tide the maximum dispersal to the north was increased by 114 m and in all other directions by 19 m. During neap tide dispersal distances were reduced to the north (by 76 m) and the south (by 19 m) but did not change in the east or west. The distance from the farm boundary where settling rates were higher than 100 faecal pellets m^{-2} h^{-1} was increased by 38 m during spring tide and reduced by 19 m during neap tide.

The initial dispersal of faecal pellets showed little sensitivity to changes in the tested parameters (Fig. 5.12, Table 5.2). The pattern of dispersal remained the same but there were some changes in the dispersal distances. For all tested

Table 5.2. Dispersal distances of mussel faecal pellets (FP) predicted by the initial dispersal and resuspension models.

Model description/ tested parameter value	Maximum distance of FP dispersal (m) North	South	East	West	Distance to 100 FP m^{-2} h^{-1} (m)
Initial dispersal model					
Original	320	57	38	95	57
Spring tide	434	38	57	114	95
Neap tide	244	57	38	76	38
D_l=D_t=0.02 m^2 s^{-1}	320	57	19	57	57
D_l=D_t=0.5 m^2 s^{-1}	377	95	95	133	57
D_v =0.0001 m^2 s^{-1}	282	76	38	76	57
D_v =0.01 m^2 s^{-1}	738	76	38	247	57
z_0=0.0002 m	320	57	38	95	57
z_0=0.005 m	320	57	38	95	57
Resuspension model					
Original	1368	1197	380	494	171
ρ=1.28 g cm^{-3}	1311	1026	228	342	266

parameter values the footprint of the farm, where settling rates were higher than 100 faecal pellets m^{-2} h^{-1}, was identical to that of the original simulation and changes affected only the areas with low settling rates. Dispersal distances are given in metres; however, their accuracy is limited by the 19 m grid cell size.

A decrease in the horizontal dispersion coefficients resulted in a slightly reduced dispersion to the west (by 38 m) and east (19 m) but there were no changes toward the north or south (Fig. 5.12a). Increasing this parameter enhanced dispersal by 38 m in the south and west and 57 m in the north and east (Fig. 5.12b).

Lowering the vertical dispersion coefficient caused slightly reduced dispersal to the west (19 m) and north (38 m) and increased dispersal to the south (19 m; Fig. 5.12c). The initial dispersal was stronger to the north following the increase of the vertical dispersion coefficient (Fig. 5.12d). Particles were found up to 418 m further north than in the original simulation, however, concentrations were very

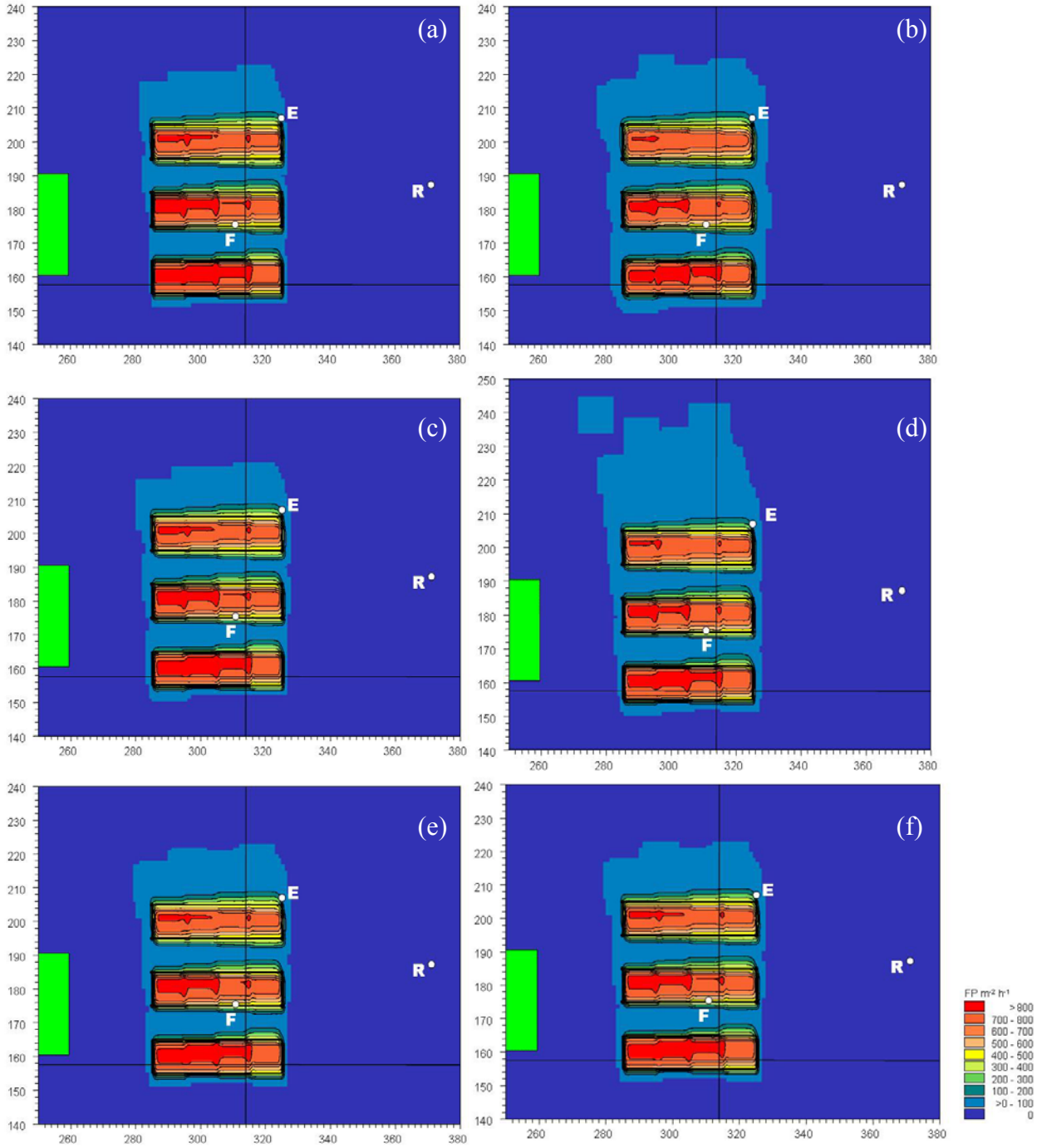

Figure 5.12. Results of sensitivity analysis (a) $D_l = D_t = 0.02$ m^2 s^{-1}, (b) $D_l = D_t = 0.5$ m^2 s^{-1}, (c) $D_v = 0.0001$ m^2 s^{-1}, (d) $D_v = 0.01$ m^2 s^{-1}, (e) $z_0 = 0.0002$ m and (f) $z_0 = 0.005$ m. White dots represent study sites (F = Farm, E = Edge, R = Reference) where faecal pellet sedimentation rates had been measured. Coordinate labels show grid cells.

low in this area (<2 faecal pellets m^{-2} h^{-1}). Particles dispersed 19 m further to the south and up to 152 m to the west. The dispersal was found to be insensitive to changes in the bed roughness (Fig. 5.12e and f).

5.2.3.3. Resuspension model

Particle dispersal was enhanced when pellets were allowed to redistribute via resuspension after their initial sedimentation (Fig. 5.13a). After the 25 h simulation period, particles could be found up to 1368 m north, 1197 m south, 494 m west and 380 m east of the farm. The maximum distance from the farm where settling rates higher than 100 faecal pellets m^{-2} h^{-1} were predicted was 171 m in the north. The highest settling rate under the farm was 754 faecal pellets m^{-2} h^{-1} under the middle farm block.

Increasing the particle density to 1.28 g cm^{-3} (which required the fall diameter to be set to 0.042 cm in order that sinking velocities implied by the Stokes equation remain consistent with measured values) did not change the particle dispersal substantially. It was reduced by 152 m to the west and the east of the farm structure, 171 m to the south and 57 m to the north (Fig. 5.13b). Settling rates were higher under the south-western part of the farm but dispersal was stronger in the eastern parts, especially in the north. The distance from the farm where settling rates were higher than 100 faecal pellets m^{-2} h^{-1} was 266 m.

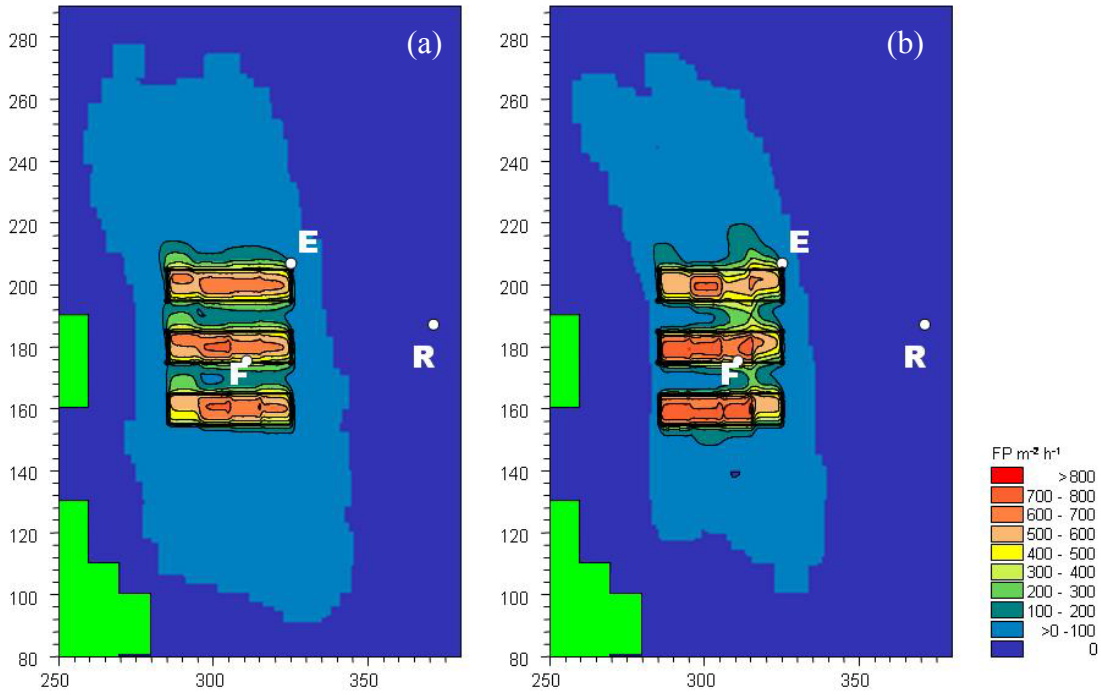

Figure 5.13. Faecal pellet sedimentation rates predicted by resuspension model with (a) density (ρ) = 1.048 g cm^{-3} and (b) ρ = 1.28 g cm^{-3}. White dots represent study sites (F = Farm, E = Edge, R = Reference) where faecal pellet sedimentation rates had been measured. Coordinate labels show grid cells.

5.2.4 Discussion

5.2.4.1. Hydrodynamic model

The hydrodynamic model did not predict the currents near the mussel farm well. It generally overestimated the tidal component of the current flow but comparisons between simulated and observed current speeds and directions were inconsistent. Previous three-dimensional simulations of tidal flows in the Firth of Thames predicted strongest flows in the outer firth of 0.4 m s^{-1} with speeds gradually decreasing to the south (Stephens 2003). Due to the lack of measured current speeds in the mid-southern part of the firth I cannot prove that the strong currents my model predicted in this area are correct. However, I measured current speeds up to 0.53 m s^{-1} at the reference site (Chapter 4), which convert to a depth-averaged speed of 0.79 m s^{-1}. Even allowing for some inaccuracy in the conversion and differences caused by the different deployment periods this indicates that current speeds up to 0.68 m s^{-1} may be realistic in the Firth of Thames.

Likely reasons for the poor performance include the fact that the hydrodynamic model is only two-dimensional and issues may arise from this simplification of the real water column structure. In addition, wind measurements were made at one weather station only. This is located on land near a mountain range that may have provided shelter and therefore the wind data may not represent the winds in the Firth of Thames accurately. The mussel farm is close to shore (~1000 m) and eddies generated by headlands may affect the current flow around the farm but may not be properly reproduced by the model. No measurements are available to confirm or refute the existence of eddies. More measurements as well as a more detailed representation of shoreline and bathymetry and the inclusion of seabed variability and waves may be necessary to improve our understanding and the simulation of the hydrodynamics in this area. Furthermore, mussel farm structures affect the water flow due to the drag and turbulence from the longlines (Plew et al. 2005) which is not considered in this simple hydrodynamic model.

Despite the foregoing comment regarding overall performance the simulated and observed currents were in relatively good agreement during the particle tracking simulation period. Furthermore, the model simulated currents reasonably well during times of strong water flows when particle dispersal is greatest and for these reasons I believe that the hydrodynamic forcing of the original particle tracking model was adequate for this period.

5.2.4.2. Initial dispersal model

The initial faecal pellet dispersal shows the expected pattern of rapidly sinking debris over a reasonable smooth bathymetry with maximum settling rates under the farm and an even gradient of decreasing rates away from the farm. This gradient is steepest in shallow waters. Currents around the farm were flowing predominantly northward and southward and therefore the gradients of particle settling rates in the east and west of the farm are very sharp. Residual currents were weak in the northern part of the farm and directed to the south-east, therefore I suggest that the increased dispersal distance in the north was due to the deeper water which gave particles more time to travel through the water column during the ebb tide before settling.

A previous modelling study of the initial dispersal of mussel biodeposits from a mussel farm at Blowhole Point in the Marlborough Sounds in similar water depth (8 to 14 m) and hydrodynamic conditions (mean current speed = 0.1 m s^{-1}, maximum current speed = 0.25 m s^{-1}) predicted that approximately 50 % of the biodeposits fall within 30 m of their release point (Hartstein and Stevens 2005). I did not follow the paths of individual particles from their release points but in the centre of the farm 27 % of particles settled in the 19 m square grid cell they were released in and 70 % within one neighbouring cell, which equates to a maximum distance of 28.5 m from their release point. Considering that our farm was located in slightly shallower water where particles reach the sediment faster these estimates compare well.

The mean (± SD) predicted faecal pellet sedimentation rate under the three farm blocks is 14.0 ± 3.9 g m^{-2} d^{-1}. This value is similar to sedimentation rates measured under mussel farms by Crawford et al. (2003) 7 to 15 g m^{-2} d^{-1}, Dahlbaeck and Gunnarson (1981) 20.9 g m^{-2} d^{-1}, Danovaro et al. (2004) 4.5 to 17 g m^{-2} d^{-1} and Hayakawa et al. (2001) 11 g m^{-2} d^{-1} but low compared to those measured by Hartstein and Stevens (2005) 133 g m^{-2} d^{-1} and Hatcher et al. (1994) 88.7 g m^{-2} d^{-1}. I estimated total sedimentation rates under the mussel farm of 78 g m^{-2} d^{-1} (adjusted for resuspension) but found that the contribution of faecal pellets to this flux was only 15.2 ± 3.4 g m^{-2} d^{-1} and suggested that the remainder was made up of detritus other than mussel faeces originating from the farm structures including pseudofaeces, algae and biodeposits produced by biofouling communities (Chapter 4). Therefore I believe that the sedimentation rate predicted by this model is a good estimate of faecal pellet sedimentation and that the higher rates published include the sedimentation of material other than mussel faeces.

The model predicted initial sedimentation rates at the three study sites well and it was not very sensitive to changes in the tested model parameters. The increased maximum dispersal distance during spring tide (+36 %) and the reduced distance during neap tide (-24 %) confirm the importance of currents for faecal pellet dispersal and indicate that the dispersal distances presented in this study represent average patterns. Simulated settling rates beneath the farm differ depending on the exact location and since particles were released in the centre of 19 m × 19 m grid

cells (after post-processing) and only 1, 3 and 6 metres below the sea surface the simulated spatial distribution of particle release is not as even as the true faecal pellet release. In addition, the study site under the farm was closer to the centre (approximately ¼ of the distance to the northern edge) of the middle farm block than represented in Fig. 5.10 but due to the representation of the farm in 190 × 190 m^2 grid cells the farm could not be placed accurately. Settling fluxes vary with season (Chapter 4), mussel size and diet (Chapter 2). In reality different parts of the farm contain differing cohorts of mussels, but the model assumes that cohorts are evenly distributed throughout the farm. Considering these aspects and the assumptions made in estimating the faecal pellet production from the cultured mussels I believe that the model performed well in simulating the initial dispersal pattern of faecal pellets from this farm.

The water depth of the south-eastern farm grid cell was only 4.9 m which is shallower than the actual measured water depth of 8 m. This was caused by an insufficient spatial resolution of the chart used to create the bathymetry and the grid cell size. In this cell some particles were released directly onto the sediment by the model and therefore the actual initial dispersal in this area is likely to be greater than predicted. However, due to the shallow depth and rapid sinking this would not change the dispersal pattern significantly. A more detailed bathymetry should be defined to improve the representation of water depths in the farm area. This may also lead to a better simulation of currents.

5.2.4.3. Resuspension model

The resuspension model shows that the potential for further faecal pellet transport after the initial deposition is high at our mussel farm. This is in agreement with the results of the erosion threshold measurements in Chapter 2 from which I concluded that a large fraction of biodeposits could be eroded after their initial deposition under the mussel farm of this study. Hartstein and Stevens (2005) could not trace mussel biodeposits in the sediments beneath the mussel farm at Blowhole Point and suggested that biodeposits may have been resuspended. Cromey et al. (2002) concluded that the frequency of resuspension events for deposited salmonid farm waste (food and faecal material) in an area with slightly lower maximum current speeds than those measured at our farm is high.

This model contains only a very simplified description of the resuspension process and several biodeposit parameters are poorly estimated. Because no decay rates are implemented into the model the simulated transport distances are only an estimate of their scale. The half-life time of faecal pellets is approximately 4.3 d and therefore the estimated dispersal distances after the 25 h simulation period are minimum estimates. However, this model reinforces that resuspension may play an important role in the dispersal of biodeposits from mussel farms.

Particle resuspension is a function of depth, currents, bottom type and roughness and shear stress as well as particle characteristics such as shape, density and degradation state. These parameters differ among mussel cultures and may also vary on the spatial scale of a single farm. The mathematical description of resuspension parameters and characteristics is complex and not well developed and resuspension is one of the key areas of uncertainty in models of the environmental impacts of marine aquaculture (Henderson et al. 2001, Grant et al. 2005). The results of this study indicate that resuspension is an important pathway of biodeposit dispersal and more research is needed in the development of models simulating biodeposit resuspension. These models should take into consideration biodeposit specific features such as shape and adhesiveness that modify their resuspension behaviour (Jumars and Nowell 1984). In addition better descriptions of seabed variability and measurements of biodeposit characteristics such as density are needed.

5.3 Modelling nitrogen remineralisation in sediments affected by biodeposition

5.3.1 Introduction

Biodeposits produced by cultured bivalves are dispersed while sinking through the water column and redistributed on the sediment surface via resuspension. Ultimately they accumulate and their remineralisation modifies nutrients dynamics and can lead to changes in sediment characteristics (e.g. Dahlbaeck and Gunnarsson 1981). In coastal ecosystems benthic nutrient regeneration can provide up to 100 % of the nutrients required for primary production (e.g. Nixon 1981, Herbert 1999, Cromey et al. 2002, Gibbs et al. 2005) and therefore an enhancement of the benthic-pelagic coupling can have significant local and far-field impacts. Despite the widespread use of numerical models for predicting carrying capacity, nutrient limitation, growth and production for suspended bivalve culture (e.g. Dowd 1997, Bacher et al. 1998, Gangnery et al. 2001) only very few models consider biodeposition and its effects on benthic nutrient regeneration (Bacher et al. 1995, Chapelle 1995, Chapelle et al. 2000, Dowd 2005). The models by Bacher et al. (1995), Chapelle (1995) and Chapelle et al. (2000) were designed to simulate the impacts of oyster cultivation in a shallow, almost closed lagoon (average depth 4 metres) and Dowd (2005) presented a bio-physical ecosystem model for intensive bivalve culture in shallow coastal bays. These models include a pelagic ecosystem component consisting of phytoplankton, zooplankton, nutrients, detritus and bivalves as well as a benthic detritus component.

The aim of this study was to simulate the impact of increased organic material deposition from a mussel farm on sediment nitrogen release rates by simulating the benthic remineralisation of organic material. Only limited data were available for this modelling study and therefore a model had to be developed that had a simple structure and few parameters but simulated the desired processes. None of the existing bivalve culture models fulfilled these requirements and therefore I chose a model of nitrogen recycling in marine sediments that was originally developed by Billen (1982) and has previously been applied to the Hauraki Gulf as part of my MSc research (Giles 2001). It is an idealised model of nitrogen

recycling in marine sediments that has successfully predicted the impacts of increased organic material deposition to North Sea sediments (Billen 1982). The model is not intended to predict accurately the absolute concentrations and fluxes. Rather it is designed to predict trends of the variations of the relative values as the result of variations in parameter values, as might arise when the model is applied to different sites. While more complex models of organic material mineralisation exist (e.g. Rabouille and Gaillard 1991) I was not able to use them due to the lack of available data.

5.3.2 Methods

Model description and application

The model simulates the distribution of organic nitrogen, organic carbon, ammonium and nitrate in the sediment, ammonification (ammonium release from organic matter), nitrification, denitrification and the fluxes of nitrate and ammonium between sediment and the overlying water column (Fig. 5.14). It has only four state variables (organic carbon, organic nitrogen, nitrate and ammonium in the sediment) and ten parameters which makes it suitable for applications in locations where only limited data are available. The original

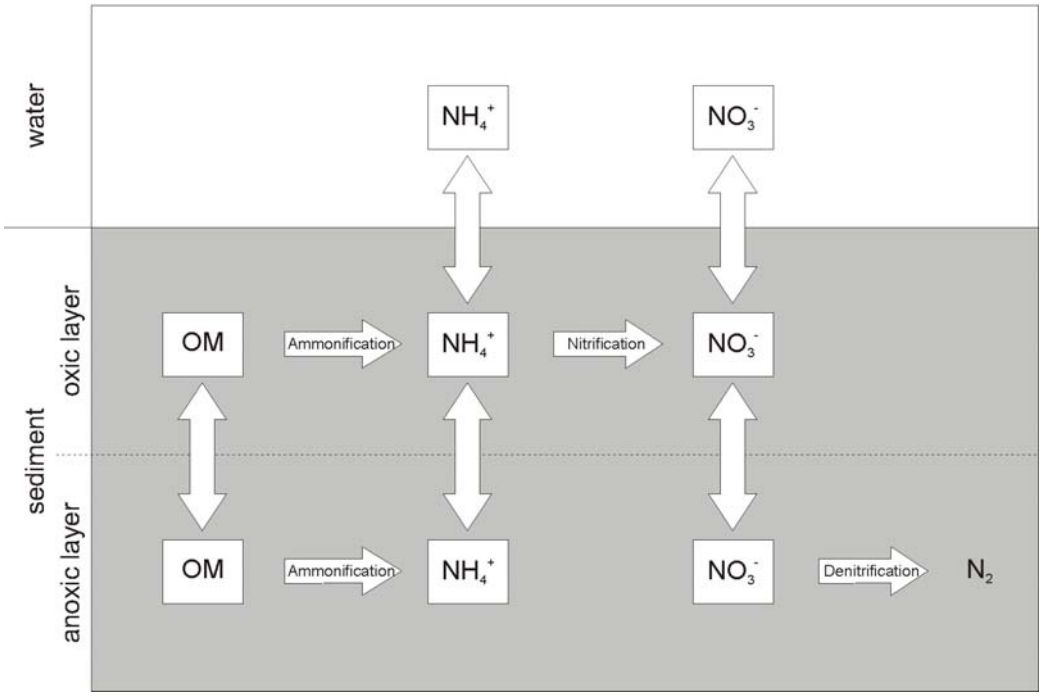

Figure 5.14. Modelled state variables and simulated processes.

Table 5.3. List of abbreviations and symbols used in this section.

Symbol	Definition	Unit
C_{NO3}	nitrate concentration	µmol cm^{-3}
C_{NH4}	ammonium concentration	µmol cm^{-3}
C^0_{NO3}	nitrate bottom water concentration	µmol cm^{-3}
C^0_{NH4}	ammonium bottom water concentration	µmol cm^{-3}
C_{orgC}	biodegradable fraction of organic carbon	µmol cm^{-3}
C_{orgN}	biodegradable fraction of organic nitrogen	µmol cm^{-3}
C^0_{orgC}	carbon concentration at sediment-water interface	µmol cm^{-3}
C^0_{orgN}	nitrogen concentration at sediment-water interface	µmol cm^{-3}
$\overline{C}_{orgC}$	mean biodegradable organic carbon concentration of top sediment layer	µmol cm^{-3}
C:N	molar carbon to nitrogen ratio	–
$D_{i,NO3}$	interstitial diffusion coefficient for nitrate	$cm^2\ s^{-1}$
$D_{i,NH4}$	interstitial diffusion coefficient for ammonium	$cm^2\ s^{-1}$
D_s	solid phase diffusion coefficient	$cm^2\ s^{-1}$
D_s^0	free diffusion coefficient in water	$cm^2\ s^{-1}$
I_{nit}	depth integrated rate of nitrification	µmol $cm^{-2}\ s^{-1}$
I_{denit}	depth integrated rate of denitrification	µmol $cm^{-2}\ s^{-1}$
J^0_{NO3}	flux of nitrate across the sediment-water interface	µmol $cm^{-2}\ s^{-1}$
J^0_{NH4}	flux of ammonium across the sediment-water interface	µmol $cm^{-2}\ s^{-1}$
k_a	organic material decay rate	s^{-1}
k_d	denitrification rate	s^{-1}
k_n	nitrification rate	µmol $cm^{-3}\ s^{-1}$
REF	fraction of refractory organic material	%
t	time	S
T	temperature	°C
TOC	total organic carbon	dry weight %
z	sediment depth	cm
z_n	depth of the oxic layer	cm
γ	proportionality coefficient between nitrification and ammonification	–
ρ	sediment density	g cm^{-3}
ϕ	sediment porosity	–

model by Billen (1982) was based on data collected in sandy sediments in the North Sea but some modifications have been made (Giles 2001) to make it applicable for finer sediments. I applied this model to sites beneath and at the edge of the mussel farm as well as to a reference site (Chapter 4). Unfortunately it was beyond the scope of this study to modify the model to include two organic

carbon and two nitrogen components, respectively, and this precluded the differentiation of biodeposits from other organic material in the sediment. However, by simulating benthic remineralisation at two study sites with different levels of biodeposition and at one site outside the influence of deposition from the farm it is still possible to model the effects of biodeposition. The following is a brief description of the model equations and parameters. A more detailed description of the model, its numerical implementation and the results of a sensitivity analysis can be found in Giles (2001).

Model equations

The vertical profiles of organic carbon, organic nitrogen, nitrate and ammonium are simulated by solving the corresponding partial differential equation at a number of equidistant depths. Organic carbon and nitrogen comprise of two components: a non-biodegradable fraction (k = 0) and a biodegradable fraction with first-order decay rate k_a (s^{-1}) that is assumed to be independent of depth and of the microbiological process of degradation. Mixing of the solid phase due to biological processes such as bioturbation or irrigation and physical processes such as resuspension is taken into account by means of a solid phase dispersion coefficient D_s ($cm^2\ s^{-1}$). The diagenetic equation describing the concentration of organic material per unit sediment volume (µmol cm^{-3}) at any depth is therefore:

$$\frac{\partial C_{org}}{\partial t} = D_s \frac{\partial^2 C_{org}}{\partial z^2} - k_a C_{org} \qquad (5.5)$$

where C_{org} (µmol cm^{-3}) is the biodegradable fraction of organic carbon (C_{orgC}) or nitrogen (C_{orgN}), respectively.

With the boundary conditions:

$C_{org} = C^0_{org}$ for $z = 0$

$C_{org} \to 0$ for $z \to \infty$

the stationary solution of Eqn. 5.5 is:

$$C_{org} = C^0_{org} e^{-\alpha z} \qquad (5.6)$$

where $\alpha = \sqrt{\frac{k_a}{D_s}}$

The carbon and nitrogen concentrations at the sediment surface (C^0_{org}, µmol cm^{-3}) are artificial model parameters. They were derived from the corresponding concentration in the upper (top 1 cm) sediment layer ($\overline{C}_{org}$, µmol cm^{-3}) that was

calculated from sediment density (ρ, g cm^{-3}), total organic carbon (TOC, dry weight %) and the fraction of refractory organic material (REF, %).

$$\overline{C}_{orgC} = \int_0^1 C^0{}_{orgC}\ e^{-\alpha x} dx = C^0{}_{orgC}\left(\frac{1-e^{-\alpha}}{\alpha}\right) \tag{5.7}$$

The nitrate distribution in the sediment is modelled taking into consideration nitrification, denitrification and diffusion in the pore water. Nitrification only takes place in the oxic layer and the depth of this layer depends on the redox conditions prevailing in the sediments. Nitrification is limited by ammonium availability it is therefore modelled by a zero order rate constant (k_n, µmol cm^{-3} s^{-1}) that is proportional, at any depth within the oxic layer, to the rate of ammonification:

$$k_n(z) = \gamma\, k_a C^0{}_{orgN} e^{-\alpha z} = k_n{}^0 e^{-\alpha z} \tag{5.8}$$

where γ is the proportionality coefficient between nitrification and ammonification rate in the top sediment layer. Denitrification was modelled by a first order rate constant (k_d, s^{-1}) with respect to nitrate that is proportional to the organic material concentration:

$$k_d = \gamma k_a C^0{}_{orgN} e^{-\alpha z_n} \frac{1}{C_{NO_3,z_n}} \tag{5.9}$$

Consequently the nitrate concentration is described by:

$$\frac{\partial C_{NO_3}}{\partial t} = D_{i,NO3} \frac{\partial^2 C_{NO_3}}{\partial z^2} + \varepsilon k_n - (1-\varepsilon) k_d C_{NO_3} \tag{5.10}$$

where ε = 1 for $z \le z_n$ (oxic layer)

ε = 0 for $z > z_n$ (anoxic layer)

and $D_{i,NO3}$ (cm^2 s^{-1}) is the interstitial phase dispersion coefficient for nitrate characterising the overall mixing of nitrate due to biological and physical processes. The boundary conditions are:

$$C_{NO_3} = C^0{}_{NO_3} \quad for \quad z = 0,$$

$$\left.\begin{aligned} C_{NO_3}\big|_{\text{base of oxic layer}} &= C_{NO_3}\big|_{\text{roof of anoxic layer}} \\ \left.\frac{dC_{NO_3}}{dz}\right|_{\text{base of oxic layer}} &= \left.\frac{dC_{NO_3}}{dz}\right|_{\text{roof of anoxic layer}} \end{aligned}\right\} z = z_n,$$

$C_{NO3} \ge 0 \quad for\ all\ z,$

$C_{NO3}\ finite \quad for\ z = \infty.$

The diffusive flux of nitrate across the sediment water interface (µmol cm^{-2} s^{-1}) is:

$$J^{0}{}_{NO_3} = D_{i,NO3}\left[\frac{dC_{NO_3}}{dz}\right]_{z=0} \tag{5.11}$$

The integrated rate of nitrification (I_{nit} in µmol cm^{-2} s^{-1}) is given by:

$$I_{nit} = \int_0^{z_n} k_n{}^0 e^{-\alpha z} dz = \frac{k_n{}^0}{\alpha}\left(1 - e^{-\alpha z_n}\right) \tag{5.12}$$

From the flux of nitrate diffusing from the oxic layer into the anoxic layer the integrated rate of denitrification (I_{denit}, µmol cm^{-2} s^{-1}) can be calculated as:

$$I_{denit} = \int_{z_n}^{\infty} k_d C_{NO_3} dz = D_{i,NO3}\left[\frac{dC_{NO_3}}{dz}\right]_{z=z_n} \tag{5.13}$$

Ammonium is produced by ammonification and consumed by nitrification in the oxic layer with ammonification being aerobic in the oxic layer and anaerobic in the anoxic layer:

$$\frac{\partial C_{NH_4}}{\partial t} = D_{i,NH4}\frac{\partial^2 C_{NH_4}}{\partial z^2} + k_a C^0{}_{orgN} e^{-\alpha z} - \varepsilon k_n \tag{5.14}$$

where $D_{i,NH4}$ (cm^2 s^{-1}) is the interstitial phase dispersion coefficient for ammonium.

The boundary conditions are:

$$C_{NH_4} = C^0{}_{NH_4} \qquad for\ z = 0,$$

$$\left.\begin{aligned} C_{NH_4}\big|_{\text{base of oxic layer}} &= C_{NH_4}\big|_{\text{roof of anoxic layer}} \\ \left.\frac{dC_{NH_4}}{dz}\right|_{\text{base of oxic layer}} &= \left.\frac{dC_{NH_4}}{dz}\right|_{\text{roof of anoxic layer}} \end{aligned}\right\} z = z_n,$$

The ammonium flux (µmol cm^{-2} s^{-1}) between the sediment and the overlying water is given by:

$$J^{0}{}_{NH_4} = D_{i,NH4}\left[\frac{dC_{NH_4}}{dz}\right]_{z=0} \tag{5.15}$$

Parameters and model calibration

The model assumes steady-state and this assumption is only valid if the characteristic time of parameter variations is longer than the turnover time of the model compartments (Billen 1982). The longest turnover time is given by the reciprocal of k_a. In the original model this value was about one year and because

Table 5.4. Measured and estimated model parameters. Estimated values were used in the initial (not calibrated) model and some were modified to calibrate the model.

Model parameter	Farm	Edge	Reference	Source
Measured				
TOC (dry weight %)	4.43	1.74	1.77	Chapter 4
C:N (-)	11.6	9.7	10.0	Chapter 4
ϕ (-)	0.71	0.85	0.88	Chapter 4
ρ (g cm^{-3})	0.80	0.41	0.34	Chapter 4
T (ºC)	16.6	16.2	16.3	Chapter 4
C^0_{NO3} (µmol cm^{-3})	3.1×10^{-4}	*	4.5×10^{-4}	Chapter 4
C^0_{NH4} (µmol cm^{-3})	1.2×10^{-3}	*	1.0×10^{-3}	Chapter 4
Estimated				
k_a (s^{-1})$^+$	5×10^{-7}	5×10^{-7}	5×10^{-7}	Ref. in Chapter 4
D_s (cm^2 s^{-1})$^+$	1×10^{-7}	1×10^{-7}	1×10^{-7}	Billen 1982
γ (-)	0.8	0.8	0.8	Billen 1982
$D_{i,NH4}$ (cm^2 s^{-1})	8.26×10^{-6}	1.17×10^{-5}	1.26×10^{-5}	Ullmann and Aller 1982
$D_{i,NO3}$ (cm^2 s^{-1})	7.96×10^{-6}	1.13×10^{-5}	1.21×10^{-5}	Ullmann and Aller 1982
z_n (cm)	0.35	0.35	0.35	K. Vopel, pers. comm.
REF (%)	17	17	17	Billen 1982

* no data available, the average of farm and reference sites was used
$^+$ modified during model calibration

k_a was modified during the model calibration the model may also not be able to predict the response to seasonal variations. Therefore I parameterised it with annual averages of measured values where these were available from Chapters 3 and 4. These parameters were TOC, C:N ratio, ρ, $C^0_{NO_3}$ and $C^0_{NH_4}$ as well as temperature and porosity (ϕ) required for calculating $D_{i,NO3}$ and $D_{i,NH4}$. The values of the measured parameters are presented in Table 1 and this section contains a description of the parameters for which published values were used in the initial (not calibrated) model or that were calculated (values given in Table 5.4). The model was calibrated by modifying some of these parameters to obtain the best possible fit of measured (Chapter 4) and simulated sediment ammonium and nitrate release rates.

Decomposition Rate

In Chapter 3, I summarised decay rates for sediments without organic additions and for this model a relatively high value of 5×10^{-7} s^{-1} was used to estimate k_a at all three study sites. This value was chosen because it is in the range of the

published rates and similar to the decay rate used to predict nitrogen transformation processes on the Hauraki Shelf (Giles 2001). However, due to a lack of measured data the Hauraki Shelf model could not be calibrated and therefore the decay rate used may be not be correct. k_a was used to calibrate the model and the fitted parameter compared to the biodeposit decay rate.

Dispersion coefficients

The solid (D_s) and interstitial (D_i) phase dispersion coefficients represent the mixing of the solid and interstitial phases of the sediment due to physical (e.g. resuspension) and biological (e.g. bioturbation, irrigation) processes. These processes are very complex and quantifying their impact on sediment nutrient fluxes is difficult (e.g. Nickell et al. 2003). D_s is usually calculated from experimental data and values for D_s found in the literature range from 3×10^{-8} cm^2 s^{-1} to 4.4×10^{-5} cm^2 s^{-1} (e.g. summary in Billen 1982, Nickell et al. 2003). The solid phase dispersion coefficient from the original model was 1×10^{-7} cm^2 s^{-1}. It was used for the initial model runs in this study and modified to calibrate the model. $D_{i,NO3}$ and $D_{i,NH4}$ were approximated by the diffusion coefficients for nitrate and ammonium. They were calculated by correcting the free diffusion coefficient of the solute in water, D_s^0, for sediment type (characterised by ϕ) and temperature (Ullman and Aller 1982).

Proportionality factor

Billen (1982) used a value of 0.8 for the proportionality factor γ between nitrification and ammonification rate in the top sediment layer which was obtained from measurements in sandy North Sea sediments. I could not find any equivalent published ratios and therefore used this value.

Oxic layer depth

The oxygenated zone varies considerably between sediments. Studies of organic rich sediments showed that oxygen does not penetrate deeper than a few millimetres (Revsbech et al. 1980) whereas in organically poor sediments oxygen can still be measured in 40 cm depth (e.g. Kepkay and Novitsky 1980). No sediment oxygen profiles were available for my study sites but oxygen penetration depths of ~0.35 cm have been measured at the edge of a mussel farm at Wilson's

Bay in the eastern Firth of Thames (Kay Vopel, pers. comm.). These rates are not expected to vary significantly among the muddy sediments in the Firth of Thames (Kay Vopel, pers. comm.) and this estimate of z_n was used at all three sites.

Fraction of refractory organic material

I only measured total sedimentary organic carbon and nitrogen (Chapter 4) and could not find any published estimates of the fraction of refractory organic material in coastal sediments. Therefore I used the original value of 17 % (Billen 1982) for the parameter REF.

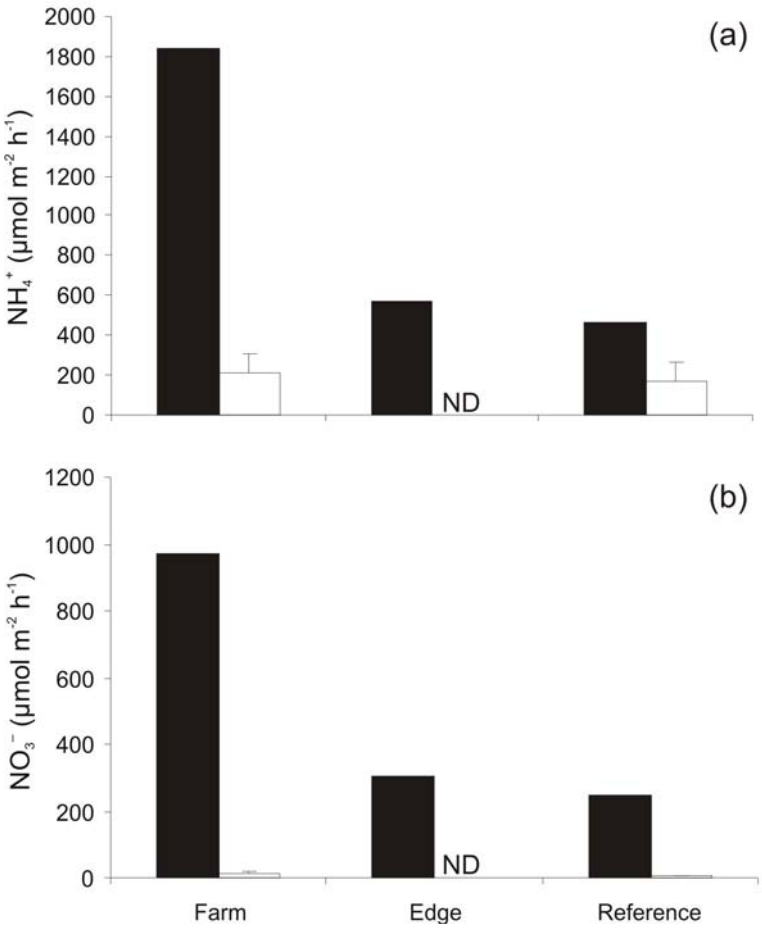

Figure 5.15. Initial (not calibrated) model results (black bars) and measurements (+ SD, white bars) of (a) sediment ammonium (NH_4^+) and (b) nitrate (NO_3^-) release rates. ND = not determined.

5.3.3 Results

Initial model simulation

Nutrient fluxes predicted by the model before calibration using the default parameters were much higher under the farm than at the other two sites (3.2 to 3.9×) and appear driven by the sediment organic material concentrations (Table 5.4). Predicted sediment-water ammonium and nitrate fluxes were 9 and 65× higher at the farm site and 3 and 47× higher at the reference site compared to the rates measured in Chapter 4 (Fig. 5.15). Consequently the model significantly underestimated the ammonium to nitrate flux ratios at both sites. No nutrient flux measurements were available for the edge site but the predicted rates appear sensible in relation to the other two sites considering the similar organic carbon and nitrogen concentrations in the sediments of the edge and reference sites (Table 5.4).

Model calibration

I calibrated the model separately for the farm and reference sites by modifying the estimated parameters. The aim of the calibration was to reduce the predicted ammonium and nitrate fluxes and increase the ammonium to nitrate flux ratio. The model is insensitive to changes in $D_{i,NO3}$ and $D_{i,NH4}$ (Giles 2001) which leaves the parameters k_a, D_s, γ, z_n and REF for the model calibration. The sensitivity analysis of the model indicated that changes of the parameters D_s, γ and z_n always result in an increased flux of one nutrient and a decreased flux of the other (Giles 2001). Therefore they could not be used to reduce the total flux rates, however, increasing D_s or decreasing γ or z_n leads to an increased ammonium to nitrate ratio (Giles 2001) and so these parameters could be used to adjust this ratio once the overall fluxes are reduced.

Increasing REF has the same effect as decreasing the organic content of the sediment and thus causes a reduction of the nutrient fluxes. An increase of REF to 50 % resulted in a decrease of the nutrient fluxes under the farm by 40 % which is still 5.3× higher than the measured ammonium and 39.1× higher than the measured nitrate flux. I could not find published estimates of REF for coastal marine sediments but believe that values above 50 % are not realistic. For this reason I retained the original value of 17 %. Another means of reducing the

nutrient flux rates was to reduce the sediment decay rate k_a and I used this parameter for the model calibration. The range of published sediment decay rates is very large (5.8×10^{-9} to 5.1×10^{-7} s^{-1}) and the simulated changes in nutrient fluxes are almost directly proportional to the changes in k_a (Giles 2001) which makes this a good calibration parameter. Nickell et al. (2003) derived dispersal coefficients from modelled sediment chlorophyll *a* profiles to quantify bioturbation and other mixing processes beneath a salmon cage farm and to compare them to unaffected sites. Under the salmon farm D_s was 6.9×10^{-7} cm^2 s^{-1} indicating less mixing than at the edge of their farm and at a reference site where D_s was ~3.9×10^{-6} cm^2 s^{-1}. However, at another reference site the calculated dispersion coefficient was even lower than under the farm (4.6×10^{-7} cm^2 s^{-1}) and the only sediment parameter that showed a strong correlation to the mixing coefficients was macrofauna mean size (Nickell et al. 2003). I modified the dispersal coefficient at the farm and reference site to adjust the predicted ammonium to nitrate flux ratios.

Satisfactory model fits were obtained for $k_a = 1\times10^{-8}$ s^{-1} and $D_s = 2\times10^{-7}$ cm^2 s^{-1} at the farm site and $k_a = 2\times10^{-8}$ s^{-1} and $D_s = 1\times10^{-6}$ cm^2 s^{-1} at the reference site (Fig. 5.16). At the farm site predicted ammonium fluxes were 1.3× higher and nitrate fluxes 1.3× lower than measured rates. At the reference site the model calculated 1.3× higher ammonium and 1.1× higher nitrate release rates. The fitted dispersal coefficient was almost an order of magnitude higher at the reference site than at the farm site, indicating less mixing under the farm. However, macrofauna abundance and biomass were higher in the sediments at the farm site (Chapter 4) and this lack of correlation as well as the large variability of the dispersal coefficient is consistent with the findings of Nickell et al. (2003) who suggested that different mixing mechanisms are responsible for the site-specific values of D_s.

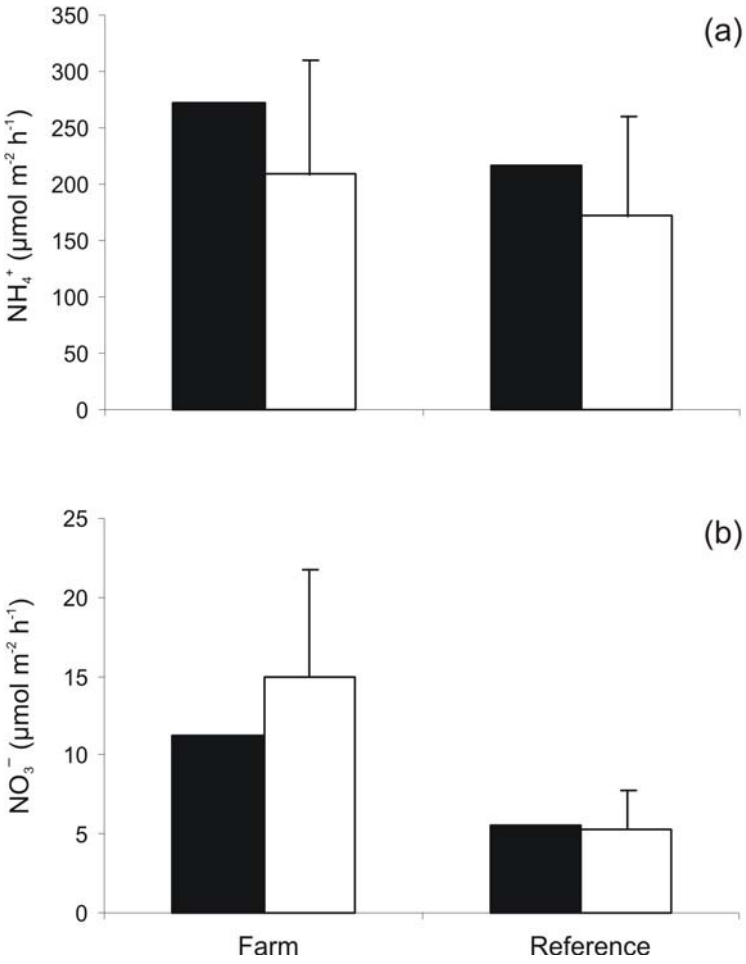

Figure 5.16. Calibrated model results (black bars) and measurements (+ SD, white bars) of (a) sediment ammonium (NH_4^+) and (b) nitrate (NO_3^-) release rates.

Interestingly, the fitted decay rate at the reference site was twice as high than that at the farm site. This may indicate that the organic material at the reference site is more labile compared to the material under the farm. Unfortunately no data is available to test this hypothesis since the common method of comparing gross measures of carbon and nitrogen are of limited value in determining the quality of organic material (Gunnarsson et al. 1999). The decay rate at the farm site is 185× lower than the decay rate measured for biodeposits (Chapter 3). Only a small fraction of the material depositing under the farm comprises of biodeposits (Chapter 4) and resuspension may further reduce the amount of biodeposits accumulating in the sediments beneath the farm (Section 5.2). Neither the composition nor the decay rate of the greater part of depositing and accumulating material is known and therefore I cannot assess if this decay rate is realistic.

Considering the accuracy of the model results and the uncertainty of many parameters no definite conclusions can be drawn from the difference of the two fitted decay rates.

Similarly accurate model results could most likely also be produced by modifying the other two estimated parameters z_n and γ. To increase the ammonium to nitrate flux ratio z_n would have to be decreased because a thinner oxic layer would result in less ammonium to be converted to nitrate and consequently the ammonium flux would increase relative to the nitrate flux (Giles 2001). An oxygen penetration depth of 0.45 cm has been measured at a site just north of the Firth of Thames (Downes unpublished data, presented in Giles 2001) so values less than 0.35 cm are possible in the shallower firth, especially beneath the mussel farm. However, since the surface sediments at the study sites appeared well-oxygenated I think the chosen value of 0.35 cm for z_n is a sensible estimate of the oxic layer depth. I could not find any publications of combined nitrification and ammonification measurements for coastal sediments and therefore decided to retain the original value for γ.

Nutrient flux rates at the edge of the farm

I applied the model to the study site at the edge of the farm using the parameters obtained from the calibrations at the farm ("farm parameters") and at the reference sites ("reference parameters") to examine how these different parameters influence the predicted nutrient fluxes. Fig. 5.17 illustrates that using the two sets of parameters significantly influenced the model results. Estimates of ammonium and nitrate fluxes based on the reference parameters were much higher (3.1× and 1.9× respectively) than those predicted from the farm parameters. Since no measurements were available at the edge site I cannot say if either of these predictions was accurate. The sediment characteristics and consequently the model input parameters of the edge and reference sites were similar (Table 5.4) but the ammonium release at the edge of the farm predicted from the reference parameters was almost as high as rates predicted under the farm. This application demonstrates how important it is to parameterise the model well and to investigate how the model responds to parameter changes, e.g. to the application at different sites.

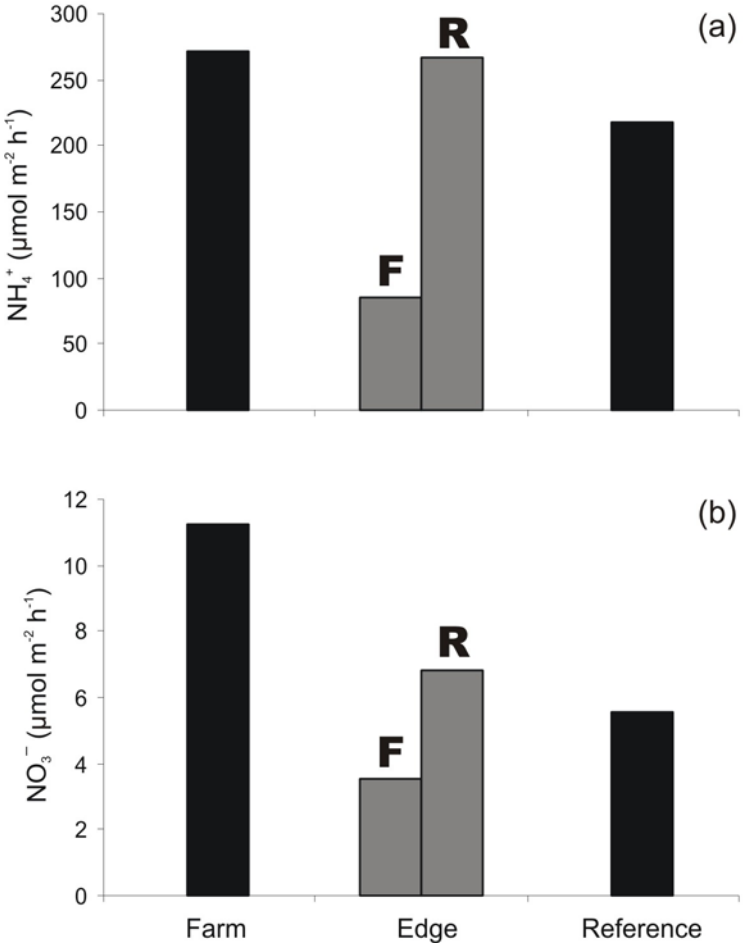

Figure 5.17. Predicted (a) sediment ammonium (NH_4^+) and (b) nitrate (NO_3^-) release rates. 'F' denotes rates modelled using parameters obtained from calibration at the farm site ($k_a = 1\times10^{-8}$ s^{-1}, $D_s = 2\times10^{-7}$ cm^2 s^{-1}) and 'R' those obtained from calibration at the reference site ($k_a = 2\times10^{-8}$ s^{-1}, $D_s = 1\times10^{-6}$ cm^2 s^{-1}).

5.3.4 Model limitations

The calibrated model could fit the data well; however, this study clearly indicated that more local data are required to obtain realistic model predictions. In addition to the measurements that were available in this study the key parameters that need to be determined are k_a, D_s, z_n, REF and γ. Estimates of decay rates can be derived from incubation experiments similar to that presented in Chapter 3, however, more research must be done to ensure that the calculated decay rates are valid for the decay of nitrogen as well as carbon. Dispersal coefficients can be calculated from sufficiently deep chlorophyll *a* profiles (Nickell et al. 2003) or radio-isotope measurements (McCall and Tevesz 1982). Oxygen penetration depth measurements can be made with microelectrodes (e.g. Kristensen 2000). The

composition of organic material and its refractory component can be analysed by measuring the content of amino acids, lipids, C, N, and polyphenolic compounds (Gunnarsson et al. 1999). To calculate γ measurements of ammonification and nitrification are needed. These are complex processes and their quantification is not easy (Herbert 1999)**.** Providing all other parameters are measured I suggest using γ as a calibration parameter.

In addition to improving the accuracy of model parameters, the model should be applied to a range of sites with different characteristics, e.g. in and out of the influence of mussel farms or in areas with different sediment properties. This would allow a comprehensive calibration of the model and demonstrate whether this simple model, when parameterised correctly, is able to simulate nitrogen remineralisation in these environments.

The model used in this study has some considerable limitations that restrict its capacity in reproducing detailed processes involved in the remineralisation of organic material. The level of detail considered in a model depends on its purpose and including more variables and parameters does not necessarily improve it. The explanatory power of any model depends on the quality of data available for parameterisation and our understanding on the modelled processes and to develop an adequate model of organic material remineralisation in sediments affected by biodeposition more research is needed in both areas. The following provides some aspects that should be considered in a modified model.

Firstly, the model considers only the fate of nitrogen but to adequately describe the benthic nutrient regeneration it should also include phosphorus, silicate and oxygen and in addition to denitrification it should incorporate other anaerobic mineralisation processes (e.g. Kristensen 2000). Also, the model ignores adsorption and while this is acceptable for the simulation of nitrogen in sandy sediments (Billen 1982) it is a very important process in muddy sediments, especially if sedimentary phosphate dynamics are considered (Ruardij and van Raaphorst 1995). In areas with high deposition rates sedimentation and consequent advection due to sediment accumulation should be included.

Furthermore, some parameters and processes should be modified to represent the underlying sedimentary processes more realistically. The vertical transport of organic material should be examined and possibly represented in a different way. However, the mathematical description of this transport process is complicated (e.g. Ebenhoeh et al. 1995) and one option would be to include several dispersion coefficients that vary with depth and represent the prevailing mixing processes in the different sediment layers (Billen 1982). Organic material was considered as made of only one biodegradable and one refractory component. Biodeposits have rapid decay rates (Chapter 3) and should be considered separately from other detritus. The decay of several organic material components can be modelled using "multi-G's-first order kinetics" (Joergensen 1978, Berner 1980) but to develop a more sophisticated representation of organic material remineralisation more research needs to be done on the composition of sedimentary organic material and decay rates of the different components.

Chapter 6

General conclusions

6.1 Summary

Bivalve biodeposition represents a significant link between the pelagic and benthic environments by transferring organic material from the water column to the sediments where its remineralisation releases nutrients that are available to primary producers. I examined dispersal characteristics of biodeposits to assess the spatial extent of their sedimentary impacts and biodeposit remineralisation to assess the contribution of biodeposits to the benthic regeneration of nutrients.

Chapter 2 of this thesis has shown that faecal pellet and pseudofaeces sinking velocities are functions of mussel diet and size and that pseudofaeces generally settle slower than faecal pellets. I provided first measurements of mussel biodeposit erosion thresholds and showed that they vary with mussel diet but are not correlated to mussel size. Estimates of dispersal distances based on these results demonstrated that the initial dispersal of biodeposits produced by cultured mussels is not far. Depending on the hydrodynamic conditions, secondary dispersal via resuspension potentially plays a more important role in the dispersal of biodeposits from mussel farms than initial dispersal and almost certainly serves as the major means of transport of biodeposits from natural mussel beds.

The decay rate calculated in Chapter 3 is the first published mussel biodeposit decay rate. It is substantially higher than decay rates for sediments without additions of organic matter or that of plant material confirming the importance of using specific decay rates for models of mussel biodeposit remineralisation. Nutrient fluxes generally showed the expected responses to organic input and illustrated that biodeposit remineralisation alters the stoichiometry of the nutrients released from the sediments which could affect primary production and may potentially be more significant than the changes of the individual fluxes.

The field study of the impacts of sedimentation from a mussel farm on sediment characteristics and benthic fluxes (Chapter 4) provided important information on mussel culture impacts in an area where major expansions are planned as well as calibration data for the models. Sedimentation was highest under the farm and elevated at the edge of the farm compared to the reference site; however, faecal pellets made up only 14 % of the additional deposition at the farm site compared to the reference site and 6 % of the additional deposition at the edge of the farm. Sediment characteristics as well as sediment-water oxygen and nutrient fluxes under the farm showed a range of attributes commonly associated with enhanced organic flux under shellfish culture and the results indicated a potential increase in denitrification under the farm in summer. Estimates showed that benthic nitrogen release could supply 74 % of the nitrogen requirements of primary producers at the reference site and 94 % at the farm site, confirming the importance of benthic nutrient regeneration in maintaining primary production in this region and the potential redistribution of nutrients caused by mussel farms.

The biodeposit dispersal model in Chapter 5 has shown that the maximum initial dispersal of faecal pellets from the mussel farm is approximately 300 m and that pellets can be transported several times this distance via resuspension. These models did not include faecal pellet decay and therefore were not able to predict maximum resuspension distances, however, they showed that the accumulation of faecal pellets is likely to affect sediments a long distance away from the farm. The remineralisation model was able to simulate the increased nitrogen fluxes from the sediments well and highlighted the need for thorough calibration and parameterisation of the model.

6.2 Conclusions and suggestions for future research

The results from Chapters 2 to 4 were used to parameterise, calibrate and validate the numerical models of biodeposit dispersal and remineralisation (Chapter 5). Because the modelling study linked all Chapters of this thesis the conclusions drawn from it will form the structure of this section. Specific conclusions and the key suggestions for future research of the other Chapters will be presented within this structure.

The modelling and laboratory studies demonstrated that while the initial deposition of biodeposits occurs close to the mussel farm the potential for further transport via resuspension is very high. The resuspension process is represented by a simplified mathematical description and problems arising during the parameterisation illustrated that this description is not adequate for the simulation of biodeposit resuspension. Therefore future studies should analyse this process and derive a more suitable mathematical expression.

The dispersal model predicted only the flux of faecal pellets, however, faecal pellets comprise only a relatively small part of the material originating from the mussel farm, thus the model only simulated a fraction of the total organic matter flux reaching the sediments. I believe that due to the relatively high suspended particle concentration in the Firth of Thames mussels produce about equal amounts of faeces and pseudofaeces. Pseudofaeces have only a slightly lower organic content compared to faeces and may therefore contribute significantly to the organic material flux to the sediments. Because they break up easily pseudofaeces may be represented best as suspended particulate material rather than particles. Therefore more research needs to be done to find a suitable mathematical description of their transport behaviour. In this study sediment organic carbon and nitrogen concentrations measured *in situ* were used as input parameters for the remineralisation model. Future studies should link the dispersal and remineralisation models and simulate the changes in sediment nutrient fluxes with distance from the farm. This would create an estimate of the spatial extent of the farm influence and demonstrate how the benthic processes react to different amounts of organic loading. These models should simulate the entire deposition, including faecal pellets, pseudofaeces and other material sedimenting from the farm.

Sinking velocity and erosion thresholds are key parameters for biodeposit dispersal and both vary with mussel diet. The regeneration of nutrients from organic material depends on its quality (Herbert 1999) and for mussel biodeposits that also depends on the mussel diet. The diet available to cultured mussels is subject to tidal, seasonal and inter-annual variations (Berg and Newell 1987) and

therefore the model should be improved to enable the simulation of shot-term impacts, such as seasonal variations and the resulting changes in mussel diet.

This thesis demonstrated the potential for denitrification under the mussel farm. Denitrification removes nitrogen from the ecosystem by converting nitrate to nitrogen gas, thus bivalve culture may increase nitrogen limitation or limit eutrophication. The impacts of mussel culture on denitrification are not well understood because denitrification requires oxic as well as anoxic sediment conditions and therefore increased organic matter input may impede denitrification rather than enhance this anaerobic mineralisation pathway. Measuring denitrification is difficult (e.g. Herbert 1999) and was beyond the scope of this thesis. Future models should include denitrification and measurements of this important process should be made.

One important motivation for this study was the planned expansion of mussel cultivation in the Firth of Thames and the consequently expected increase of biodeposition and associated environmental impacts. Because the dispersal of mussel biodeposits is well beyond the footprint of a single farm I suggest that all existing and planned mussel farms should be included in one model simulation to examine their cumulative environmental impacts. The model could be coupled to existing models of other aspects of mussel culture, such as carrying capacity and mussel growth and consequently would provide a very useful tool for comprehensive assessments of mussel culture impacts.

References

Ahn I-Y (1993) Enhanced particle flux through the biodeposition by the Antarctic suspension-feeding Bivalve *Laternula elliptica* in Marian Cove, King George Island. J Exp Mar Biol Ecol 171: 75-90

Aller RC (1994) Bioturbation and remineralization of sedimentary organic matter: Effects of redox oscillation. Chem Geol 114: 331-345

Andersen TJ (2001) Seasonal variation in erodibility of two temperate, microtidal mudflats. Est Coast Shelf Sci 53: 1-12

Andersen TJ, Jensen KT, Lund-Hansen L, Mouritsen KN, Pejrup M (2002) Enhanced erodibility of fine-grained marine sediments by *Hydrobia ulvae*. J Sea Res 48(1): 51-58

Arar EJ, Collins GB (1997) *In vitro* determination of chlorophyll *a* and pheophytin *a* in marine and freshwater algae by fluorescence. National Exposure Research Laboratory, Office of Research and Development, U.S. Environmental Protection Agency. http://web1.er.usgs.gov/nemi/method_pdf/7222.pdf

Asmus H, Asmus RM (1992) Benthic-pelagic flux rates on mussel beds. Helgol Meeresunters 46: 341-361

Austen I, Andersen TJ, Edelvang K (1999) The influence of benthic diatoms and invertebrates on the erodibility of an intertidal mudflat, the Danish Wadden Sea. Est Coast Shelf Sci 49: 99-111

Bacher C, Bioteau H, Chapelle A (1995) Modelling the impact of a cultured oyster population on the nitrogen dynamics: the Thau Lagoon case (France). Ophelia 42: 29-54

Bacher C, Duarte P, Ferreira JG, Heral M, Raillard O (1998) Assessment and comparison of the Marennes-Oleron Bay (France) and Carlingford Lough (Ireland) carrying capacity with ecosystem models. Aquat Ecol 31: 379-394

Baudinet D, Alliot E, Berland B, Grenz C, Plante-Cuny M-R, Plante R, Salen-Picard C (1990) Incidence of mussel culture on biogeochemical fluxes at the sediment-water interface. Hydrobiologia 207: 187-196

Bayne BL (1993) Feeding physiology of bivalves: Time-dependence and compensation for changes in food availability. In: Dame RF (ed.) Bivalve

filter feeders in estuarine and coastal ecosystem processes. Springer-Verlag, Berlin Heidelberg, pp. 1-24

Berg JA, Newell RIE (1987) The role of physical factors in regulating temporal and spatial variations in seston. In: Neilson B, Brubker J, Kuo A (eds.) Estuarine Circulation. Humana Press, Clifton, NJ, pp. 235-253

Berner RA (1980) Early diagenesis. A theoretical approach. Princeton University Press, Princeton, New Jersey, 241 pp.

Billen G (1982) An idealized model of nitrogen recycling in marine sediments. Am J Sci 282: 512-541

Black KP, Bell RG, Oldman JW, Carter GS, Hume TM (2000) Features of 3-dimensional barotropic and baroclinic circulation in the Hauraki Gulf, New Zealand. N Z J Mar Freshw Res 34: 1-28

Black KP, McShane PE (1990) Influence of surface gravity waves on wind-driven circulation in intermediate depths on an exposed coast. Aust J Mar Freshw Res 41: 353-363

Bloesch J, Burns NM (1980) A critical review of sediment trap technique. Schweiz Z Hydrol 42(1): 15-55

Bray JT, Bricker OP, Troup BN (1973) Phosphate in interstitial waters of anoxic sediments: Oxidation effects during sampling procedure. Science 180: 1362-1364

Broekhuizen N, Ren J, Zeldis J, Stevens S (2004) Ecological sustainability assessment of Firth of Thames shellfish aquaculture: Tasks 2-4 - Biological Modelling. Environment Waikato Technical Report 2005/06, Auckland Regional Council Technical Publication 253, 62 pp.

Broekhuizen N, Zeldis J, Stephens SA, Oldman JW, Ross AH, Ren J, James MR (2002) Factors related to the sustainability of shellfish aquaculture operations in the Firth of Thames: a preliminary analysis. Environment Waikato Technical Report 2002/09, Auckland Regional Council Technical Publication 182, 109 pp.

Butler M, Dam HG (1994) Production rates and characteristics of fecal pellets of the copepod *Acartia tonsa* under simulated phytoplankton bloom conditions: implications for vertical fluxes. Mar Ecol Prog Ser 114: 81-91

Campbell DE, Newell CR (1998) MUSMOD, a production model for bottom culture of the blue mussel, *Mytilus edulis* L. J Exp Mar Biol Ecol 219: 171-203

Canfield DE, Thamdrup B, Hansen JW (1993) The anaerobic degradation of organic matter in Danish coastal sediments: Iron reduction, manganese reduction, and sulfate reduction. Geochim Cosmochim Acta 57: 3867-3883

Chamberlain J, Fernandes TF, Read P, Nickell TD, Davies IM (2001) Impacts of biodeposits from suspended mussel (*Mytilus edulis* L.) culture on the surrounding surficial sediments. ICES J Mar Sci 58(2): 411-416

Chapelle A (1995) A preliminary model of nutrient cycling in sediments of a Mediterranean lagoon. Ecol Model 80: 131-147

Chapelle A, Menesguen A, Deslous-Paoli J-M, Souchu P, Mazouni N, Vaquer A, Millet B (2000) Modelling nitrogen, primary production and oxygen in a Mediterranean lagoon. Impact of oysters farming and inputs from the watershed. Ecol Model 127: 161-181

Christensen PB, Glud RN, Dalsgaard T, Gillespie P (2003) Impacts of longline mussel farming on oxygen and nitrogen dynamics and biological communities of coastal sediments. Aquaculture 218(1-4): 567-588

Cloern JE (1982) Does the benthos control phytoplankton biomass in South San Francisco Bay? Mar Ecol Prog Ser 9: 191-202

Cole RG, Hull PJ, Healy TR (2000) Assemblage structure, spatial patterns, recruitment, and post-settlement mortality of subtidal bivalve molluscs in a large harbour in north-eastern New Zealand. N Z J Mar Freshw Res 34: 317-329

Cranford P, Dowd M, Grant J, Hargrave B, McGladdery S (2003) Ecosystem level effects of marine bivalve aquaculture. A scientific review of the potential environmental effects of aquaculture in aquatic ecosystems. Hargrave B, Canadian Technical Report of Fisheries and Aquatic Sciences No. 2450. Fisheries and Oceans Canada, Science Sector**:** 51-84

Crawford CM, Macleod CKA, Mitchell IM (2003) Effects of shellfish farming on the benthic environment. Aquaculture 224(1-4): 117-140

Cromey CJ, Nickell TD, Black KD (2002) DEPOMOD - modelling the deposition and biological effects of waste solids from marine cage farms. Aquaculture 214(1-4): 211-239

Dahlbaeck B, Gunnarsson LAH (1981) Sedimentation and sulphate reduction under a mussel culture. Mar Biol 63: 269-275

Dame RF (1993) The role of bivalve filter feeder material fluxes in estuarine ecosystems. In: Dame RF (ed.) Bivalve filter feeders in estuarine and coastal ecosystem processes. Springer-Verlag, Berlin Heidelberg, pp. 245-269

Dankers N, Zuidema DR (1995) The role of the mussel (*Mytilus edulis* L.) and mussel culture in the Dutch Wadden Sea. Estuaries 18(1A): 71-80

Danovaro R, Gambi C, Luna GM, Mirto S (2004) Sustainable impact of mussel farming in the Adriatic Sea (Mediterranean Sea): evidence from biochemical, microbial and meiofaunal indicators. Mar Pollut Bull 49(4): 325-333

Davies MS, Hawkins SJ (1998) Mucus from marine molluscs. In: Advances in Marine Biology, Vol 34pp. 1-71

Deibel D (1990) Still-water sinking velocity of fecal material from the pelagic tunicate *Dolioletta gegenbauri*. Mar Ecol Prog Ser 62: 55-60

Dowd M (1997) On predicting the growth of cultured bivalves. Ecol Model 104: 113-131

Dowd M (2005) A bio-physical coastal ecosystem model for assessing environmental effects of marine bivalve aquaculture. Ecol Model 183(2-3): 323-346

Ebenhoeh W, Kohlmeier C, Radford PJ (1995) The benthic biological submodel in the European Regional Seas Ecosystem Model. Neth J Sea Res 33(3/4): 423-452

Enoksson V (1993) Nutrient recycling by coastal sediments: Effects of added algal material. Mar Ecol Prog Ser 92: 245-254

Eyre BD, Ferguson AJP (2002) Comparison of carbon production and decomposition, benthic nutrient fluxes and denitrification in seagrass, phytoplankton, benthic microalgae- and macroalgae-dominated warm-temperate Australian lagoons. Mar Ecol Prog Ser 229: 43-59

Fabiano M, Danovaro R, Olivari E, Misic C (1994) Decomposition of faecal matter and somatic tissue of *Mytilus galloprovincialis*: changes in organic matter composition and microbial succession. Mar Biol 119: 375-384

Falconer RA, Owens PH (1990) Numerical modelling of suspended sediment fluxes in estuarine waters. Est Coast Shelf Sci 31: 745-762

Fegley SR, MacDonald BA, Jacobsen TR (1992) Short-term variation in the quantity and quality of seston available to benthic suspension feeders. Est Coast Shelf Sci 34: 393-412

Feinberg LR, Dam HG (1998) Effects of diet on dimensions, density and sinking rates of fecal pellets of the copepod *Acartia tonsa*. Mar Ecol Prog Ser 175: 87-96

Finelli CM, Hart DD, Fonseca DM (1999) Evaluating the spatial resolution of an acoustic Doppler velocimeter and the consequences for measuring near-bed flows. Limnol Oceanogr 44(7): 1793-1801

Frankenberg D, Smith KL (1967) Coprophagy in marine animals. Limnol Oceanogr 12: 443-450

Frechette M, Butman CA, Geyer WR (1989) The importance of boundary-layer flows in supplying phytoplankton to the benthic suspension feeder, *Mytilus edulis*. Limnol Oceanogr 34(1): 19-36

Gangnery A, Bacher C, Buestel D (2001) Assessing the production and the impact of cultivated oysters in the Thau lagoon (Mediterranee, France) with a population dynamics model. Canadian Journal of Fisheries and Aquatic Science 58(5): 1012-1020

Garber JH (1984) ^{15}N tracer study of the short-term fate of particulate organic nitrogen at the surface of coastal marine sediments. Mar Ecol Prog Ser 16: 89-104

Gasith A (1975) Tripton sedimentation in eutrophic lakes - simple correction for the resuspended matter. Verh Internat Verein Limnol 19: 116-122

Gibbs M, Funnell G, Pickmere S, Norkko A, Hewitt J (2005) Benthic nutrient fluxes along an estuarine gradient: influence of the pinnid bivalve *Atrina zelandica* in summer. Mar Ecol Prog Ser 288: 151-164

Gilbert F, Souchu P, Bianchi M, Bonin P (1997) Influence of shellfish farming activities on nitrification, nitrate reduction to ammonium and

denitrification at the water-sediment interface of the Thau lagoon, France. Mar Ecol Prog Ser 151: 143-153

Giles H (2001) Modelling denitrification in continental shelf sediments. MSc Thesis. University of Waikato, Hamiton, 110 pp.

Giles H, Pilditch CA (2004) Effects of diet on sinking rates and erosion thresholds of mussel *Perna canaliculus* biodeposits. Mar Ecol Prog Ser 282: 205-219

Gonzales H, Biddanda B (1990) Microbial transformation of metazoan (*Idotea granulosa*) faeces. Mar Biol 106: 285-295

Graf G, Bengtsson W, Diesner U, Schulz R, H. T (1982) Benthic response to sedimentation of a spring phytoplankton bloom: Process and budget. Mar Biol 67: 201-208

Graf G, Rosenberg R (1997) Bioresuspension and biodeposition: a review. J Mar Syst 11: 269-278

Grall J, Chauvaud L (2002) Marine eutrophication and benthos: the need for new approaches and concepts. Global Change Biol 8(9): 813-830

Grant J, Cranford P, Hargrave B, Carreau M, Schofield B, Armsworthy S, Burdett-Coutts V, Ibarra D (2005) A model of aquaculture biodeposition for multiple estuaries and field validation at blue mussel (*Mytilus edulis*) culture sites in eastern Canada. Can J Fish Aquat Sci 62(6): 1271-1285

Grant J, Hargrave BT (1987) Benthic metabolism and the quality of sediment organic carbon. Biol Oceanogr 4(3): 243-264

Grant J, Hatcher A, Scott DB, Pocklington P, Schafer CT, Winters GV (1995) A multidisciplinary approach to evaluating impacts of shellfish aquaculture on benthic communities. Estuaries 18(1A): 124-144

Green MO, Hewitt JE, Thrush SF (1998) Seabed drag coefficient over natural beds of horse mussels (*Atrina zelandica*). J Mar Res 56(3): 613-637

Greenway JPC (1969) Survey of mussels (mollusca: lamellibranchia) in the Firth of Thames, 1961-67. N Z J Mar Freshw Res 3: 304-317

Grenz C, Hermin M-N, Baudinet D, Daumas R (1990) *In situ* biochemical and bacterial variation of sediments enriched with mussel biodeposits. Hydrobiologia 207: 153-160

Griffiths CL, Griffiths RJ (1987) Bivalvia. In: Pandian TJ, Vernberg FJ (eds.) Animal energetics. Academic Press, New York, pp. 1-88

Gunnarsson JS, Granberg ME, Nilsson HC, Rosenberg R, Hellman B (1999) Influence of sediment-organic matter quality on growth and polychlorobiphenyl bioavailability in echinodermata (*Amphiura filiformis*). Environ Toxicol Chem 18(7): 1534-1543

Hansen B, Fotel FL, Jensen NJ, Madsen SD (1996) Bacteria associated with a marine planktonic copepod in culture. II. Degradation of fecal pellets produced on a diatom, a nanoflagellate or a dinoflagellate diet. J Plankton Res 18(2): 275-288

Hansen LS, Blackburn TH (1992) Effect of algal bloom deposition on sediment respiration and fluxes. Mar Biol 112: 147-152

Hargrave BT (1973) Coupling carbon flow through some pelagic and benthic communities. J Fish Res Board Can 30: 1317-1326

Hargrave BT (1976) The central role of invertebrate faeces in sediment decomposition. In: Anderson JM, Macfayden A (eds.) The role of terrestrial and aquatic organisms in decomposition processes. Blackwell Scientific Publications, Great Britain, 301-321

Harris JM (1993) The presence, nature and role of gut microflora in aquatic invertebrates: A synthesis. Microb Ecol 25: 195-231

Hartstein ND, Stevens CL (2005) Deposition beneath long-line mussel farms. Aquac Eng 33(3): 192-213

Hatcher A, Grant B, Schofield B (1994) Effects of suspended mussel culture (*Mytilus* spp.) on sedimentation, benthic respiration and sediment nutrient dynamics in a coastal bay. Mar Ecol Prog Ser 115: 219-235

Haven DS, Morales-Alamo R (1968) Occurence and transport of faecal pellets in suspension in a tidal estuary. Sediment Geol 2: 125-140

Hawkins AJS, James MR, Hickman RW, Hatton S, Weatherhead M (1999) Modelling of suspension-feeding and growth in the green-lipped mussel *Perna canaliculus* exposed to natural and experimental variations of seston availability in the Marlborough Sounds, New Zealand. Mar Ecol Prog Ser 191: 217-232

Hawkins AJS, Smith RFM, Bayne BL, Heral M (1996) Novel observations underlying the fast growth of suspension-feeding shellfish in turbid environments: *Mytilus edulis*. Mar Ecol Prog Ser 131: 179-190

Hawkins AJS, Smith RFM, Tan SH, Yasin ZB (1998) Suspension-feeding behaviour in tropical bivalve molluscs: *Perna Viridis*, *Crassostrea Belcheri*, *Crassostrea Iradelei*, *Saccostrea Cucculata* and *Pinctada Margarifera*. Mar Ecol Prog Ser 166: 173-185

Hayakawa Y, Kobayashi M, Izawa M (2001) Sedimentation flux from mariculture of oyster (*Crassostrea gigas*) in Ofunato estuary, Japan. ICES J Mar Sci 58(2): 435-444

Henderson A, Gamito S, Karakassis I, Pederson P, Smaal A (2001) Use of hydrodynamic and benthic models for managing environmental impacts of marine aquaculture. J Appl Ichthyol 17(4): 163-172

Herbert RA (1999) Nitrogen cycling in coastal marine ecosystems. FEMS Microbiol Rev 23: 563-590

Hertweck G, Liebezeit G (1996) Biogenic and geochemical properties of intertidal biosedimentary deposits related to *Mytilus* beds. PSZN I: Mar Ecol 17(1-3): 131-144

Horppila J, Nurminen L (2005) Effects of calculation procedure and sampling site on trap method estimates of sediment resuspension in a shallow lake. Sedimentology 52(4): 903-913

Ingalls AE, Aller RC, Lee C, Sun M-Y (2000) The influence of deposit-feeding on chlorophyll-*a* degradation in coastal marine sediments. J Mar Res 58: 631-651

Jaramillo E, Bertran C, Bravo A (1992) Mussel biodeposition in an estuary in southern Chile. Mar Ecol Prog Ser 82: 85-94

Jeffs AG, Holland RC, Hooker SH, Hayden BJ (1999) Overview and bibliography of research on the Greenshell mussel, *Perna canaliculus*, from New Zealand waters. J Shellfish Res 18(2): 347-360

Jensen MH, Lomstein E, Soerensen J (1990) Benthic NH_4^+ and NO_3^- flux following sedimentation of a spring phytoplankton bloom in Aarhus Bight, Denmark. Mar Ecol Prog Ser 61: 87-96

Joergensen BB (1978) A comparison of methods for the quantification of bacterial sulfate reduction in coastal marine sediments. II. Calculation from mathematical models. Geomicrobiology Journal 1: 29-47

Joergensen BB, Revsbech NP (1985) Diffusive boundary layers and the oxygen uptake of sediments and detritus. Limnol Oceanogr 30(1): 111-122

Johannes RE, Satomi M (1966) Composition and nutritive value of fecal pellets of a marine crustacean. Limnol Oceanogr 11: 191-197

Jumars PA, Nowell ARM (1984) Effects of benthos on sediment transport: difficulties with functional grouping. Cont Shelf Res 3(2): 115-130

Kaiser MJ, Laing I, Utting SD, Burnell GM (1998) Environmental Impacts of Bivalve Mariculture. J Shellfish Res 17(1): 59-66

Kaspar HF, Gillespie PA, Boyer IC, MacKenzie AL (1985) Effects of mussel aquaculture on the nitrogen cycle and benthic communities in Kenepuru Sound, Marlborough Sounds, New Zealand. Mar Biol 85: 127-136

Kautsky N, Evans S (1987) Role of biodeposition by *Mytilus edulis* in the circulation of matter and nutrients in a Baltic coastal ecosystem. Mar Ecol Prog Ser 38: 201-212

Keeley NB (2001) Seston supply and scallop (*Pecten novaezelandiae*) production in the Firth of Thames, New Zealand. M.Phil Thesis. University of Waikato, Hamilton, 170 pp.

Kelly JR, Nixon SR (1984) Experimental studies of the effect of organic deposition on the metabolism of a coastal marine bottom community. Mar Ecol Prog Ser 17: 157-169

Kepkay PE, Novitsky JA (1980) Microbial control of organic carbon in marine sediments: coupled chemoautotrophy and heterotrophy. Mar Biol 55: 261-266

Komar PD, Morse AP, Small LF, Fowler SW (1981) An analysis of sinking rates of natural copepod and euphausiid fecal pellets. Limnol Oceanogr 26(1): 172-180

Kristensen E (2000) Organic matter diagenesis at the oxic/anoxic interface in coastal marine sediments, with emphasis on the role of burrowing animals. Hydrobiologia 426(1-3): 1-24

Kristensen E, Blackburn TH (1987) The fate of organic carbon and nitrogen in experimental marine sediment systems: Influence of bioturbation and anoxia. J Mar Res 45: 231-257

Kristensen E, Holmer M (2001) Decomposition of plant materials in marine sediment exposed to different electron acceptors (O_2, NO_3^-, and SO_4^{2-}), with emphasis on substrate origin, degradation kinetics, and the role of bioturbation. Geochim Cosmochim Acta 65(3): 419-433

Kristensen E, Mikkelsen OL (2003) Impact of the burrow-dwelling polychaete *Nereis diversicolor* on the degradation of fresh and aged macroalgal detritus in a coastal marine sediment. Mar Ecol Prog Ser 265: 141-153

La Rosa T, Mirto S, Favaloro E, Savonna B, Sara G, Danovaro R, Mazzolla A (2002) Impact on the water column biogeochemistry of a Mediterranean mussel and fish farm. Water Res 36: 713-721

Ladle M, Welton JS, Bell MC (1987) Sinking rates and physical properties of faecal pellets of freshwater invertebrates of the genera *Simulium* and *Gammarus*. Arch Hydrobiol 108(3): 411-424

Lohrer AM, Thrush SF, Gibbs MM (2004) Bioturbators enhance ecosystem function through complex biogeochemical interactions. Nature 431(7012): 1092-1095

Loo L-O, Rosenberg R (1989) Bivalve suspension-feeding dynamics and benthic-pelagic coupling in an eutrophicated marine bay. J Exp Mar Biol Ecol 130: 253-276

MacIntyre HL, Geider RJ, Miller DC (1996) Microphytobenthos: The ecological role of the "secret garden" of unvegetated, shallow-water marine habitats. I. Distribution, abundance and primary production. Estuaries 19(2A): 186-201

Masini RJ, McComb AJ (2001) Production by microphytobenthos in the Swan-Canning Estuary. Hydrol Process 15(13): 2519-2535

Mattsson J, Linden O (1983) Benthic macrofauna succession under mussels, *Mytilus edulis* L. (bivalvia), cultured on hanging long-lines. Sarsia 68: 97-102

Mazouni N, Gaertner J-C, Deslous-Paoli J-M, Landrein S, d'Oedenberg MG (1996) Nutrient and oxygen exchanges at the water-sediment interface in a shellfish farming lagoon (Thau, France). J Exp Mar Biol Ecol 205: 91-113

McCall PL (1979) The effects of deposit feeding oligochaetes on particle size and settling velocity of Lake Erie sediments. J Sediment Petrol 49: 813-818

McCall PL, Tevesz MJZ (1982) Animal-sediment relations. The biogenic alteration of sediments. Topics in GeoBiology Vol. 2. Pelnum Press, New York and London, 336 pp.

Miller DC, Norkko A, Pilditch CA (2002) Influence of diet on dispersal of horse mussel *Atrina Zelandica* biodeposits. Mar Ecol Prog Ser 242: 153-167

Minoura K, Osaka Y (1992) Sediments and sedimentary processes in Mutsu Bay, Japan: Pelletization as the most important mode in depositing argillaceous sediments. Mar Geol 103: 487-502

Miron G, Landry T, Archambault P, Frenette B (2005) Effects of mussel culture husbandry practices on various benthic characteristics. Aquaculture 250(1-2): 138-154

Mirto S, La Rosa T, Danovaro R, Mazzola A (2000) Microbial and meiofaunal response to intensive mussel-farm biodeposition in coastal sediments of the Western Mediterranean. Mar Pollut Bull 40(3): 244-252

Morton J, Miller M (1973) The New Zealand sea shore. William Collins and Sons, London, 653 pp.

Muschenheim DK, Grant J, Mills EL (1986) Flumes for benthic ecologists: theory, construction and practice. Mar Ecol Prog Ser 28: 185-196

Naylor RL, Goldburg RJ, Primavera JH, Kautsky N, Beveridge MCM, Clay J, Folke C, Lubchenco J, Mooney H, Troell M (2000) Effect of aquaculture on world fish supplies. Nature 405(6790): 1017-1024

Newell R (1965) The role of detritus in the nutrition of two marine deposit feeders, the prosobranch *Hydrobia ulvae* and the bivalve *Macoma balthica*. Proc Zool Soc Lond 144(1): 25-45

Newell RIE (2004) Ecosystem influences of natural and cultivated populations of suspension-feeding bivalve molluscs: A review. J Shellfish Res 23(1): 51-61

Newell RIE, Cornwell JC, Owens MS (2002) Influence of simulated bivalve biodeposition and microphytobenthos on sediment nitrogen dynamics: A laboratory study. Limnol Oceanogr 47(5): 1367-1379

Nickell LA, Black KD, Hughes DJ, Overnell J, Brand T, Nickell TD, Breuer E, Harvey SM (2003) Bioturbation, sediment fluxes and benthic community structure around a salmon cage farm in Loch Creran, Scotland. J Exp Mar Biol Ecol 285: 221-233

Nielsen P (1992) Coastal bottom boundary layers and sediment transport. World Scientific Publishing, Singapore, 324 pp.

Nixon SW (1981) Remineralization and nutrient cycling in coastal marine ecosystems. In: Nielson BJ, Cronin LE (eds.) Estuaries and nutrients. Humana Press, New Jersey, pp. 111-138

Nizzoli D, Welsh DT, Bartoli M, Viaroli P (2005) Impacts of mussel (*Mytilus galloprovincialis*) farming on oxygen consumption and nutrient recycling in a eutrophic coastal lagoon. Hydrobiologia 550: 183-198

Nodder SD, Alexander BL (1999) The effects of multiple trap spacing, baffles and brine volume on sediment trap collection efficiency. J Mar Res 57: 537-559

Norkko A, Hewitt JE, Thrush SF, Funnell GA (2001) Benthic-pelagic coupling and suspension-feeding bivalves: linking site-specific sediment flux and biodeposition to benthic community structure. Limnol Oceanogr 46(8): 2067-2072

Nowell ARM, Jumars PA, Eckman JE (1981) Effects of biological activity on the entrainment of marine sediments. Mar Geol 42: 133-153

Owen G (1966) Digestion. In: Wilbur KM, Yonge CM (eds.) Physiology of Mollusca II. Academic Press, New York, pp. 53-96

Pamatmat MM (1975) *In situ* metabolism of benthic communities. Cah Biol Mar 16: 613-633

Parsons TR, Takahashi M, Hargrave B (1977) Biological oceanographic processes, 2nd ed. Pergamon Press, Oxford, New York, 332 pp.

Parsons TR, Takahashi M, Hargrave B (1984) Biological oceanographic processes, 3rd ed. Pergamon Press, Oxford, New York, 330 pp.

Plew DR, Stevens CL, Spigel RH, Hartstein ND (2005) Hydrodynamic implications of large offshore mussel farms. IEEE J Ocean Eng 30(1): 95-108

Porter ET, Cornwell JC, Sanford LP (2004) Effect of oysters *Crassostrea virginica* and bottom shear velocity on benthic-pelagic coupling and estuarine water quality. Mar Ecol Prog Ser 271: 61-75

Prins TC, Smaal AC (1989) Carbon and nitrogen budgets of the mussel *Mytilus edulis* L. and the cockle *Cerastoderma edule* (L.) in relation to food quality. Topics in Marine Biology. Ros JD (ed.). Scient Mar 53(2-3): 477-482

Prins TC, Smaal AC (1994) The role of the blue mussel *Mytilus edulis* in the cycling of nutrients in the Oosterschelde estuary (The Netherlands). Hydrobiologia 282/283: 413-429

Rabouille C, Gaillard J-F (1991) Towards the EDGE: Early diagenetic global explanation. A model depicting the early diagenesis of organic matter, O_2, NO_3, Mn and PO_4. Geochim Cosmochim Acta 55: 2511-2525

Redfield AC (1934) On the proportions of organic derivatives in sea water and their relation to the composition of plankton. In: Daniel RJ (ed.) James Johnstone Memorial Volume. University Press, Liverpool, pp. 176-192

Revsbech NP, Soerensen J, Blackburn TH, Lomholt JP (1980) Distribution of oxygen in marine sediments measured with microelectrodes. Limnol Oceanogr 25(3): 403-411

Roditi HA, Strayer DL, Findlay SEG (1997) Characteristics of zebra mussel (*Dreissena polymorpha*) biodeposits in a tidal freshwater estuary. Arch Hydrobiol 140(2): 207-219

Rowe GT, Clifford CH, Smith KL, Hamilton PL (1975) Benthic nutrient regeneration and its coupling to primary productivity in coastal waters. Nature 255: 215-217

Ruardij P, van Raaphorst W (1995) Benthic nutrient regeneration in the ERSEM ecosystem model of the North Sea. Neth J Sea Res 33(3/4): 453-483

Rueda JL, Smaal AC (2002) Physiological response of *Spisula Subtruncata* (Da Costa, 1778) to different seston quantity and quality. Hydrobiologia 475(1): 505-511

Rysgaard S, Christensen PB, Nielsen LP (1995) Seasonal variation in nitrification and denitrification in estuarine sediment colonized by benthic microalgae and bioturbating infauna. Mar Ecol Prog Ser 126: 111-121

Singer JK, Anderson JB, Ledbetter MT, McCave IN, Jones KPN, Wright R (1988) An assessment of analytical techniques for the size analysis of fine-grained sediments. J Sediment Petrol 58(3): 534-543

Smaal AC, Prins TC (1993) The uptake of organic matter and the release of inorganic nutrients by bivalve suspension feeder beds. In: Dame RF (ed.) Bivalve filter feeders in estuarine and coastal ecosystem processes. Springer-Verlag, Berlin Heidelberg, pp. 271-298

Sobral P, Widdows J (2000) Effects of increasing current velocity, turbidity and particle-size selection on the feeding activity and scope for growth of *Ruditapes decussatus* from Ria Formosa, southern Portugal. J Exp Mar Biol Ecol 245: 111-125

Stenton-Dozey J, Probyn T, Busby A (2001) Impact of mussel (*Mytilus galloprovincialis*) raft-culture on benthic macrofauna, in situ oxygen uptake, and nutrient fluxes in Saldanha Bay, South Africa. Can J Fish Aquat Sci 58: 1021-1031

Stephens S (2003) Ecological sustainability assessment of Firth of Thames shellfish aquaculture: Task 1 - Hydrodynamic modelling. NIWA Report HAM2003-113, Environment Waikato Technical Report 2005/06, Auckland Regional Council Technical Publication 252, 34 pp.

Strasser M, Walensky M, Reise K (1999) Juvenile-adult distribution of the bivalve *Mya arenaria* on intertidal flats in the Wadden Sea: why are there so few year classes? Helgoland Marine Research 53(1): 45-55

Stuart V, Newell RC, Lucas MI (1982) Conversion of kelp debris and faecal material from the mussel *Aulacomya ater* by marine micro-organisms. Mar Ecol Prog Ser 7: 47-57

Sun M-Y, Lee C, Aller RC (1993) Laboratory studies of oxic and anoxic degradation of chlorophyll-*a* in Long Island Sound sediments. Geochim Cosmochim Acta 57: 147-157

Sundback K, Miles A (2000) Balance between denitrification and microalgal incorporation of nitrogen in microtidal sediments, NE Kattegat. Aquat Microb Ecol 22(3): 291-300

Sundby B, Gobeil C, Silverberg N, Mucci A (1992) The phosphorus cycle in coastal marine sediments. Limnol Oceanogr 37(6): 1129-1145

Taghon GL, Nowell ARM, Jumars PA (1984) Transport and breakdown of fecal pellets: Biological and sedimentological consequences. Limnol Oceanogr 29(1): 64-72

Tenore KR, Boyer LF, Cal RM, Corral J, Garcia-Fernandez C, Gonzalez N, Gonzalez-Gurriaran E, Hanson RB, Iglesias J, Krom M, Lopez-Jamar E, J. M, Pamatmat MM, Perez A, Rhoads DC, de Santiago G, Tietjen J, Westrich J, Windom HL (1982) Coastal upwelling in the Rias Bajas, NW Spain: Contrasting the benthic regimes of the Rias de Arosa and de Muros. J Mar Res 40(3): 701-772

Tenore KR, Dunstan WM (1973) Comparison of feeding and biodepositon of three bivalves at different food levels. Mar Biol 21: 190-195

Turner JT, Ferrante JG (1979) Zooplankton fecal pellets in aquatic ecosystems. BioScience 29(11): 670-677

Ullman WJ, Aller RC (1982) Diffusion coefficients in nearshore marine sediments. Limnology and Oceanogaphy 27(3): 552-556

Urban-Rich J (1999) Release of dissolved organic carbon from copepod fecal pellets in the Greenland Sea. J Exp Mar Biol Ecol 232(1): 107-124

van Duyl FC, van Raaphorst W, Kop AJ (1993) Benthic bacterial production and nutrient sediment-water exchange in sandy North Sea sediments. Mar Ecol Prog Ser 100: 85-95

Verardo DJ, Froelich PN, McIntyre A (1990) Determination of organic carbon and nitrogen in marine sediments using the Carlo Erba NA-1500 analyzer. Deep-Sea Res 37(1): 157-165

Westrich JT, Berner RA (1984) The role of sedimentary organic matter in bacterial sulfate reduction: The *G* model tested. Limnol Oceanogr 29(2): 236-249

Widdows J, Brinsley MD, Salkeld PN, Elliott M (1998) Use of annular flumes to determine the influence of current velocity and bivalves on material flux at the sediment-water interface. Estuaries 21(4): 552-559

Widdows J, Brinsley MD, Salkeld PN, Lucas CH (2000) Influence of biota on spatial and temporal variation in sediment erodability and material flux on a tidal flat (Westershelde, The Netherlands). Mar Ecol Prog Ser 194: 23-37

Widdows J, Fieth P, Worrall CM (1979) Relationships between seston, available food and feeding activity in the common mussel *Mytilus edulis*. Mar Biol 50: 195-207

Willows RI, Widdows J, Wood RG (1998) Influence of an infaunal bivalve on the erosion of an intertidal cohesive sediment: A flume and modeling study. Limnol Oceanogr 43(6): 1332-1343

Witbaard R, Bergman MJN (2003) The distribution and population structure of the bivalve *Arctica islandica* L. in the North Sea: what possible factors are involved? J Sea Res 50(1): 11-25

Wotton RS, Malmqvist B (2001) Feces in aquatic ecosystems. BioScience 51(7): 537-544

Wotton RS, Malmqvist B, Muotka T, Larsson K (1998) Fecal pellets from a dense aggregation of suspension-feeders in a stream: An example of ecosystem engineering. Limnol Oceanogr 43(4): 719-725

Yoon WD, Kim SK, Han KN (2001) Morphology and sinking velocities of fecal pellets of copepod, molluscan, eupausiid, and salp taxa in the northeastern tropical Atlantic. Mar Biol 139: 923-928

Yoon WD, Marty J-C, Sylvain D, Nival P (1996) Degradation of faecal pellets in *Pegea confoederata* (Salpidae, Thaliacea) and its implication in the vertical flux of organic matter. J Exp Mar Biol Ecol 203: 147-177

Zeitzschel B (1980) Sediment-water interactions in nutrient dynamics. In: Tenore KR, Coull BC (eds.) Marine benthic dynamics. University of South Carolina Press, Columbia, SC, pp. 195-218

Zeldis JR (2004) New and remineralised nutrient supply and ecosystem metabolism on the northeastern New Zealand continental shelf. Cont Shelf Res 24(4-5): 563-581

Zeldis JR (2005) Magnitudes of natural and mussel farm-derived fluxes of carbon and nitrogen in the Firth of Thames. Report No. CHC2005-048. Environment Waikato Technical Report 2005/30, 42 pp.